SEA SURFACE TEMPERATURE ANOMALIES IN THE SOUTH INDIAN OCEAN: OBSERVATIONS AND ATMOSPHERIC MODELLING

KABUMBWE HANSINGO

UNIVERSITY OF CAPE TOWN, ENVIRONMENTAL AND GEOGRAPHICAL SCIENCES
2001-2003, CAPE TOWN, SOUTH AFRICA

SEA SURFACE TEMPERATURE ANOMALIES IN THE SOUTH INDIAN OCEAN: OBSERVATIONS AND ATMOSPHERIC MODELLING

SUBMITTED IN FULFILMENT OF THE UNIVERSITY OF CAPE TOWN DEGREE OF MASTER OF SCIENCE

TO MY FAMILY AND FRIENDS:
CLORITY, NICHOLAS
AND
JOMO (Jr.)

JEREMIAH 33 VERSE 3

Call unto me, and I will answer thee, and shew thee great and mighty things, which thou knowest not (King James Version of the Bible).

DECLARATION

This is to certify that the dissertation entitled 'Sea Surface Temperature Anomalies in the South Indian Ocean: Observations and Atmospheric Modelling' submitted in fulfillment of the requirements of the degree of Master of Science of the University of Cape Town is a record of bonafide research work. The subject matter embodied in this report has not been submitted at any other university.

Name; Kabumbwe Hansingo

Signature; Signed by candidate

Signed this ..4th.... day of August 2003.

ACKNOWLEDGEMENT

During the course of this research there have been a number of people whose help, support and advise has helped very much. I therefore find it necessary to acknowledge and thank them here. First and foremost I would like to thank my family and friends for their understanding and allowed me to be so many miles away from them for the duration of my study –special thanks to Mark.

I would like to thank all my colleagues and friends at the Climate System Analysis Group (**CSAG**) for demonstrating the virtue of selflessness. Special thanks to Chris Jack, Ruwan and Andrew for helping me run the model and Prof. Hewiston who helped me so much, financially, when I was faced with unforeseen problems.

I would like to thank the **Water Research Commission** for the financial support that they have provided for this research.

Finally, unalloyed thanks go to my supervisor Prof. Chris Reason for his enviable responsibility of providing guidance and his inspirational hard work to get this work done –thanks for not giving up on me when things seemed not to move.

ABSTRACT

Sea surface temperature (SSTs) variations in the South Indian Ocean have been found to influence rainfall over Southern Africa. As one of the modes of South Indian Ocean SST variability, the subtropical South Indian Ocean dipole is observed to be associated with dry and wet summer conditions over Southern Africa. The positive phase of the subtropical South Indian Ocean dipole is characterized by warm SST anomalies in the southwest South Indian Ocean and cool SST anomalies in the southeast. This phase is associated with above average summer rainfall over the subcontinent. The negative phase is associated with dry conditions over Southern Africa and is characterized by cool SST anomalies in the southwest and warm anomalies in the southeast South Indian Ocean.

In order to investigate the atmospheric response over Southern Africa to this phenomenon, this study uses the MM5 regional climate model in which the model is forced with a warm pole SST anomaly south of Madagascar. Subtropical South Indian Ocean events are identified using GISST 2.3b monthly data and the model is then validated over the Southern Africa for the strong and most recent wet and dry seasons, 1980/1 and 1997/8 respectively, associated with the dipole events against NCEP. The forcing is similar to the strongest and most recent observed positive phase dipole pattern except that the cold pole is removed. A run with climatological SSTs served as the control run in this study.

A low pressure anomaly is generated over the warm pole forcing; in agreement with the previous AGCM experiments. The 850 and 500 hPa anomalies indicate that this low decays with height consistent with the linear quasi-geostrophic theory. An associated cyclonic low level wind anomaly is observed to evaporate water over the warm pole. However, there is no strong indication of it advecting moist air to the southeastern parts of the subcontinent. This low weakens the predominately southeasterlies in the southwest Indian Ocean. The forcing also generated changes in other atmospheric fields like, out-going longwave radiation, specific humidity and moisture flux.

TABLE OF CONTENTS

LIST OF FIGURES

LIST OF TABLES

Chapter 1

Introduction

1.1 Indian Ocean SSTs

Sea surface temperature anomalies have, over the past two or more decades, emerged to be a significant indicator of regional and global climate variability (Jury *et al.*, 1999; Klopper *et al.*, 1998; Wang, 2001). On the regional scale, Indian Ocean sea surface temperature (SST) variability is important for influencing the climate over the surrounding subcontinents (e.g., Black *et al.*, 2003; Clark *et al.*, 2000; Streten, 1983), particularly Southern Africa (e.g., Nicholson, 2003; Reason and Mulenga, 1999). These variations may or may not be related to the El Niño-Southern Oscillation in the equatorial Pacific region. The Indian Ocean sometimes evolves SST patterns that are associated with extreme weather conditions (droughts and floods) over the subcontinent. Among the anomaly patterns displayed in this ocean, particularly in the tropical and southern subtropical regions, are those that appear dipole in nature (e.g., Baquero-Bernal *et al.*, 2002; Behera and Yamagata, 2001; Saji *et al.*, 1999; Webster *et al.*, 1999).

1.2 The Indian Ocean Dipole Modes

A number of studies (e.g., Saji *et al.*, 1999; Webster *et al.*, 1999; Behera and Yamagata, 2001; Rao *et al.*, 2002; Reason, 2002; Vinayachandran *et al.*, 2002) have studied an Indian Ocean SST anomaly dipole pattern, in the tropical and subtropical South Indian Ocean in particular. Controversy exists as to whether these patterns are strictly a dipole (e.g. Dommenget and Latif, 2000; Allan *et al.*, 2001; Hasternrath, 2002). It is not the purpose of this thesis to determine whether or not these modes of Saji et al (1999) and Behera and Yamagata (2001) are truly dipole or not. For consistency with Behera and Yamagata (2001), we use the term dipole to refer to an SST anomaly with opposite sign on either side of the Indian Ocean basin. In the tropical Indian Ocean, the dipole mode is referred to as the tropical Indian Ocean dipole or Indian Ocean Zonal Mode and is observed to have influence on East African rainfall (Saji *et al.*, 1999; Rao *et al.*, 2002;

Vinayachandran *et al.*, 2002). In the South Indian Ocean, the dipole mode is referred to as the subtropical dipole and is observed to influence Southern African rainfall (Behera and Yamagata, 2001; Reason, 2001, 2002). Observations (Behera and Yamagata, 2001) indicate that the subtropical South Indian Ocean dipole is seasonally-phase locked to the austral summer. The positive phase is characterized by warm (cool) sea surface temperature anomalies in the southwest (southeast) Indian Ocean and the negative phase by the reverse. Observational work (Behera and Yamagata, 2001) suggests that the positive (negative) phase of the subtropical dipole mode is associated with above (below) normal rainfall over Southern Africa. Modeling work (Reason, 2001 and 2002) supports the above observations. However, the above study uses a low resolution GCM, which does not capture regional processes associated with the subtropical dipole. We therefore need to examine processes, on a regional scale, in the Indian South Indian Ocean to assist in seasonal forecasting and improve understanding of climate variability over Southern Africa.

The Global Ice and Sea Surface Temperature dataset (GISST2.3b) is used to identify the positive and negative phase events of the subtropical South Indian Ocean dipole. Circulations associated with these events are analysed in this thesis by examining sea level pressure, surface winds and latent heat fluxes of each event. These are then related to wet or dry conditions that may be associated with the event.

This thesis focuses on the positive phase of the southern subtropical Indian Ocean dipole, the warm pole in particular, because the response over southern Africa appears to be sensitive to the warm pole and its proximity to the subcontinent (Reason, 2001 and 2002). An elliptical shaped sea surface temperature anomaly pattern, +2°C in magnitude, is imposed on climatological sea surface temperatures to south of Madagascar close to the subcontinent. This is one of the four simulations carried out in this thesis using the MM5 regional model. Two simulations use SST anomalies from the observed subtropical South Indian Ocean dipoles during the wet (1980/1) and dry (1997/8) seasons. The final simulation uses climatological SSTs but 1981 National Center for Environmental Prediction (NCEP) boundary conditions. This serves as a control simulation since a long

term climatology of the MM5 model is not currently available over the southern Africa region and the model difference between the above events (i.e., 1980/1–1997/8) for various fields are compared for MM5 and NCEP.

1.3 STUDY OBJECTIVES AND MOTIVATION

Much work on the role of tropical oceans in atmospheric variability has been done with much emphasis on the Pacific, Atlantic and eastern Indian Ocean. Relatively little work has been done on the western tropical and particularly, the South Indian Ocean. From the discussions in the above paragraphs, it is evident that there is lack of sufficient knowledge and insight into climate variability observed in the Indian Ocean, particularly in these tropical and subtropical regions. In order to gain more understanding of this Indian Ocean variability, there is a need to supplement GCM experiments with higher resolution regional model experiments. This study is motivated by the need to gain more insight into the effects of the forcing that is local to the South Indian Ocean. The objective of this research is to study the atmospheric response over southern Africa to the SST dipole pattern in the South Indian Ocean using the MM5 regional circulation model developed at National Centre for Atmospheric Research (NCAR) and Pennsylvania State University (PSU). A brief description of this model is given in the next chapter. To help achieve the above objective, this research will try to address the following questions:

- How does MM5 respond to SST forcing over the domain under study?
- What atmospheric circulation changes are produced by this SST forcing?
- What summer conditions, wet or dry, are associated with dipole patterns?
- How do atmospheric parameters other than rainfall respond to these SST forcing?
- What is the time scale of the atmospheric response to these SST anomalies and what are the implications for seasonal forecasting?

1.4 The Outline of the Thesis

Chapter two reviews the literature on Indian Ocean SSTs and their relation to southern African climate. **Sections 2.2** and **2.3** look at the definition of the Indian Ocean dipole modes and their possible relationship ENSO. **Sections 2.4**, **2.5**, and **2.6** discuss the tropical and southern subtropical Indian Ocean dipole modes and the possible mechanisms involved in generating them. Reported atmospheric responses over Southern Africa to SST anomalies in the Indian Ocean and a discussion on global and regional circulation models are presented in **sections 2.7** and **2.8** respectively. The last section, **section 2.9**, of the chapter presents the objectives and motivation of the study.

Chapter three presents a brief description of the MM5 regional climate model and its diagnostics (**sections 3.2** and **3.3** respectively). It gives further details on the boundary conditions used, the domain and the experiments carried out (**sections 3.4**, **3.5**, and **3.6** respectively) to address the objectives presented in **chapter 2**.

The index showing positive and negative subtropical South Indian Ocean dipole events is reproduced in **Chapter four**. Strong positive and negative events are identified from the index and their composite plotted. This is done in **sections 4.2.2** and **4.3.2**. Intra-composite variations for each phase are discussed in **sections 4.2** and **4.3**. The two strongest events of opposite phases and the associated circulation are discussed in **sections 4.2.1** and **4.3.1**. Possible weaknesses and flaws of previously published work on the subtropical South Indian Ocean are presented in **section 4.9**. The two strongest events identified in **chapter four** are simulated in **chapter five**. These simulations are used to investigate the model response over southern Africa and compare with NCEP data. The validation is done using sea level pressure, geopotential height and zonal winds and precipitation related variables.

The model is forced with idealised SST, an idealisation of the observed 1981, this summer being the strongest positive event, in **Chapter six**. **Section 6.3** presents the

model's response to this forcing while **section 6.4** considers the circulation changes. The summary and conclusions of the study are presented in **chapter seven**.

Chapter 2

Literature review

2.1 Introduction

The Indian Ocean has influence on the climate of the surrounding continents. Li *et al.* (2001) have shown the relationship between Indian Ocean sea surface temperatures (SSTs) and Asian summer monsoon while Nicholls (1989), Smith (1994), and Smith *et al.* (2000) have demonstrated the existence of significant correlations between Indian Ocean SST and Australian winter rainfall. The Indian Ocean SSTs also play a major role in forcing East African rainfall anomalies (Goddard and Graham, 1999; Latif *et al.*, 1999). In their review of climate variability and change over southern Africa, Mason and Jury (1997) have indicated that sea surface temperature (SST) anomalies in the Indian Ocean are important for influencing interannual climate variability over the subcontinent.

A number of observational and general circulation model (GCM) modeling studies (e.g., Walker (1990), Jury and Pathack (1991), Rocha and Simmonds (1997), Landman and Mason (1999) and Reason and Mulenga (1999)) provide strong evidence of links between interannual variability of SST in the Indian Ocean and observed rainfall variability over southern Africa. Particular South Indian Ocean areas of importance to southern Africa include that northeast of Madagascar (Jury, 1996), the southwest Indian Ocean east of South Africa (Walker, 1990; Mason, 1995; Reason and Mulenga, 1999), south of South Africa (Walker, 1990; Reason, 1999), south and southeast of Madagascar (Behera and Yamagata, 2001; Reason, 2002), areas in the tropical Indian Ocean (Rocha and Simmonds, 1997). Jury (1996) has pointed out that SSTs in the Central Indian Ocean may be significant predictors/modulators of southern African rainfall. Anomalous rainfall occurs in large parts of South Africa during warm and cool events in the South Indian Ocean (Reason, 1999 and Reason *et al.*, 1998). The events may have influence on the

frequency and intensity of rainfall-producing systems, such as extra-tropical cyclones and tropical temperate troughs, over the region (Reason, 2002; Mason and Jury, 1997). Although the Indian Ocean region exhibits ENSO-induced interannual variability (Reason *et al.*, 2000; Venzke *et al.*, 2000), there are debates (e.g. Chambers et al., 1999; Saji et al., 1999; Allan et al., 2001; Dommenget and Latif, 2001) as to whether all anomalous events in the Indian Ocean are linked to ENSO or not. In this chapter, a summary of relevant studies is presented with the aim of outlining some key aspects of the so-called Indian Ocean tropical and subtropical modes (Saji et al, 1999; Webster et al., 1999; Behera and Yamagata, 2001).

2.2 Indian Ocean Dipole Modes and their possible relationships with ENSO

At times, the Indian Ocean appears to display sea surface temperature anomaly patterns that appear dipole in nature in the tropics (Behera *et al.*, 1999; Saji *et al.*, 1999; Webster et al., 1999) or in the southern subtropics (Behera and Yamagata, 2001). Local ocean-atmosphere interaction (Iizuka *et al.*, 2000; Yu and Rienecker, 1999; Ansell *et al.*, 2000) may force Indian Ocean SST anomalies while some may originate remotely via ENSO (e.g. Reason et al., 2000) or via some other process such as Indonesian throughflow variations (e.g. Hirst and Godfrey, 1993; Reason *et al.*, 1996).

For the tropical dipole pattern, Iizuka *et al.* (2000) have indicated local ocean-atmosphere interaction through the analysis of the heat budget at both the warm and cold poles as the tropical dipole pattern evolves. This Indian Ocean phenomenon was initially suggested to be essentially independent of forcing by external phenomena such as the El Nino/Southern Oscillation (ENSO) (Saji *et al.*, 1999; Webster *et al.*, 1999). The time series of the two phenomena are not orthogonal (Yamagata et al., 2002) except at zero lag (Allan et al., 2001). Yamagata *et al.* (2002) have suggested that although the Indian Ocean and ENSO time series are non-orthogonal, the two phenomena are not necessarily connected in a physical space. They have shown this ENSO-independence of the Indian Ocean via the analysis of the atmospheric bridge, the Walker circulation, between the

Indian and Pacific oceans. The presence of an anomalously strong Walker cell operating only in the Indian Ocean in the composite for Indian Ocean dipole events suggests the independent occurrence of pure Indian Ocean dipoles (an Indian Ocean dipole event is considered pure when it is not accompanied simultaneously by El Niño or La Niña) (Yamagata *et al.*, 2002). Saji et al (1999) have reported weak correlations (<0.35) between an index of the dipole, the dipole mode index (DMI), and NINO-3 SST (5ºN-5ºS, 150ºW-90ºW) anomaly time series whereas Webster et al. (1999) have reported a strong correlations of the above time series. The above authors suggest that these correlations are insignificant. However, Allan *et al.* (2001) and Nicholls and Drosdowsky (2001) debate the independence of the Indian Ocean dipoles from ENSO.

Chambers *et al.* (1999) have found a similar SST dipole in the Indian Ocean but have related it to ENSO through analysis of TOPEX/POSEIDON altimeter data. Saji *et al.* (1999) and Webster *et al.* (1999) used a mixture of EOF and correlation techniques to identify the Indian Ocean dipole SST patterns and indices. However, Allan *et al.* (2001) argues that Saji *et al.* (1999) fail to take account of the spatio-temporal evolution of ENSO events when using a standard EOF analysis of data in a non-temporally stratified form. This may have led Saji *et al.* (1999) to mistakenly assume that EOF1 and 2 modes in their results are distinct phenomena, being ENSO and an independent Indian Ocean dipole signal respectively (Allan *et al.*, 2001). Allan *et al.* (2001) have argued further that, although these EOFs are orthogonal at zero lag, they are confounded and have considerable shared variance as their time series correlate significantly with one another at leads and lags of around 9-10 months. When the correlations are calculated on monthly or seasonally-stratified values of the indices, the correlation between mean September-November values of Saji *et al.* (1999) Indian Ocean dipole index and NINO-3 is 0.52, using data from 1872-1997 (Allan *et al*, 2001). Allan *et al.* (2001) have suggested that these correlations and those reported in Webster *et al* (1999) are statistically significant. However, if the correlations in Saji *et al.* (1999) are done using March-May means, they give weakly negative values (and not statistically significant) (Allan *et al.*, 2001). Further evidence of significant correlations between ENSO and the Indian Ocean dipole is given by Goddard and Graham (1999). Allan *et al.* (2001) caution that the above EOF and

correlation over-simplified techniques are still repeated in Behera *et al.* (2000), Behera and Yamagata (2001), and Iizuka *et al.* (2000). The ENSO-dependence of the Indian Ocean dipole is further supported by Nicholl and Drosdowsky (2001). Correlations between SSTs in the two boxes used by Webster *et al.* (1999) (5°N-5°S, 45°E-55°E to represent the western and Eq-10°S, 95°E-105°E the eastern) and NINO-3 SSTs are strong and vary through the year; with positive correlations in the first half of the year (Nicholls and Drosdowsky, 2001).

2.3 DEFINITION OF THE DIPOLE MODES

By examining long-term data sets of SST (GISST2.3b) and (NCEP reanalysis), Saji *et al.* (1999) and Webster *et al.* (1999) identified several occurrences of the dipole patterns in the tropical Indian Ocean and have found two modes of variability using empirical orthogonal function (EOF) analysis. According to Saji *et al.* (1999), the first mode (EOF1), ENSO mode, explains 30% of the total variation of anomalous Indian Ocean SSTs and the second mode (EOF2), the dipole mode, (e.g **Fig 2.1**) explains 12%. They have suggested that a strong correlation (>0.7) between the simple index time series (defined as the difference in SST anomaly between the tropical western Indian ocean (50°E-70°E, 10°S-10°N) and the tropical south-eastern Indian ocean (90°E-110°E, 10°S-Equator)), referred to as the dipole mode index (DMI), and the time series associated with EOF2, indicates the accuracy of the DMI in representing the dipole mode in SST.

The subtropical dipole mode (SDM) events are seasonally phase-locked to the austral summer (Behera and Yamagata, 2001). In the subtropical Indian Ocean, a positive (negative) event, **Fig 2.2,** is characterized by cold (warm) SST anomalies in the eastern part i.e. off Australia. When in positive phase, there is evidence that this mode may produce above normal rainfall over many regions in southern Africa and drier conditions when in the opposite phase (Behera and Yamagata, 2001; Reason, 2001 and 2002). Six strong positive events (1968, 1974, 1976, 1981, 1982, and 1993) in the subtropical Indian Ocean have been identified by Behera and Yamagata (2001). Inspection of the SDI time series of Behera and Yamagata (2001) and examination of regional SST anomalies in this

thesis suggests that 1957/8, 1958/9, 1959/60, 1963/4, 1964/5, 1966/7, 1969/70, and 1997/8 are negative events.

In the tropical Indian Ocean the dipole mode, known as the tropical dipole mode (TDM), is in positive (negative) phase, **Fig 2.1**, when there is cooling (warming) of SST in the southeastern Indian Ocean off Sumatra and warming (cooling) in the western Indian Ocean and is phase locked to the boreal summer. Increased (reduced) precipitation in western (eastern) tropical Indian Ocean is associated with the positive phase of the TDM. Six strong positive events (1961, 1967, 1972, 1982, 1994, and 1997) in the tropical Indian Ocean have been identified by Saji et al. (1999).

Significant SST anomalies for the tropical Indian Ocean dipole appear around June in the equatorial Indian Ocean. They intensify in the following months and peak in October (Saji et al., 1999). The southeastern tropical Indian Ocean SST anomalies weaken after November while those in western tropical Indian Ocean continue to increase until the following January (Iizuka et al., 2000).

In the southern subtropical Indian Ocean, the SDM is usually observed to develop in December-January, peak in February and die down by May (Behera and Yamagata, 2001). During certain occasions, the event is observed not to die down completely, but may revive again to become the second consecutive event e.g. the 1980-81 and 1981-82 events (Behera and Yamagata, 2001).

2.4 THE SUBTROPICAL DIPOLE MODE

Behera and Yamagata (2001) have described the evolution of SDM events using monthly composite analysis of the observed SST, wind, sea level pressure and latent heat flux anomalies for February, March and April of the six strong positive events. At this time of the year, mean surface winds in the southern Indian Ocean north (south) of 35°S are predominantly easterly (westerly) in association with the subtropical high. These winds are however, more southeasterly off Australia during January because the centre of the

South Indian high shifts eastward during austral summer. The low surface pressure over the warm Australian landmass gives rise to a pressure gradient along the edge of the subtropical high, the centre of which migrates seasonally between 30°S and 35°S, which results in southeasterlies in the south east Indian Ocean.

Behera and Yamagata (2001) showed that during the mature phase of the subtropical dipole pattern event, the South Indian Ocean anticyclone is strengthened and shifts slightly southward. Since the West Coast Trough that forms over Western Australia during summer months (Fandry and Leslie, 1984) tends to migrate nearer to the west coast during January-March, the resultant pressure gradient between the eastern edge of the South Indian Ocean anticyclone and this trough further enhances the southeasterlies off the coast of Australia. During SDM events, these high pressure anomalies in the South Indian Ocean lead to anomalous southwesterlies southwest of Australia. The anomalous winds in the eastern South Indian Ocean essentially represent a strengthening of the mean wind and, as a result cause cooling due to increased evaporation and upper-ocean mixing. Even in the absence of the other processes, a change of 10 Wm^{-2} in latent heat loss can lead to a local change of 0.5°C in the SST over a season for a typical mixed layer depth of 50m (Behera and Yamagata, 2001).

The deformation of the South Indian Ocean anticyclone (**Fig 2.3**) during SDM positive phase events causes anomalous easterlies around 40°S in the subtropical Indian Ocean around February, when the dipole pattern peaks, leading to weakening of the midlatitude westerlies. The weakening of the midlatitude westerlies may cause reduction of the seasonal latent heat loss, which in turn leads to the warming of the southwestern Indian Ocean. As stated earlier, February is the month of maximum SST anomalies. In addition, the reduction in the midlatitude westerlies may decrease the equatorward Ekman transport of colder high latitude waters, thereby contributing to the warming. As the austral summer ends, the subtropical anticyclone migrates to the northwest i.e. south of Madagascar when the Australian landmass cools and an anticyclone establishes over the continent. The associated northward shift in the westerlies and easterlies causes decay of the SDM.

The SDM does not occur every austral summer, however. The occurrence of SDM may be related to the location and intensity of the South Indian Ocean anticyclone in a particular year. An anomaly east or southern centre of the anticyclone may favour the occurrence of the dipole mode.

2.5 THE TROPICAL DIPOLE MODE

For the TDM, Iizuka *et al.* (2000) and Saji *et al.* (1999) have reported that cool SST anomalies first appear in the vicinity of the Lombok strait by May–June accompanied by moderate southeasterly wind anomalies. These winds enhance upwelling along Java and Sumatra coasts leading to local cooling. From late May to August, negative anomalies of the heat budget occur over this region. This may be due to the vertical and horizontal divergence of heat transport in the southeastern tropical Indian Ocean (Iizuka *et al.*, 2000). The vertical divergence indicates that cold water is brought into the surface as the thermocline shallows in response to the southeasterly wind anomaly over the Indian Ocean. The horizontal divergence corresponds to the advection of relatively cold surface water induced by the anomalous westward current excited by the southeasterly wind anomaly leading to the cold pole of the TDM.

In the following months, the cold SST anomalies intensify and appear to migrate towards the Equator along the Indonesian coastline, while the western tropical Indian Ocean begins to warm up. The deepening of the thermocline in the western tropical Indian Ocean, in response to the anomalous easterly winds along the equatorial Indian Ocean, leads to warmer (cooler) than usual SSTs in the western (eastern) Indian Ocean region because of reduced (increased) cold-water entrainment from the subsurface layer and weaker than average Wyrtki jets (Iizuka *et al.*, 2000; Vinayachandran *et al.*, 1999; Vinayachandran *et al.*, 2002). Equatorial waves also affect the depth of the thermocline and hence the ocean's temperature profile, through their downwelling/upwelling effects, as well as the sea surface height. During the positive phase of the TDM, Kelvin (Rossby) waves generated by the anomalous winds reflect from the eastern (western) boundary as

an upwelling (downwelling) Rossby (Kelvin) wave, lowing (raising) SSTs there (Vinayachandran *et al.*, 2002). Zonal wind anomalies along the Equator and alongshore wind anomalies of Sumatra intensify as the SST dipole evolves (Saji *et al.*, 1999). In September, the zonal wind anomaly over the tropical Indian Ocean further intensifies while the southeasterly wind anomaly along the Sumatra weakens. A rapid peaking of these features occurs in October. The heat exchange over the warm pole starts to increase, mainly due to the vertical convergence of heat transport brought about by the anomalous westward bound Rossby currents, in late October. This is followed by a rapid demise of these features, which may be due to the strong monsoon associated with the warm West Indian Ocean. These strong winds may induce greater mixing, greater Ekman transports forcing coastal upwelling, and greater evaporation, all of which would contribute to rapid cooling (Webster *et al.*, 1999). This is also a monsoon transitional period, which is associated with equatorial westerlies. These winds relax the SSH fields, which would force eastward-propagating and downwelling Kelvin waves that deepen the eastern mixed layer and return the system towards its previous state (Webster *et al.*, 1999).

2.6 MECHANISMS

Coupling between the ocean and the atmosphere is purported to be strong in the tropical Indian Ocean and is important for generating the anomalous events in the region (e.g. Ansell *et al.*, 2000; Behera *et al.*, 1999; Iizuka *et al.*, 2000). However, in the subtropical South Indian Ocean, Reason (1999) suggests that atmospheric forcing may be important in driving SST. Anomalous wind conditions and cloud-cover have been identified as influencing SSTs in the tropical and the subtropical Indian Ocean regions (e.g. Behera and Yamagata, 2001; Iizuka *et al.*, 2000; Reason *et al.*, 2000). Oceanic processes like entrainment, upwelling, Ekman drift, and variation in surface heat flux exchange are observed to play a role in influencing SSTs in both the tropical and subtropical Indian Ocean. Variations in thermocline depth, sea surface height (SSH), Rossby and Kelvin waves and Wyrtki jets may play a major role in the evolution of observed and modeled SSTs anomalies in the tropical Indian Ocean (e.g Ansell *et al*, 2000; Behera *et al*, 2000;

Vinayachandran *et al.*, 2002). How the above processes may influence the SST anomalies is briefly described in the following paragraphs.

Strong southeasterly wind stress is reported to prevail over the cold pole while easterly wind anomalies dominate over the warm pole in the tropical Indian Ocean (Behera *et al.*, 1999). According to Iizuka *et al.* (2000) the anomalous easterly winds during the positive phase of the dipole mode generate a westward current over the tropical Indian Ocean, which causes the shoaling (deepening) of the thermocline in the eastern (western) equatorial Indian Ocean. This may result in the cooling (warming) of SSTs in the east (west) by increasing (decreasing) entrainment from below the thermocline (Iizuka *et al.*, 2000). A similar process has been reported by Vinayachandran *et al.* (2002). They have reported that the easterly wind anomalies excite an upwelling equatorial Kelvin wave that reflects from the eastern boundary as an upwelling Rossby wave propagating westward across the equatorial Indian Ocean. This Rossby wave initiates the deepening of the thermocline in the western tropical Indian Ocean weakening the influence of the Wyrtki jets. The latter are eastward equatorial jets, which typically occur during the monsoon transition seasons of Oct/Nov and Apr/May when equatorial westerlies prevail and accumulate water in the eastern Indian Ocean leading to warm SST and a deep mixed layer and thermocline (Vinayachandran *et al.*, 2002; Hastenrath *et al.*, 1993). These jets are weak during positive TDM events because of the anomalous easterly winds and strong during negative TDM events (Vinayachandran *et al.*, 2002).

In addition to Wyrtki jet modulation, Behera *et al.* (1999) have reported that entrainment cooling produced most of the negative SST anomaly near the coasts of Java and Sumatra whereas evaporative cooling dominated the process away from these coasts during the 1994 dipole mode event. They have suggested that stronger entrainment, higher latent heat loss, and a decrease in radiative flux may produce colder SST while a higher-radiative flux, in the absence of strong entrainment and latent heat loss, may produce warmer SST.

Unlike in the tropical region where the atmosphere and the ocean are tightly coupled, atmospheric forcing may be important in the southern subtropical region (Reason, 1999). The deformation of the South Indian Ocean anticyclone causes anomalous easterlies around 40°S, 90°E during the peak of the positive SDM event, leading to the weakening of the midlatitude westerlies (Behera and Yamagata, 2001). Reason (1999) and Behera and Yamagata (2001) have proposed that enhanced evaporation, upper-ocean mixing and surface fluxes, which may be as a consequence to stronger southeasterly winds in the eastern subtropical Indian Ocean, may cool the SST there. Weakening of the midlatitude westerlies in the southwest subtropical Indian Ocean reduce surface flux losses and upper-ocean mixing, conditions favourable for warm SSTs (Behera and Yamagata, 2001; Reason 1999). Weaker midlatitude westerlies tend to warm the subtropical SST by reduced Ekman drift of higher latitude water equatorwards, additionally the anticyclonic and easterly wind anomalies south east of South Africa during SDM events may imply relative Ekman drift of more tropical waters polewards further warming the SST there (e.g Reason, 1999). Cloud cover changes may influence SST through the amount of insolation received at the surface. Reduced (increased) cloud cover is favourable for warmer (cooler) SST in large regions of the subtropics/midlatitudes during anomalous events (Reason, 1999). Weaker winds and reduced cloud cover would favour warming if the latter is mainly responding via latent and sensible heat fluxes and upper ocean mixing to atmospheric changes (Reason *et al.*, 2000) rather than dynamically through anomalies in wind-driven currents.

2.7 ATMOSPHERIC RESPONSE

Large-scale SST anomalies lead to differences in atmospheric convection and pressure gradient fields, which in turn can set up anomalous atmospheric circulation and rainfall patterns. However, it is still unclear to what extent Indian Ocean SST anomalies are a causal factor as opposed to simply being a response to large-scale circulation changes that produce both Indian Ocean SST and South African rainfall anomalies (Rocha and Simmonds, 1997a). A number of observational and experimental studies (e.g. Goddard

and Graham, 1999; Jury, 1996; Reason, 1998, 2001, 2002; Reason and Mulenga, 1999; Rocha and Simmonds, 1997b) have been performed to investigate the influence of the Indian Ocean SST anomalies on rainfall and atmospheric circulation over southern Africa. Mason and Jury (1997) have reported that ENSO events and SST anomalies in the Indian and Atlantic oceans can influence both the tropical and the midlatitude atmospheric circulation and moisture fluxes over the subcontinent. More specifically, SST anomalies in the southwest Indian Ocean may have an important influence upon the formation of southern Africa's tropical-temperate troughs, the main summer rain-bearing synoptic systems (Walker, 1990; Mason, 1995, Reason and Mulenga, 1999). Goddard and Graham (1999) have indicated the influence of the Indian Ocean SST anomalies on formation of anomalous cyclonic (anticyclonic) circulations southeast of Africa, which may influence moisture convergence and rainfall over southern Africa. As discussed below, the Indian Ocean SST may also influence the number and intensity of the extra-tropical cyclones (e.g. Reason, 2002; Reason and Murray, 2001) that influence tropical temperate troughs and tropical cyclones (Jury *et al.*, 1999) in the region. Mason (1995) has suggested the occurrence of strong associations between rainfall over southern Africa and western equatorial Indian Ocean SSTs. Thus SST anomalies of the Indian Ocean may be related to southern African seasonal rainfall variability in different ways.

Traditionally, warm SST anomalies in the Indian Ocean have been linked to ENSO (Cadet, 1985; Allan *et al.*, 1996) events in the tropical Pacific Ocean. The latter are associated with dry conditions over southern Africa and anomalous weather conditions in other parts of the world (Ropelewski and Halpert, 1987). However, Landman and Mason (1999) suggested that since the late-1970s, warm (cool) events in the tropical western Indian Ocean have become associated with wet (dry) conditions over the southern Africa, especially the north-eastern half of South Africa and northern Namibia. There are strong indications that El Niño-related warm events are associated with the ascending (descending) branch of the Walker circulation found over the central Indian Ocean (African continent) and that the opposite configuration occurs during cool events associated to La Niña (Reason *et al.*, 2000). However, Rocha and Simmonds (1997 ab) have indicated that warm SSTs in the central Indian Ocean, which are partially

independent of ENSO, may dominate the rainfall response. They have suggested that warming of the central Indian Ocean may generate low-level cyclonic atmospheric anomalies there. This may in turn weaken the predominantly easterly flow across the eastern coast of Africa, thus less moisture enters the continent and reduced precipitation takes place. A circulation gyre off the coast of southeast Africa, identified in Jury (1996), is believed to control the flux of moisture between southern Africa and northern Mozambique Channel. This has been supported by the studies of Mason (1995) in which, he suggested that high SSTs to north of Madagascar may induce the development of tropical easterly disturbances over the western equatorial Indian Ocean rather than over the interior of the subcontinent. Hence, this may result in drier conditions over the land.

The Indian Ocean, particularly the western tropical Indian Ocean, is thought to be an important source of atmospheric moisture throughout the austral rainfall season (D'Abreton and Tyson, 1995). During a dry austral rainfall season (DJF), associated with cool tropical Indian Ocean SST, weaker winds between 15° and 25°S (Reason *et al.*, 1998) advect little moist air onshore and strong negative mean sea-level pressure anomalies occur in the central Indian Ocean, east of Madagascar. This may be related to the fluctuation of the preferred position of the ridge associated with the standing wave 3, which is normally located over the south-western Indian Ocean. The southern African tropical temperate or tropical-extratropical cloud band (one of the most important rain-bearing systems in the region during summer) forms ahead of the mid-latitude trough associated with wave number 3 (Rocha and Simmonds, 1997).

Warmer (cooler) SSTs in the western (eastern) tropical Indian Ocean may produce convergent (divergent) flow and enhanced (diminished) convective heating in that region (Behera *et al.*, 1999; Goddard and Graham, 1999; Iizuka *et al.*, 2000). This results in decelerating and convergent westerly (accelerating and divergent easterly) low-level flow over central east Africa. Increased (decreased) convective heating in the low-latitude western Indian Ocean induces the formation of cyclonic (anticyclonic) circulations off southeast Africa, producing southeasterly (northwesterly) low-level flow and divergence (convergence) of moisture flux over southern Africa, reducing (increasing) rainfall in that

region. The same circulation changes contribute to moisture flux convergence (divergence) and increased (decreased) rainfall over central-east Africa (Goddard and Graham, 1999). The intensified easterly wind anomalies over the central Indian Ocean (Behera *et al.*, 1999; Lizuka *et al.*, 2000) result in an anomalous Walker Circulation over the tropical Indian Ocean. This anomalous Walker Circulation associated with the easterly wind anomaly in the lower troposphere leads to decreased (increased) precipitation over the eastern (western) tropical Indian Ocean (Lizuka *et al.*, 2000). Model results of Rocha and Simmonds (1997) suggest that positive and negative evaporation anomalies coincide with anomalously warm and cold surface waters, respectively.

Not much study has been done on the influence of the subtropical Indian Ocean SST dipole on atmospheric circulation and rainfall over southern Africa. However, studies of Reason (1999,2001, and 2002) and Behera and Yamagata (2001) have suggested a potential influence. Behera and Yamagata (2001) have suggested that cold anomalies elongated obliquely from the eastern subtropical region to the western tropical region in the southern Indian Ocean may weaken the maritime ITCZ by reducing local atmospheric convergence. The anomalous southeasterlies lead to increased tropospheric moisture divergence from the eastern subtropical Indian Ocean. Enhanced lower tropospheric southeasterlies may then transport the surplus moisture downstream to south-central Africa, leading to the moisture convergence there. This may give rise to increased convective activity and increased rainfall over these regions. The situation is then reversed during a negative phase of the SDM. The warmer water associated with anomalous northwesterlies strengthens the maritime ITCZ giving rise to increased precipitation in the maritime region. Further, the cold western pole and the opposite anomalies in the tropospheric flow result in less precipitation over the regions of southern Africa and southern Madagascar.

2.8 LOW AND HIGH RESOLUTION CIRCULATION MODELS.

Earlier experiments (e.g. Reason, 2001; Rocha and Simmonds, 1997) and analyses (e.g Yamagata and Behera, 2001) on Indian Ocean climate variability have been carried out using GCMs or NCEP re-analysis data. However, GCMs have limitations. One of the limitations of the GCMs is their weakness to represent local topographic, SST and vegetation gradients, with high accuracy (Reason, 2001 and 2002). This is because of their low resolution, which in turn is restricted by computational capabilities on which they are run. However, RCMs have been developed to try to overcome these limitations. RCMs are high-resolution climate models appropriate for studies over smaller domain and are able to better represent these local features.

Peng *et al.* (1997) have suggested that high- and low- resolution general circulation model (GCM) experiments may give different results concerning the effects of the midlatitude SST anomalies on the atmosphere. Three types of results from low-resolution model simulations have been obtained (e.g., Pitcher et al., 1988; Ting 1991; Kushnir and Lau, 1992; Lau and Nath, 1994; Kushnir and Held, 1996, cited in Peng *et al.*, 1997). The first result indicates that there is no atmospheric response to the midlatitude SST forcing. The second result indicates that there is a baroclinic response to the surface heating, similar to that given by a linear model, with a low-level trough and an upper-level ridge downstream. The third result indicates that there is an equivalent barotropic response to the heating with a trough growing with height. On the other hand, a different response has emerged from experiments with high-resolution GCMs (e.g., Palmer and Sun, 1985; Ferranti et al., 1994; Latif and Bernett, 1994; Peng et al., 1995, cited in Peng *et al*, 1997). An equivalent barotropic response structure but with a downstream anomalous ridge was found when the models are forced with positive SST anomalies. Peng et al, (1997) suggest that such a response is realistic but is not captured by low resolution models. Furthermore, Peng and Whitaker (1998) have noted that different results among models of comparably high resolution GCMs exist and these differences may be due to differences in their background circulation states and approach on the physics of the boundary layer.

Low resolution GCM experiments of Reason (2001 and 2002) in the subtropical Indian Ocean indicate that a low (high) pressure anomaly which decays with height, consistent with the linear quasi-geostrophic theory, is generated over, and downstream of the warm (cold) pole. The anticyclonic wind anomaly over the South West Indian Ocean, during the positive phase, evaporates more moisture over the warm pole and enhances the mean summer onshore advection of moisture over eastern South Africa and Mozambique. The local Walker circulation over the western Indian Ocean/southern African region is relatively enhanced and relatively weakened over northern Australia /Indonesia (Reason, 2001 and 2002). Anomalously strong high level easterlies over low latitude Africa, that are associated with increased summer rainfall over southeastern Africa, are observed during warm events. Further, the model results suggest that it is the warm part of the SDM, and particularly its proximity to eastern South Africa/ Mozambique, that is important for the response over Southern Africa. The response over tropical (subtropical) Southern Africa appears to be sensitive (not sensitive) to the cold part of the dipole off Western Australia.

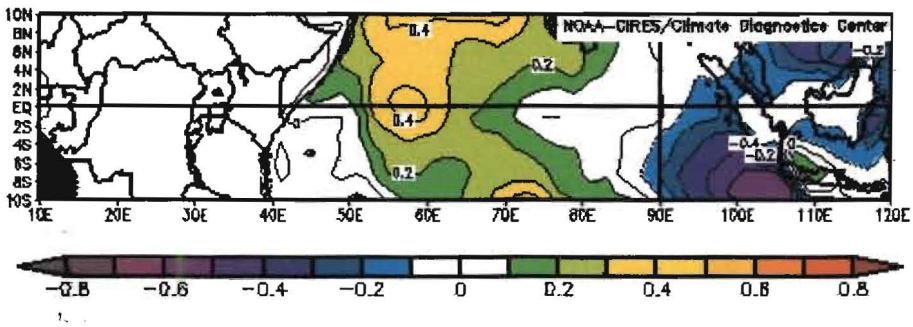

Fig 2.1 Oct 1967 Tropical Indian Ocean SST dipole obtained from reconstructed Reynolds SST data on the CDC www.cdc.noaa.gov/Composite.

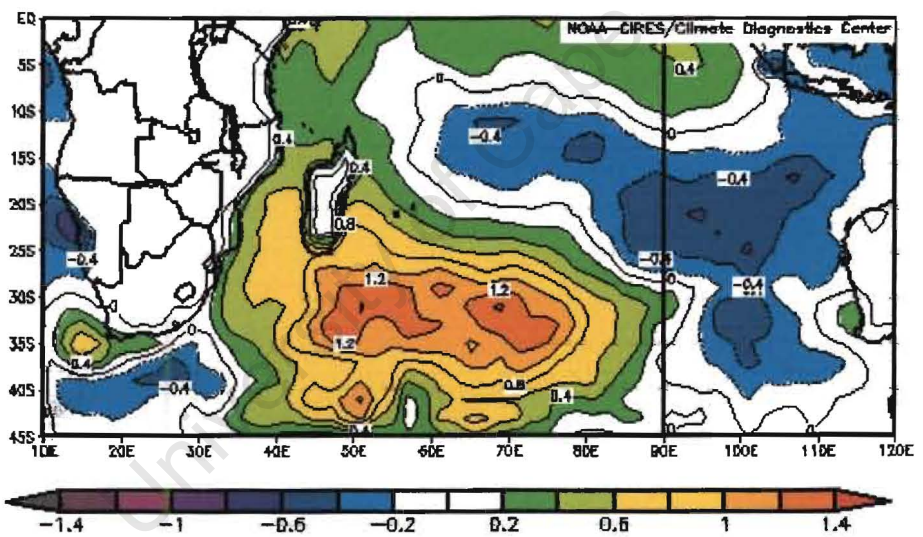

Fig 2.2 JFM 1981 Subtropical Indian Ocean SST dipole obtained from reconstructed Reynolds SST data on the CDC WWW.cdc. noaa.gov/Composite.

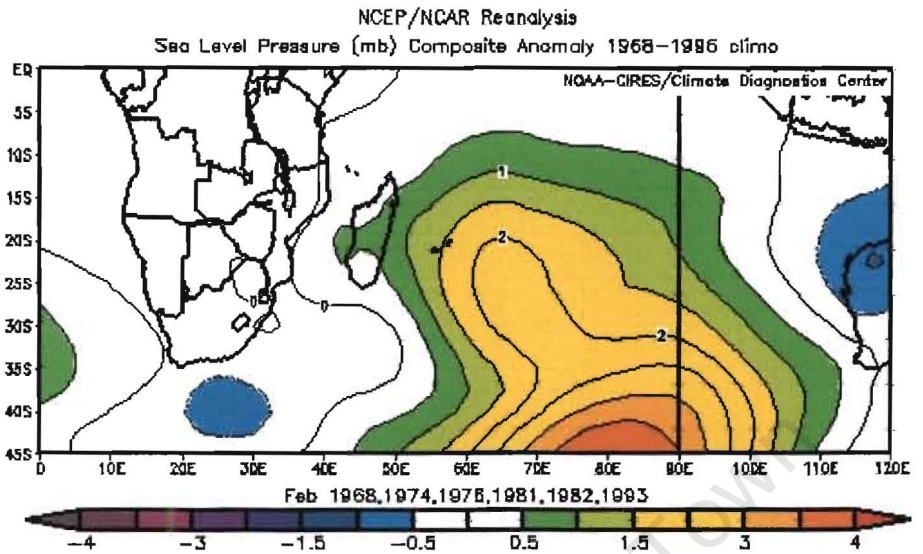

Fig 2.3 *February sea level pressure composite anomaly for six strong subtropical dipole events obtained from www.cdc.noaa.gov/Composite web site*

Chapter 3

Data and Methodology

3.1 Introduction

The Pennsylvania State University (PSU)-National Center for Atmospheric Research (NCAR) fifth generation mesoscale model version 3 (MM5V3, hereafter referred to as MM5) is used in this study. This is a high resolution model and is likely to better represent SST gradients that are known to be significant for Southern African weather and climate (e.g. Rouault *et al.* 2002, 2003) than a global model. Additionally, MM5 may better represent the tight vegetation and orography gradients that exist over Southern Africa. This model is expected to bring out features, associated with the dipole, that may be difficult to simulate in GCMs. Six hourly National Center for Environmental Prediction (NCEP) reanalyses were used for the model's initial and boundary conditions. Four sets of experiments, each with an ensemble member of five integrations using different initial conditions, were carried out. Two of the experiments are simulations of the strong dipole mode events (1980/81 and 1997/98) of opposite orientation as found from the subtropical dipole index of Behera and Yamagata (2001). The third experiment was similar to the 1980/81 experiment, except that the model was forced with NCEP reanalysis 30yr daily skin temperature (SKT) climatological data derived from the six hourly dataset. This served as the control run for the study. The fourth experiment was an idealized run of the 1980/81 positive event (positive SST anomalies in southwest Indian Ocean). Following Reason (2001, 2002), an elliptical shaped positive pole anomaly of +2°C in magnitude was imposed on NCEP reanalysis 30yr daily climatology skin temperature (SKT) to represent an idealization of the warm pole observed south of Madagascar during 1980/1. The purpose of this experiment was to assess the response of the model to a large scale coherent idealized SST anomaly which hopefully would be easier to diagnose in terms of theory than the response to an observed pattern. In this chapter, a brief description of the model used is given. The integration is done over a

period of six months in all the four experiments. The domain, data and method used in this study are also discussed.

3.2 MODEL DESCRIPTION

MM5 is a limited-area, nonhydrostatic, terrain-following sigma co-ordinate model designed to simulate mesoscale and regional scale atmospheric circulation. It has been developed at PSU and NCAR as a community mesoscale model and is continuously being improved by contributions from users at several universities and government laboratories. There are over 200 peer-reviewed publications that focus on MM5 model development, applications, and various levels of evaluation (Koracin and Dorman, 2001). In its weather mode, MM5 is an advanced numerical weather prediction model used for research and operational forecasting around the world. A general description of the model is given by Dudhia (1993, cited in Bromwich et al., 2001; Roebber and Reuter, 2002). The model has variable resolution and is supported by several auxiliary programs, which are referred to collectively as the MM5 modeling system. However, not all the programs were used in this study. Only four; Terrain, Regrid, Interpf and MM5 of the complete modeling system were used. A schematic diagram of the complete modeling system and the order of the programs and the flow of data can be found on the World Wide Web site http://www.mmm.ucar.edu/mm5/. Since MM5 is a regional model, it requires initial conditions as well as lateral and surface boundary conditions to run. A large number of physics parameterization schemes are available in the MM5 model. Detailed information on the optional parameters of the MM5 code is provided by Grell *et al.* (1995, cited in Koracin and Dorman, 2001) and the above mentioned Web site. The physical parameterisation used for all the runs in this study include a mixed phase explicit moisture scheme, the Grell cumulus parameterisation scheme and the MRF planetary boundary layer scheme. The cloud-radiation and no-shallow convection implicit cumulus schemes are used.

MM5 has been used in various studies, ranging from sensitivity studies to short-range (1-2 days) prediction of mesoscale phenomena (e.g Zou *et al.*, 1998; Colle and Mass, 2000),

in North America. Colle and Mass (2000) have indicated that the model's skill in forecasting precipitation improves as the grid spacing decreases from 36 to 4 km and that the model produces excessive precipitation at 12 and 4 km resolutions. However, little work has been done with this model over Africa, particularly southern Africa. Therefore, the skill of the model in representing atmospheric circulation over this region is not completely known.

3.3. Boundary Conditions

As mentioned in the previous section, MM5 requires initial and boundary conditions to simulate atmospheric circulations. These were generated by first interpolating the six hourly NCEP global re-analyses (2.5° lat × 2.5° long resolution) to the model grid. This dataset is a research quality dataset suitable for many uses, including weather and short-term climate research. The system used to produce this dataset has many new features, which include a frozen state-of-the-art global data assimilation, an improved quality control system etc. All the analysis output fields are monitored with a complex quality control monitoring system, in which the statistics of the data, e.g. tendency checks, time tendencies etc, are compared to climatological statistics in order to detect errors (Kalnay *et al.*, 1996). From this dataset the following fields, which are a minimum requirement to run the MM5 model, were used for initial and boundary conditions.

i.) Air temperature (K)
ii.) U-component of the horizontal wind (ms^{-1})
iii.) V-component of the horizontal wind (ms^{-1})
iv.) Relative humidity (%)
v.) Geopotential height (m)
vi.) Sea level pressure (Pa)
vii) Sea surface temperature (SST) or Skin temperature (SKT) (K)

Note the sea surface temperature field represents the temperature of the water (whether that is the temperature at the ocean surface or temperature of some layer near the surface). Over land, this field does not have meaning, and in many datasets the values are smoothly interpolated from water points. A skin temperature field represents the temperature of the surface of the earth, whether that surface is land or water. In MM5 these fields are interpreted differently. The SST field is interpreted as one that can be used as an instantaneous field appropriate for water temperatures, which may vary in time. The SKT field is averaged for all times, and the average is written as a single-invariant field. This averaging is done to remove the diurnal variation of the skin temperature over land (www.mmm.ucar.edu/mm5/mm5v3/tutorial/regrid/sst_note.html). In this study, the SKT field was used because six hourly SST data was not available. In addition to the above fields, the model is forced with level one (0-10cm) and two (10-200cm) NCEP soil moisture data.

3.4. Domain

For this study, a model grid of 140 × 90 horizontal points, centered at 22.5°S and 35°E (**Fig.3.1**) with a grid distance of 60 km and 23 levels in the vertical sigma coordinates was used. The domain extends from 0° to 45°S; 5°W to 70°E, covering the whole of southern Africa, Madagascar and part of the South Indian and Atlantic Oceans. This domain is smaller than that originally intended, which extended further east to about 120°E and south to about 60°S, but computational resources were limiting. However, the size of the domain used is such that any signal from the lateral boundary conditions is not likely to have a significant influence to the response over Southern Africa and the local SST forcing should dominate. This domain is of interest because observations and GCM modelling attribute a robust rainfall signal (from Zambia to southeastern south Africa) that seems to be linked with the dipole SST patterns in the South Indian Ocean (Behera and Yamagata, 2001; Reason, 2001,2002).

3.5. Method

In order to investigate the atmospheric response over southern Africa to the dipole pattern, four sets of experiment were performed. Each set had an ensemble member of five integrations of the model with different initial conditions. In each set, the model was integrated from five different starting times spaced at intervals of six hours starting from 00:00UTC 01 November 1980. Given that our interest is in intraseasonal to interannual variability, in all the experiments the model output frequency was set to twenty-four hours (1440 minutes). Because of the length of the model integration and magnitude of the temporal resolution difference between the initial conditions and the output it is reasonable to use a five member ensemble to assess whether there are any intra-ensemble variations. These variations are discussed in **chapter five.**

The first experiment was a simulation of one of the strongest and coherent positive events (1981) of the six events defined by Behera and Yamagata (2001). Furthermore, the 1980/1 austral summer rainy season was wetter than average over large parts of Southern Africa. In this experiment, the model was forced with NCEP's six hourly reanalysis data for the simulated period for all the variables required by the model. As mentioned earlier, each ensemble member had different initial conditions. The second experiment is similar to the first experiment except that a negative event (1998) (cool in southwest Indian Ocean, warm in SE Indian Ocean) noted by the author from Behera and Yamagata's (2001) SDI time series, was used to force the model.

In experiment three, the model was forced with a 30yr (1970 to 1999) daily SKT climatological data obtained from six hourly data to produce a control data set. This was done because the model climatology for all the variables required by the model was not available. This experiment is similar to experiment one except that climatological SKT was used over the ocean. Forming anomalies from the ensemble mean of experiment one minus experiment three would, in theory, represent the model's response to the 1980/1 SST anomalies. Unfortunately, due to computational limitations, a MM5 run forced by observed SST over the last 30yrs, which one would ideally use to form a climatology was

not possible. The five ensemble member integrations also started from different early November days of 1980 and the same NCEP boundary conditions as from experiment one were imposed. This experiment served as the control run for the study.

The fourth experiment is similar to experiment three except for a spatially constant positive anomaly pole, centred at 30°S, 42°E with a temporal constant magnitude of +2°C (**Fig. 3.2**) imposed on the climatological SKT. This experiment can be compared with the third global AGCM experiment in Reason (2002) whose purpose was to test the sensitivity of the southern African atmospheric response to forcing originating only from the nearby ocean with the southeast Indian Ocean pole removed. Experiment four can be used to assess the model's response to a smooth, large SST anomaly and hopefully facilitates diagnosis of the model's response in terms of theory. Lau and Nath (1990) have suggested that it is necessary to use anomaly amplitudes which a much higher than the observed values, so as to yield statistically significant atmospheric signals. To make the response that much clearer and more straightforward to diagnose, an anomaly magnitude of +2°C (Reason 2001 and 2002) was used. Note that some of the six individual austral summers that went into the Behera and Yamagata (2001) SST dipole composite had a maxima of about 2°C.

In all the above experiments, the first and second months were regarded as the spin-up periods for the model. Given that the dipole reaches maximum in February, results are presented as summer season (JFM) and intraseasonal (January, February and March) wet and dry spell differences between ensemble means (Reason 2001). In order to isolate the atmospheric response to the SST forcing, the anomalies from the idealized run are compared with those from the 1981 simulation. In order to obtain amplified signals of the 1980/1 wet event, the results from the 1997/8 dry event are subtracted from this event to form a wet-dry model response. A summary of the experiments is given in **Table 3.1**

Behera and Yamagata's (2001) SDI indicates 1997/8 to have been a strong negative dipole mode event. Examination of negative events as per the above index by the author, from the CDC website www.cdc.noaa.gov/Composite, however indicates that the dipole

pattern during this event is not as clear as in other events. However, this event was modeled because it is the only negative event after 1980 and there are concerns about the quality of the daily NCEP data set (used for model boundary conditions) prior to this year. As a result of this concern and the fact that the observed rainfall anomaly was appropriate, it was deemed preferable to use 1997/8 as the negative event modeled in this thesis rather than one of the earlier cases.

EXPERIMENT	SIMULATION
Experiment One	1980/1 Positive Event.
Experiment Two	1997/8 Negative Event.
Experiment Three	1980/1 with climatological SKT.
Experiment Four	1980/1 Idealised SST.

Table 3.1 *Summary of all the experiments.*

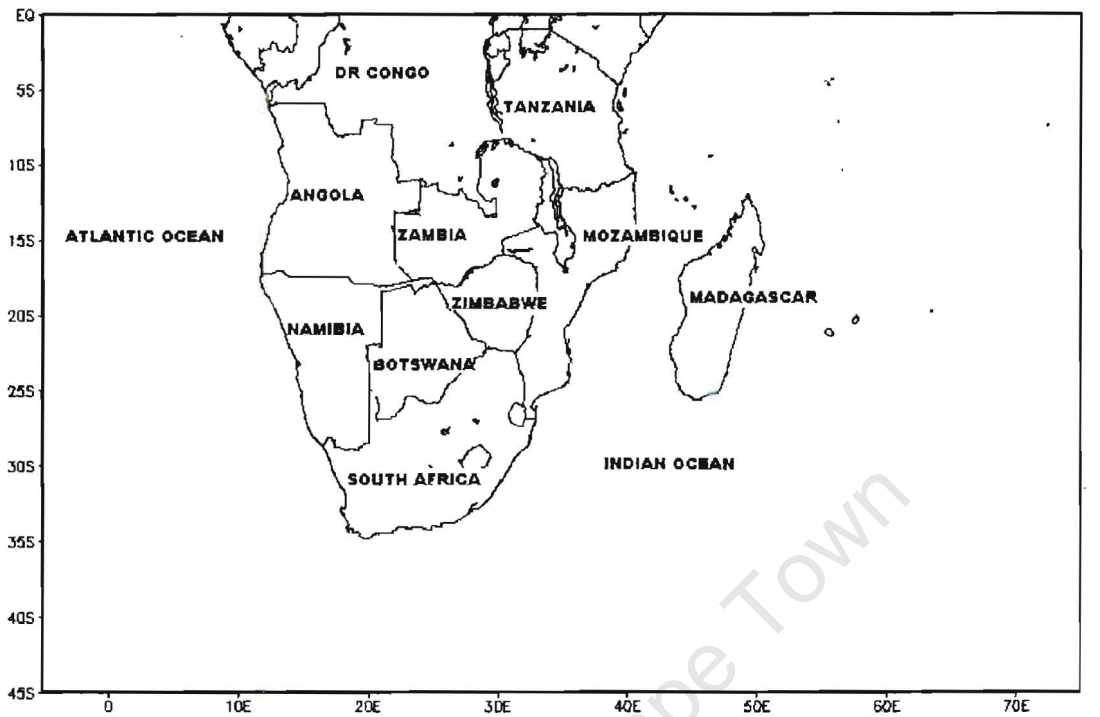

Fig 3.1 Model domain covering southern Africa and southern Indian Ocean.

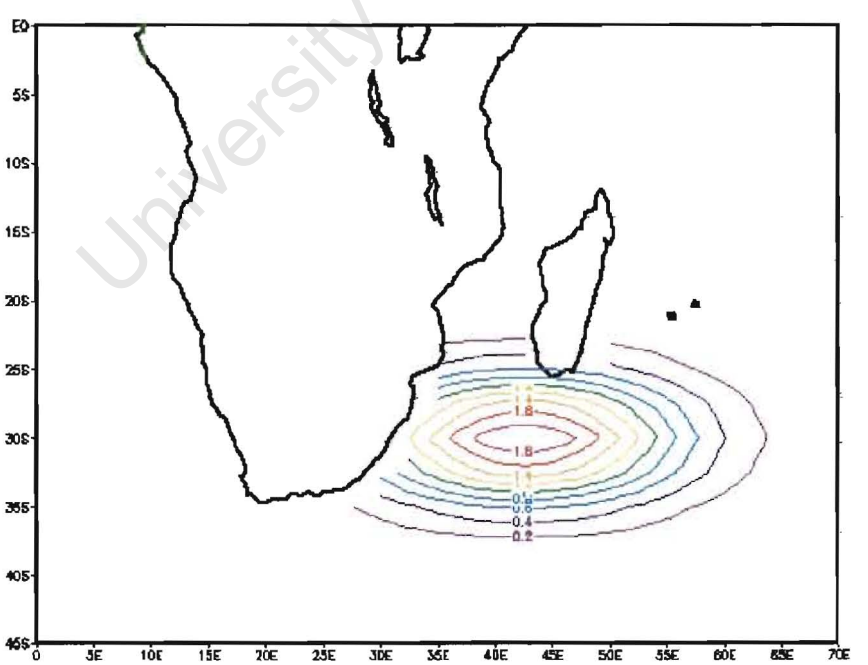

Fig 3.2 SST anomaly pattern forcing imposed on SST climatology.

Chapter 4

Observations of Dipole SST Patterns in the South Indian Ocean.

4.1 Introduction

Based on an EOF analysis of the GISST 2.3b SST data set, and composites of associated NCEP re-analyses of sea level pressure winds and latent heat fluxes, Behera and Yamagata (2001) suggested that dipole modes that are seasonally phase locked to the austral summer (January to March) occur in the subtropical South Indian Ocean. To measure them, they constructed an index time series, referred to as the subtropical dipole index (SDI). The SDI was obtained from the SST anomaly difference between the western (55-65°E, 37-27°S) and eastern (90-100°E, 28-18°S) subtropical South Indian Ocean (Behera and Yamagata, 2001). The boxes used to define the index appear to have been derived by these authors from the EOF analysis. Six strong positive events (i.e. warm southwest Indian pole, cold southeast Indian pole) (1967/8, 1973/4, 1975/6, 1980/1, 1981/2, 1992/3) were identified by Behera and Yamagata (2001) according to the index.

Behera and Yamagata (2001) did not identify specific negative events, in which the southwest Indian Ocean pole is cold and the southeast Indian Ocean pole is warm. Therefore, to identify negative events, the index was reproduced in this thesis (**Fig 4.1**) from the same dataset used by these authors, to identify negative events. The index runs from January 1955 to October 1999 and index values of about +1 and −1 are used to define positive and negative events respectively. Therefore, the index (**Fig 4.1**) suggests that 1957/8, 1958/9, 1963/4, 1964/5, 1966/7, 1969/70, 1977/8, 1983/4 and 1997/8 may be considered as negative events. In addition to the six positive events identified by Behera and Yamagata (2001), three more positive events (1955/6, 1960/1 and 1998/9) are identified. From the SDI, the 1980/1 and 1997/8 events are identified to be the most recent strong cases among the positive and negative events with associated wet and dry conditions over southern Africa respectively. The events of 1963/4 and 1997/8 are

identified to be the strongest among the negative and positive events respectively. It is noted that several of the events occurred during El Niño or La Niña years. In particular the 1997/8 dipole mode event, which is a negative event and associated with dry conditions over southern Africa, coincided with a strong El Niño event (Latif *et al.*, 1999; Grotzner *et al.*, 2000; Anyamba *et al.*, 2001) while the strong positive 1980/1 event is a pure dipole mode event i.e. there was no El Niño or La Niña during this event. It is also noted that during the last fifty years, most of the negative dipole mode events occurred in the late 1950s and 60s while the positive events tended to mainly occur in the late 1960s to early 80s period. Whether this reflects the influence of long-term climate change or decadal to multidecadal modes in the Indian Ocean (e.g. Allan et al., 1995; Reason and Rouault, 2002) is unknown. This question is not investigated in this thesis since the primary objective is to assess the atmospheric response over southern Africa to these SST dipole patterns. There is need to mention here that a positive SDI does not necessarily mean that the southwestern pole shows warm anomalies and the southeastern pole cold anomalies relative to climatology. The SDI will be positive if positive SST anomalies exist over both poles but that for the southwest pole is greater than that for the southeast pole. A similar situation applies to the negative values of the SDI. Therefore, not all the identified events show dipole patterns described in Behera and Yamagata (2001).

In this chapter, individual positive and negative events are investigated, in reference to the dipole composite in Behera and Yamagata (2001), by means of GISST2.3b SST and other variables (wind, latent heat flux and sea level pressure) available from NCEP. This analysis is done in order to assess the intra-composite variations of these events and the robustness of the composite pattern derived by Behera and Yamagata (2001). **Table 4.1** lists the SST anomalies and SDI values for each event for each month and will be referred to from time to time. Also presented in this chapter is the comparison of SST anomaly patterns of the two recent strong opposite events (1980/1 and 1997/8) that are used to force MM5, together with their respective composite mean anomalies. In addition to the two discussions mentioned above, this chapter also discusses apparent flaws in the Behera and Yamagata (2001) results.

4.2 Intra-Composite Variations of the Positive Dipole

Behera and Yamagata (2001) did not show the evolution of each of the six positive events they identified but only the composite of six events (1967/8, 1973/4, 1975/6, 1980/1, 1981/2 and 1992/3). Therefore this section discusses each individual event. The 1980/1 event is discussed first in the next section because it is one of the modelled events in this thesis and other events are discussed in the section that follows. As mentioned above, not all the positive phase events individually by the SDI show the dipole pattern described in Behera and Yamagata (2001). Of the nine positive events suggested by the SDI (Table 4.1), only during seven events (1968, 1974, 1976, 1981, 1982, 1993 and 1999) is the dipole pattern clear and these events are used in the composite anomalies (**Fig 4.2**) for the variables mentioned above.

The first panel in **Fig 4.2** indicate that during the positive phase from January to March a warm pole evolves south of Madagascar and a cool pole west of Australia. Anomalies at the centre of the cold pole vary from about –0.8°C in January to about –0.9°C in February and March. Warm pole anomalies vary from about 0.8°C in January to about 1.0°C in February and March. A weak anticyclonic anomaly (second panel **Fig 4.2**) forms east of Madagascar in January, strengthens in February and then shifts southeastward in March. As a result, predominately southeasterly winds over the subtropical south Indian Ocean are strengthened in the east and weakened in the west (third panel **Fig 4.2**). Increased (reduced) latent heat losses (fourth panel **Fig 4.2**) characterise areas of strengthened (weakened) winds and cool (warm) SST anomalies.

4.2.1 Positive Dipole Mode (1980/1)

The subtropical South Indian Ocean positive dipole events are characterized by positive SST anomalies in the western South Indian Ocean, south of the island of Madagascar, and negative SST anomalies in the eastern South Indian Ocean (Behera and Yamagata, 2001). From the SDI in Behera and Yamagata (2001) and **Fig 4.1**, 1980/1 is identified to

be the most recent strong positive phase event of the southern subtropical Indian Ocean SST dipole modes with SDI values of 1.5 in January and February and 1.3 in March (**Table 4.1**). It also had a robust and significant rainfall impact over large areas of southern Africa and hence it is one of the events modelled in this thesis. In addition to comparing the 1981 event with the composite, this section also focuses on the evolution of this event.

Behera and Yamagata (2001) reported that the dipole peaks in February and begins to die down by May. Changes in SST anomaly magnitudes over the cold pole from January to March for both 1981 and composite (first panel **Figs 4.3** and **4.2** respectively) indicate the above trend as the dipole evolves in positive phase mode. The dying down of this particular event starts in March and continues in April (not shown). Also observed from **Fig 4.3,** are month-to-month changes in the position of warmest and coldest centres of the poles that constitute the dipole. Behera and Yamagata (2001) however, do not explain these changes. They have attributed changes in the dipole's robustness during the austral summer season to atmospheric forcing, particularly focusing on changes in strength of midlatitude westerlies and lower latitude easterlies over the South Indian Ocean, which may in turn be associated with the strength and position of the subtropical anticyclone. Behera and Yamagata (2001) have suggested that warming over the warm pole is due to a decrease in latent heat loss. This decrease in latent heat loss results from reduced evaporation associated with the weakening of midlatitude westerlies on the poleward side of the subtropical anticyclone. The cold pole results from strengthening of the southeasterlies in the Southeast Indian Ocean. An examination of SST anomaly magnitude for 1981 (uppermost panel **Fig 4.3**) and the composite (**Fig 4.2**), indicate that anomalies are larger over the warm pole for all months of the austral summer season for 1981 compared to the composite. The magnitude over the warm pole is about 2.0°C in January and decreases to about 1.2°C in February and March for 1981. In the composite, January SST anomalies over the warm pole are about 0.8°C and about 1.0°C in February and March.

There are observed shifts in the sea level pressure and low level winds during the austral summer of 1981 (second and third panel **Fig 4.3**). The northwesterly anomaly in winds east of South Africa during January is consistent with warming since it implies a weakening of prevailing southeasterlies and less evaporation and upper ocean mixing. These wind anomalies shift eastward as the season progresses coinciding with the shift of the warm pole (see below). Behera and Yamagata (2001) suggested that the midlatitude westerlies weaken in February and this may lead to further warming of the warm pole. This may be as a result of reduced equatorward Ekman transport of cool midlatitude water masses. An examination of the February winds during 1981 indicates weakening of the midlatitude westerlies over the southern part of the warm pole and weaker easterlies over the northern part. The cyclonic feature implies relative cooling there via Ekman suction. During March the low level cyclonic wind anomaly shifts northeast and the anomaly over the midlatitude parts of the warm pole is a weak westerly. Though the above results differ somewhat from Behara and Yamagata (2001), they do suggest that winds play a major role in the evolution of the dipole. What is not evident from the 1981 austral summer sea level pressure anomalies however is the influence on the evolution of the low level winds and SST patterns of the subtropical high highlighted by Behera and Yamagata (2001).

The eastward shifting of the centre of the warm pole as the season progresses from January to March, is observed in both the 1980/1 (first panel **Fig 4.3**) event and the composite (first panel **Fig 4.2**) anomalies. The marked time of shifting is, however different in the two cases. In 1981, the shift occurs between January (50°E) and February (70°E) and the centre remains at about the same position in March. This may be related to eastward shift of the low level midlatitude westerly wind anomalies mentioned above. For the composite, the shift of the warm pole is apparent between February (50°E) and March (70°E). The difference in anomalous SLP and winds between 1981 (second and third panel **Fig 4.3**) and the composite reflects this difference in the shift of the warm pole. This is accompanied by the decrease in SST along the southeastern coast of Southern Africa in March in both cases.

The spatial size of the warm pole in all the three months of the season is large in 1981 compared to the composite (first panel **Figs 4.3** and **4.2**). The opposite may be true for the cold pole except for February where they appear to be about the same size. In January, the warm pole extends from the eastern coast of South Africa to about 95°E in 1981 and to about 88°E in the composite. The latitudinal extent is about the same in both cases, from about 20°S to 45°S. The shape of the warm pole is more regular (elliptical) in the composite than in 1981. The longitudinal extent is decreased to about 88°E and 80°E in February for 1981 and the composite respectively but meridionally, the warm pole extends farther north to about 15°S in both cases. In March, the latitudinal extent of the warm pole in the composite reduces and returns to that similar to the January one. The longitudinal extent however, increases to about 95°E, farther than the January extent. For 1981, both the latitudinal and longitudinal extent of the warm pole increases further north (7°S) and east (108°E) respectively in March.

Over the cold pole, a negative anomaly value of about –0.8°C is observed in January in the composite anomalies. In February and March, the anomaly is about –0.9°C and the most negative value during the season. The magnitude of the SST anomalies over the cold pole is about –0.8°C in January, peaks in February to about –1.2°C and decrease to about –0.8°C in March during the 1980/1 event. The trend in the SST evolution during 1981 over the cold pole is consistent, unlike over the warm pole, with that described in Behera and Yamagata (2001). Behera and Yamagata (2001) have associated the variations in SST anomalies over the cold pole with the Australian west coast trough, Indian Ocean subtropical high and the pressure gradient that is generated between them. At the beginning of the 1981 season (January) and the following month (February), an enhanced west coast trough is apparent over western Australia (**Fig 4.3**) and there is an anticyclonic feature over central to eastern Indian Ocean and the wind anomalies are predominantly southeasterlies over the cold pole in both months. These anticyclonic wind anomalies are however further away from coast in January compared to February. In March, an anticyclonic anomaly establishes over western Australia. Behera and Yamagata (2001) suggested that in autumn, high pressure begins to establish over the Australian continent and the ITCZ moves north over the Indian Ocean, with the

associated wind changes leading to the decay of the dipole event. Examination of the winds during March indicates the replacement of the southeasterly anomaly over the cold pole by a weak northerly anomaly. This reflects a weakening of the mean March winds here and hence may lead to warming of the cold pole via reduced evaporation (negative latent heat flux anomalies or reduced evaporation, fourth panel **Fig 4.3**) and less upper ocean mixing. A weaker cold pole is located to the west of Australia in January 1981 whereas in the composite, where it is stronger and situated more to the northwest. This is reflected in the weakening of the southeasterlies over this region in March 1981.

4.2.2 Other Positive Events

To consider the robustness of the composite of the positive phase, **Fig 4.4** plots the SST anomaly evolution from the GISST dataset of each of the other positive events. **Fig 4.5** plots the sea level pressure anomalies, **Fig 4.6** plots surface wind anomalies and **Fig 4.7** latent heat flux anomalies using NCEP dataset. Some of the dipole patterns observed in **Figs 4.4** do not obviously display the Behera and Yamagata (2001) subtropical dipole orientation. Also apparent from this figure are the variations in the extent and strength of the cold and warm poles during a particular month of the events. During most of the events, there seems to be an alternating pattern in the spatial size of the cold and warm pole. When the warm pole is large during a particular event, the cold is smaller and vice versa. The SST anomalies for the western and eastern parts of the subtropical south Indian Ocean in **Table 4.1** might not reflect the anomalies of warmest or coldest centres observed over the poles; they just indicate that one part is warmer or cooler than the other. This subsection discusses these variations in these events in comparison to the composite.

From the SDI (**Fig 4.1**), the 1968 event appears to be the strongest. The SDI values (**Table 4.1**) for each month show an increasing pattern during this event. During the 1968 event, the dipole pattern gets clearer as it evolves, with the warm pole becoming stronger (**Fig 4.4**). The magnitude of the SST anomalies over the warm pole range from about 0-

0.4°C in January to about 1.2°C in March. The SST anomalies over the cold pole appear to be constant at about -2.0°C throughout the season. Examination of SST anomalies of the western part of the southern subtropical Indian Ocean (region of warm pole) in **Table 4.1** however, shows weaker positive anomalies in January and negative anomalies in February and March. SST anomalies over the cold pole are large compared to the composite anomalies (**Fig 4.2**) in all the three months (January, February and March). This is a good example of a case where a significantly cooler southeast Indian pole leads to a relatively large SDI value even though the southwest Indian pole does not always show large positive anomalies. The location of the warm pole is however, further to the south than in the composite warm pole. The spatial extent of the cold pole is larger than that of the warm pole throughout the season. Increased subtropical easterlies (**Fig 4.6**), particularly in January and March, accompanied by increased latent heat losses (**Fig 4.7**) are observed over the central South Indian Ocean, between Madagascar and Australia. The increase in the easterlies in this region may be due to a strong pressure gradient generated between the anticyclonic and cyclonic anomalies located (**Fig 4.5**) to the southwest and northeast of Madagascar respectively in March. Increased latent heat flux losses, due to strengthened southerly flow of the subtropical easterlies on the eastern parts of South Indian Ocean coincide with the cold pole of the SST anomalies.

Table 4.1 indicates that the 1974 event (**Fig 4.4**) is one of the events with large SDI values throughout the season. Larger SST anomalies are observed over the warm pole during the 1974 dipole event (**Fig 4.4**) than in the composite (upper panel **Fig 4.2**). In the composite, the weakest anomaly is about 0.8°C (January) and the strongest is about 1.0°C (March) while during the 1974 event anomalies of about 1.2°C are observed in all three months of the season. The location of the warm and the cold poles appears to be the same as in the composite. The warm pole extends further westward to the eastern coast of South Africa. This may enhance its impact on summer rainfall over the subcontinent (Reason, 2001). Cold pole anomalies are stronger in this event than in the composite. The anomalies are about –1.2C in January, -2.0C in February and about –1.8C in March. A strengthened southeasterly flow is observed over the eastern region of the southern subtropical Indian Ocean, west of Australia, (**Fig 4.6**) throughout the season during this

event. An anticyclonic surface pressure anomaly to the southeast of Madagascar (**Fig 4.5**) strengthens in February producing anomalous southeasterlies west of Australia. These, increased southeasterlies are accompanied by increased latent heat losses over this region (**Fig 4.7**) leading to local cooling of SST.

The 1976 event is characterised by weak warm SST anomalies over the warm pole and strong cold SST anomalies over the cold pole in January and the opposite is observed in February and March (**Fig 4.4**). The January SST anomaly over the warm pole during the event is about 0.4°C, which is weaker than 0.8°C observed in the composite. In February and March, anomalies of about 1.2°C and 1.6°C are observed over the warm pole and are large compared to those in the composite. Cold anomalies of about -0.4°C, -1.2°C and -1.6°C are observed in January, February and March in the southeast Indian Ocean. **Table 4.1** however indicates positive anomalies over both the southwest and southeast regions in February and March. This situation arises because during 1976 the cold pole is displaced from the box used to calculate the SDI. The location of the warm pole is similar to the composite in February and March. During this event, weakened easterly winds (**Fig 4.6**) are observed to the southeast of Madagascar in February and March. This may be due to anticyclonic pressure anomalies to the east of the island (**Fig 4.5**). Reduced latent heat losses (**Fig 4.7**) and warm SST anomalies are observed over this region of weakened winds in the southwest Indian Ocean. This may suggest that weaker subtropical easterlies generate warm SST anomalies via reduced latent heat losses (i.e. reduced evaporation).

Colder SSTs than in the composite are observed over the cold pole during the 1982 event. A maximum magnitude of about 1.2°C compared to 1.0°C in the composite is observed in February during the event (**Fig 4.4**). Maximum warm pole SST anomalies of about 1.2°C and 1°C are observed in March during the event and in the composite respectively. During this event, the warm pole is observed to be located further east into the central south Indian Ocean compared to the composite and this may result in reduced rainfall over the subcontinent (e.g. Reason 2002). Over the central eastern South Indian Ocean, weak easterlies are observed in January (**Fig 4.6**) while strong easterlies are observed in February and March. Cyclonic sea level pressure anomalies (**Fig 4.5**)

oriented in a southeast-northwest direction stretching from southwest Australia to Madagascar may explain the observed weakening of the southeasterlies in January. Reduced latent heat fluxes (**Fig 4.7**) over the same area and similar orientation as the above wind anomalies are observed during this event, indicating links between winds and local evaporation. The strengthening of the easterlies in February and March are observed mainly over the northern and northeastern edges of the southern Indian Ocean subtropical anticyclone respectively. These wind anomalies are accompanied by increased latent heat losses and hence strong negative SSTs anomalies over these regions in February and March.

For the 1993 event, warmer SST anomalies than in the composite are observed over the warm pole while SST anomalies over the cold pole are about the same in magnitude as in the composite (**Fig 4.4**). However, the cold pole is spatially small during the 1993 event compared to the composite. Throughout the season, warm pole anomalies range from about 1.2°C to about 2.0°C during the 1993 event and from about 0.8°C to about 1.0°C in the composite (**Fig 4.2**). The centres of both poles appear to be further east during this event than in the composite. The dipole pattern is however not clear in March. A strong cyclonic sea level pressure anomaly is observed over the midlatitude South Indian Ocean in January (**Fig 4.5**) and shifts southeast in February and March. This leads to weakening of the predominantly southeasterly winds south of Madagascar (**Fig 4.6**), which in turn causes reduced evaporation there (**Fig 4.7**). Little evidence of the anticyclone anomaly noted in Behera and Yamagata (2001) is present during this event.

During the 1999 event, warmer SST anomalies than in the composite (**Fig 4.2**) are observed displaced southwards in the South Indian Ocean (**Fig 4.4**) and then constitute the warm pole during this event. Anomalies of about 2.0°C are observed over the warm pole in January through to March. Over the cold pole, anomalies of 1.2°C are observed also throughout the season. The location of the high pressure anomaly over the central South Indian Ocean in January (**Fig 4.5**) leads to increased southward Ekman transport of tropical waters south of Madagascar as well as enhanced southerly flow off the western coast of Australia, causing cooling there. The weaker westerlies in the midlatitude

weaken Ekman convergence and downwelling in the midlatitude and would force warmer SSTs there. In addition, the weaker midlatitude westerlies further, promote warming (**Fig 4.6**). In February, the high pressure anomaly shifts north to lie east of Madagascar (**Fig 4.5**), thereby weakening the southeasterly winds north of the 35°S (warm SST anomalies evolve southeast of Madagascar as a result) and strengthening the midlatitude westerlies further south (**Fig 4.6**). The high pressure anomalies are located further south in the South Indian Ocean in March and this results in strengthened southeasterly flow off the western coast of Australia in March. Stronger easterlies are also observed over the southern coast of Mozambique. Changes in the strength of the southeasterly wind during this event are reflected more in the latent heat fluxes (**Fig 4.7**) than in SSTs. This may be due to delayed response of the SSTs to changes in wind strength.

4.3 Intra-Composite Variations of the Negative Dipole

As pointed out above, nine negative phase South Indian subtropical dipole events are identified from the SDI (**Fig 4.1**). Variations observed in the positive phase events of the dipole modes in the South Indian Ocean are also observed in the negative phase. The location of the poles during some of the events is somewhat different from the Behera and Yamagata (2001) negative dipole pattern and do not necessarily align with poles as defined by these authors. Among the negative events identified from the SDI (**Fig 4.1**), the 1997/8 event is the most recent strongest event and is the negative event used to force MM5 (**Chapter 5**). The purpose of this section is to discuss this event, in detail, and other events in comparison with the composite (**Fig 4.8**).

In general the identified negative events do not show as clear an expression of the dipole as the positive events.. The composite plots of SST anomalies (**Fig 4.8** first panel) indicate a dipole pattern with the cold pole over the southwest Indian Ocean and warm pole in the southeast. SST anomalies of about –0.7°C, -0.9°C and –0.8°C are observed over the cold pole in January, February and March. SST anomalies over the warm pole are weaker in the negative phase than in the positive. Anomalies of about 0.5°C are

observed over the warm pole in January and February and about 0.4°C in March. Inspection of the sea level pressure (**Fig 4.8**) indicates that low (high) anomalies are generated over the western (eastern) parts of the subtropical South Indian Ocean in January and February. In March, the composite shows mainly low pressure anomalies over the south Indian Ocean. Southeasterly winds are weakened (strengthened) in the east (west) particularly in January and February. Reduced latent heat fluxes are observed in the western parts of the subtropical south Indian Ocean.

4.3.1 Negative Dipole Mode (1997/8)

Cool SSTs to the west and warm SSTs in the east of the South Indian Ocean characterize the negative phase of the subtropical SST dipole (Behera and Yamagata, 2001). As seen in Fig 4.9, the SST anomaly dipole pattern is not as clear during the 1997/8 event as in the composite (**Fig 4.8**) despite being a strong event (**Fig 4.1**) and having large SDI values of about -1.3, -1.1 and –0.9 in January, February and March respectively (**Table 4.1**). Therefore the dipole discussed here does not really coincide in orientation with the opposite of the positive phase as suggested by Behera and Yamagata (2001). However, this event coincides with one of the strongest El Nino events on record (Chambers *et al.*, 1999; Grotzner *et al.*, 2000) characterized by numerous climate anomalies all over the world (Latif *et al.*, 1999). Anomalously high sea surface temperatures in the Indian Ocean are observed during this period (Chambers *et al.*, 1999; Yu and Rienecker, 2000) and may explain why the dipole pattern in **Fig 4.9** (upper panel) is less well established. However, cool SST anomalies of about –0.4°C are seen to the southeast of Madagascar in January during the 1998 event (**Fig 4.9**). Strongest SST anomalies of about –1.2°C are seen to the southwest of Madagascar in February and appear to fall to about -0.4°C in March. SST anomalies over the cold pole are weaker during this event than in the composite (**Fig 4.8**) in January and March. Stronger anomalies are observed over the warm pole during the event than in the composite. In January and February, anomalies of about 1.8°C are observed over the warm pole and anomalies of about 2.0°C in March.

The pattern of SST anomaly variations over both poles is the same during the 1998 event (**Fig 4.9**) and in the composite.

The cold pole discussed in the above is spatially larger in March than in January and February (**Fig 4.8**). A region of cold SST anomalies at about 70°E, 30°S (i.e southeast of the western pole defined in Behera and Yamagata (2001)) constitute the cold pole in January. Colder anomalies in the Agulhas current region south of South Africa appear to extend northeastward up to South Madagascar in February. These anomalies and those observed in January constitute the cold pole in February. These two regions of cold SST anomalies appear to merge in March and produce the spatially large cold pole in this month. The negative phase of the subtropical dipole was not discussed by Behera and Yamagata (2001) and its forcing is not well understood. Behera and Yamagata (2001) however mention that the situation is opposite to that of the positive phase. In January during the 1997/8 dipole event, positive SST anomalies of about 2.0°C are observed to the east of Madagascar. This appears to be an extension of ENSO-induced tropical Indian Ocean warming north of Madagascar during the mature phase (Reason 2001). As already mentioned, some of the positive and negative events fall within El Niño or La Niña years; however it is not the intention of this thesis to try and establish what role ENSO may play in driving the anomalous conditions over the Indian Ocean. The extension of the warming towards the midlatitude southeast Indian Ocean becomes a large warm anomaly of about 1.8°C west of Australia in February and forms the warm pole. The anomalies over this pole increase to about 2.0°C in March. The high pressure anomalies are observed further southeast of Madagascar in January during the event (**Fig 4.9** second panel). The cool anomaly southeast of Madagascar in January seems to arise from the strong southeasterly winds seen in the central subtropical South Indian Ocean in this month. These imply increased evaporation and upper ocean mixing lead to cooling. In February, the strong southeasterlies shift towards the Southern African coast leading to cooling in the greater Agulhas current region. In March the stronger southeasterlies return to the central south Indian Ocean and the cool anomaly shifts eastward again. The cold pole seems to arise mainly during January and February from the weaker southeasterly seen in these months over the southeast Indian Ocean near Australia.

4.3.2 Other Negative Events

Though the composite of the negative phase of the subtropical South Indian Ocean dipole show a clear SST anomaly dipole pattern, a number of variations are observed among events. The obvious variation, among others, is in the orientation of the dipole. This section discusses variations among the rest of the negative events identified from the SDI (**Fig 4.1**).

The cold and warm regions, which make up the dipole during the 1958 event are orientated in the north-south direction (**Fig 4.10**) with the cold region in the south and the warm in the north. This may reflect the fact that austral summer 1958 corresponds to the mature phase of an ENSO event. The January plots of this event show a more obvious Northeast-Southwest dipole pattern. In January, cold anomalies of about –1.2°C are observed between the 70°E and 80°E longitude and near 40°S in the South Indian Ocean while warm anomalies of about 0.8°C are observed west of Australia; these areas make up the cold and warm poles respectively. Anomalies over both poles strengthen in February but shift so the orientation is more north-south. SST anomalies over the warm pole are about 1.2°C and about –1.8°C over the cold pole. In March, these anomalies weaken to about 0.4°C and –1.2°C and assume an earlier Northeast-Southwest orientation. The anomalies over the cold pole are larger in magnitude in all three months of the season during the 1958 event than those in the composite (**Fig 4.8**). The anomalies during the event are also larger over the warm pole, except in March. The weakening of the southeasterly winds over the central subtropical South Indian Ocean (**Fig 4.12**), particularly in January and March, caused by a cyclonic sea level pressure anomaly (**Fig 4.11**) over the central South Indian Ocean lead to reduce latent heat fluxes (**Fig 4.13**) west of Australia. The strengthening of the SST anomalies over the cold and warm pole in February appear to be a response to wind changes observed in January. This may suggest that the SST response to wind changes is delayed.

During the 1959 dipole event, cold anomalies are observed over the western subtropical South Indian Ocean and warm anomalies over the eastern (**Fig 4.10**). In January, cold

anomalies of -0.4°C are observed to the west of 60°E longitude and warm anomalies of about 0.8°C to the east. As the season progresses, the region of cold SST anomalies extend eastward to about 80°E in March. The SST anomalies over the cold pole also increase in magnitude. The anomalies over the warm pole do not appear to change throughout the season and are larger than in the composite. Negative sea level pressure anomalies over central the South Indian Ocean characterised this event throughout the season (**Fig 4.11**). In January high pressure anomalies in the midlatitude weaken the midlatitude westerly winds (**Fig 4.12**). A cyclonic anomaly southwest of Australia weakens the southerly flow off the southwest coast of Australia. This leads to decreased latent heat fluxes over this region and warmer SST. The weaker southeasterlies off Australia continue in February and March although the cyclonic pressure anomaly is less clear in February. Then weaker winds lead to warmer SST in the southeast Indian Ocean (**Fig 4.13**).

The1964 dipole event has a strong cold pole compared to the composite and is the strongest of the identified negative events (**Fig 4.1**) with SDI values of about –1.7, -1.4 and –1.3 in January, February and March (**Table 4.1**). SST anomalies of about -2.0°C are observed over the cold pole during the season (**Fig 4.10**). . By comparison, the anomalies over the cold pole in the composite are about –0.7°C in January, -0.9°C in February and about –0.8°C in March. However, the warm pole anomalies weaker during this event, except in March, than in the composite. Anticyclonic and cyclonic SLP anomalies (**Fig 4.11**) to the southeast and east of Madagascar respectively in January strengthen the southeasterly winds in this region as well as the midlatitude westerlies in the southwest Indian Ocean (**Fig 4.12**). These strengthened winds increase the evaporation east of Madagascar and in the midlatitude, indicated by positive latent heat flux anomalies (**Fig 4.13**). The high pressure anomaly west of Australia (**Fig 4.11**) weaken the southeasterly winds in the southeastern Indian Ocean in January (**Fig 4.12**). These weaker winds reduce the evaporation over this region leading to warm SST. The warm SST anomalies weaken in February and March consistent with the disorganised and weak wind anomalies in the two months respectively.

A strong cold and weak warm pole characterise the 1965 dipole event. **Table 4.1** indicates negative anomalies over the southwest and southeast subtropical Indian Ocean and **Fig 4.10** indicates that the orientation is more east-west than northeast-southwest. Cold SST anomalies of about -2.0°C are observed at the centre of the cold pole to the southeast of Madagascar in January and February (**Fig 4.10**). In March, anomalies over the cold pole weaken to about –1.8°C and shift northewards. These anomalies are generally large compared to those in the composite whose values are about -0.5°C in January and February and about –0.4°C in March. Apart from being weak, the warm pole is also spatially small compared to the warm pole of the composite. Warm pole SST anomalies of about 0.4°C are observed in January and March and less than that in February. Strong anticyclonic SLP anomalies (**Fig 4.11**) in the southeast Indian Ocean during January and March strengthen the easterly winds (**Fig 4.12**), south of Madagascar, in January and March. Increased latent heat flux (**Fig 4.13**) are observed over the south central Indian Ocean in January and also near to Madagascar in March. In February, large parts of the southern Indian Ocean are characterised by negative sea level pressure anomalies. These low pressure anomalies are accompanied by weakened easterly winds and reduced evaporation. SST anomalies over the cold pole are slightly weaker in February than in January but weaken further in March.

A north-south pattern of warm and cold SST anomalies characterise the 1967 event (**Fig 4.10**). Regions of cold SST anomalies extend from the southeastern Atlantic Ocean right across the southern Indian Ocean throughout the event. Anomalies of about –1.6°C are observed over the cold pole in January and March and about –2.0°C in February. Regions of warm SST anomalies extend from Madagascar to the western coast of Australia with maxima of about 0.8°C. Low pressure anomalies in the midlatitudes South Indian Ocean (**Fig 4.11**) weaken the subtropical southeasterlies and strengthens the midlatitude westerlies in January and February (**Fig 4.12**). Reduced (enhanced) latent heat fluxes (**Fig 4.13**) over these areas of weakened (strengthened) winds are observed in January and February leading to the subtropical warm (midlatitude cool) SST anomalies in the southwest Indian Ocean. The weak warm anomalies over the southeast Indian Ocean

appear to be related to the weaker southeasterlies (**Fig 4.12**) in January and lesser extent February and reduced evaporation (**Fig 4.13**)

The 1970 event is more northwest-southeast in January and March but more meridional in February (**Fig 4.10**). In January, SST anomalies of about –1.8°C are observed over the cold pole. These anomalies weaken in February to about –0.4°C and strengthen in March to about -2.0°C. Except for February these anomalies, except for in February, are large compared to those in the composite (**Fig 4.8**). Weaker anomalies over the warm pole are also observed in February. The January and March anomalies are about 0.8°C while the anomalies in February are about 0.4°C. The warming in the southeastern Indian Ocean that constitutes the warm pole appears to be an extension of warming further north. Weakening of the predominantly southeasterly winds over the southeastern Indian Ocean (**Fig 4.12**) related to cyclonic pressure anomalies (**Fig 4.11**) is observed during this event. This weakening is more pronounced in February and March. Reduced latent heat fluxes (**Fig 4.13**) related to the weaker southeasterly winds lead to SST warming in the southeast Indian Ocean.

The cold pole is observed to the southeast of Madagascar during the 1978 south Indian Ocean subtropical dipole (**Fig 4.10**). This pole is further south in February and March. The SST anomalies over the cold pole are about –1.2°C in January and February and about –0.8°C in March. The January and February cold pole anomalies are large compared to those in the composite (**Fig 4.8**). Warm SST anomalies are observed off the west coast of Australia in January and March and constitute the warm pole of this event. The SST anomalies over these regions are about 0.4°C and 1.2°C in January and March. In February, regions of warm SST anomalies are observed to the north of a region of cold anomalies extending from the midlatitude South West Indian Ocean, to the northwestern coast of Australia. Anomalies over this region are about 0.4°C. During this event warm anomalies are also observed offshore from the eastern coasts of Mozambique and South Africa. Warm anomalies close to these coasts are reported (e.g. Walker, 1990; Jury et al, 1993; Reason and Mulenga, 1999) to enhance austral summer rainfall over southern Africa. On the other hand, the negative phase of the South Indian Ocean may reduce

summer rainfall over the region (Behera and Yamagat, 2001; Reason, 2002). These features appear to counter the effect of each other. The presence of a cyclonic surface pressure anomaly east of Madagascar in January (**Fig 4.11**) weakens southeasterly winds on the equator-ward side while a midlatitude anticyclone further southwest of Australia strengthens these winds (**Fig 4.12**). An anticyclonic surface pressure anomaly in the southeast Indian Ocean near Madagascar enhances the southeasterlies flow towards the eastern coast of East Africa in February. In March, this anticyclonic anomaly moves south and low pressure anomalies are generated further east. As a result southerly to southeaterly anomalies occur east of Madagascar, which seem to enhance latent heat fluxes there via increased evaporation throughout the event but particularly in March (**Fig 4.13**). Cool SST anomalies are therefore observed over these regions.

A weak dipole pattern in January, while strengthened in February and then anomalous strong in March is observed during the 1984 event (**Fig 4.10**). SST anomalies of about –0.4°C are observed south of Madagascar in January. In February, the anomalies strengthen to about –1.2°C and weaken to about –0.4°C in March. The cold pole is spatially smaller in January than in February and March. The pattern of variation in the SST anomalies over the cold pole is similar to that of the composite (**Fig 4.8**). Warm SST anomalies of about 0.4C dominate central and eastern parts of the South Indian Ocean in January during this event. A strong warm pole is observed in February. Warm anomalies of about 2.0°C are observed over this pole and weaken to about 0.4°C in March. A cyclonic surface pressure anomaly east of Madagascar in January and February (**Fig 4.11**) strengthens the southeasterlies in the southwest Indian Ocean and weakens them in the central to eastern South Indian Ocean (**Fig 4.12**). Increased (decreased) latent heat fluxes (Fig 4.13) with cool (warm) SST anomalies are therefore found south (east) of Madagascar in March, an anticyclonic surface pressure anomaly is established east Madagascar, which leads to stronger (weaker) southeasterly winds east (south) of the islandsoutheasterlies on its northern and southern edges respectively. The associated changes in latent heat fluxes (**Fig 4.13**) southeast and the cool SST anomaly south of Madagascar shift to lie more to the east of the island in March. In the southeast Indian

Ocean, the strengthening of the warm pole in February seems to be linked to the decreased southeasterlies in the tropics and associated reduced evaporation.

4.4 Apparent Weaknesses in the Southern Subtropical Dipole Mode Analysis

The SST anomaly dipole pattern in the southern Indian Ocean defined in Behara and Yamagata (2001) via EOF analysis has its western and eastern poles at 55°-65°E, 37°-27°S and 90°-100°E, 28°-18°S respectively. The SDI index mentioned above (also reproduced in **Fig 4.1**) was obtained from the SST anomaly difference between the western and eastern pole using the GISST2.3b dataset. The anomalies used by these authors are obtained from the 1958-1998 climatology. It is from this index that Behera and Yamagata (2001) and identified six strong positive events. Extending the index back to 1955, this thesis ha identified nine positive and nine negative events (**Fig 4.1**). For their six positive events, Behera and Yamagata (2001) have computed a composite analysis and suggested circulation anomalies associated with their evolution. They however did not give much detail on the negative phase. Therefore this section presents a number of apparent weaknesses in Behera and Yamagata (2001) results.

Firstly, Behera and Yamagata (2001) have suggested that the situation during the negative phase is just the opposite of the positive. This suggestion is rather cryptic and may be flawed. For example wind anomalies, which they have suggested to play an important role during dipole modes in the Indian Ocean, may change both direction and magnitude. Over a particular pole, winds may increase or reduce in magnitude or change direction, increasing or reducing the SST anomalies there, during an opposite event via changes in evaporation, upper ocean mixing, Ekman pumping and Ekman drifts for example. As discussed in the previous sections, variations in the latent heat fluxes, which may be responding to variations in winds, may also occur.

Secondly, though composites may bring out certain features that are associated with a particular phenomenon, they also tend to leave out some features or patterns that are not

generic to the phenomenon but important to a specific event. Therefore use of composites must be used with caution especially when analysing phenomena that occur on interannual, but vary on, intra-seasonal scales. In selecting the location of the poles of the dipole, Behera and Yamagata (2001) have used EOFs. An examination of individual events (**Figs 4.4**) however, indicates that the location of the observed warm and cold poles varies substantially from event to event and from month to month within the season. A composite of the nine negative events identified in this thesis, brings out a dipole pattern opposite to the positive phase (**Fig 4.8**). However, an examination of individual events shows that none of them has a pattern all that similar to that in the composite.

Lastly, during some events the Behera and Yamagata (2001) defined poles of the dipole were both located in regions where the SST anomalies were entirely cold or warm, i.e., a clear contrast in sign of the SST anomaly between the southwest and southeast Indian Ocean did not exist. (Examples of this lack of clear dipole pattern are February and March of the 1964 event, **Table 4.1**). Picking out strong events from the index (**Fig 4.1**) must be done cautiously when a particular season is of interest. Though the index may indicate a strong event during a particular year, the season in which it peaks is important. For example, the index (**Fig 4.1**) indicates that 1956 and 1961 are strong positive phase events. However plots of SST anomalies of these events during austral summer (**Fig 4.14**) do not show the dipole pattern. In addition, SDI values in **Table 4.1** are negative for the 1956 positive event and weak for the 1961 event in January and February.

4.5 Conclusion

The investigation of the individual events of the composites of positive and negative phase of the subtropical south Indian Ocean dipole has revealed the existence of variations among events of a particular phase. The dipole is strong during some events and weak during other events. Differences in orientation of the dipole have been observed in this thesis, particularly in negative phase. Thus the robustness of the composites is

questionable. Generalising processes associated with the particular phase of this phenomena is from the composite may therefore be misleading.

Identifying strong dipole events using the index and by visualising the data may be more reliable than just using one of the two. Using the index alone may be more objective but some of the events that do not show dipole patterns during a particular season may be picked out as strong events. On the other hand, visualisation alone is subjective, hence picking out a strong event may be difficult.

Once strong events are identified, using the index and visualisation, they can be simulated using general circulation models (GCMs) or regional circulation models (RCMs). This simulations may done for the purpose of assessing the model's ability in reproducing features associated with the particular phase of the phenomena or for sensitivity studies of the atmosphere over a region to this SST anomaly pattern.

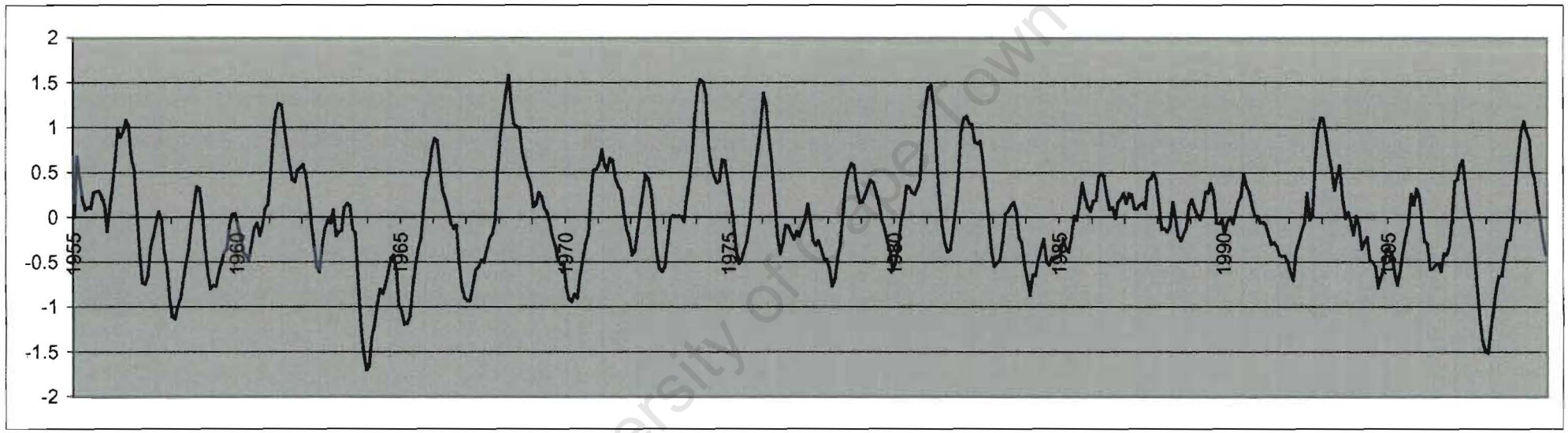

***Fig 4.1**. Time series of SDI from January 1955 to October 1999 (produced from GISST2.3b). The time series is smoothed by a five-month running mean and detrend.*

GISST2.3b DATA SET

YEARS	January			February			March			Phase
		SST ANOM. (°C)			SST ANOM. (°C)			SST ANOM. (°C)		
	SDI	EAST	WEST	SDI	EAST	WEST	SDI	EAST	WEST	
1956	-0.3	-0.6	0.0	0.0	-0.4	0.1	0.2	-1.0	-0.1	Positive
1958	-1.2	0.3	-0.9	-1.3	0.2	-0.4	-1.1	0.3	-0.6	Negative
1959	-0.4	0.6	-0.8	-0.7	0.3	-0.7	-0.9	0.4	-0.5	Negative
1961	0.4	-0.3	1.1	0.8	-0.7	0.6	1.1	-0.7	0.5	Positive
1964	-1.7	0.1	-0.3	-1.4	-0.3	-0.8	-1.3	-0.1	-1.5	Negative
1965	-1.1	-0.2	-1.2	-1.3	0.0	-1.2	-1.3	-0.2	-0.9	Negative
1967	-1.0	0.1	-0.8	-1.0	-0.1	-0.5	-0.8	0.1	-0.6	Negative
1968	0.8	-1.6	0.3	1.1	-1.5	-0.1	1.3	-1.3	-0.3	Positive
1970	-0.8	0.6	-1.0	-0.9	0.4	-0.6	-1.0	0.0	-0.9	Negative
1974	1.4	-1.2	0.4	1.5	-0.8	0.4	1.5	-0.7	0.2	Positive
1976	1.4	-0.8	1.3	1.2	0.2	0.6	0.9	0.5	0.0	Positive
1978	-0.6	0.5	-0.3	-0.7	0.4	-0.3	-0.7	0.1	0.0	Negative
1981	1.5	-0.7	0.9	1.5	-0.2	0.6	1.3	0.0	-0.2	Positive
1982	1.0	-1.4	0.6	1.2	-0.3	0.5	1.2	-0.4	0.3	Positive
1984	-0.6	0.5	-0.3	-0.8	1.1	-0.2	-0.6	-0.1	0.4	Negative
1993	1.2	0.6	0.2	1.1	0.0	0.2	0.8	-0.3	1.1	Positive
1998	-1.3	0.6	-0.3	-1.1	0.8	0.0	-0.9	0.8	0.0	Negative
1999	1.1	-0.5	1.1	1.2	-0.4	0.4	1.1	0.0	0.5	Positive

Table 4.1 *Listing the SST anomalies and SDI values for each event for each month.*

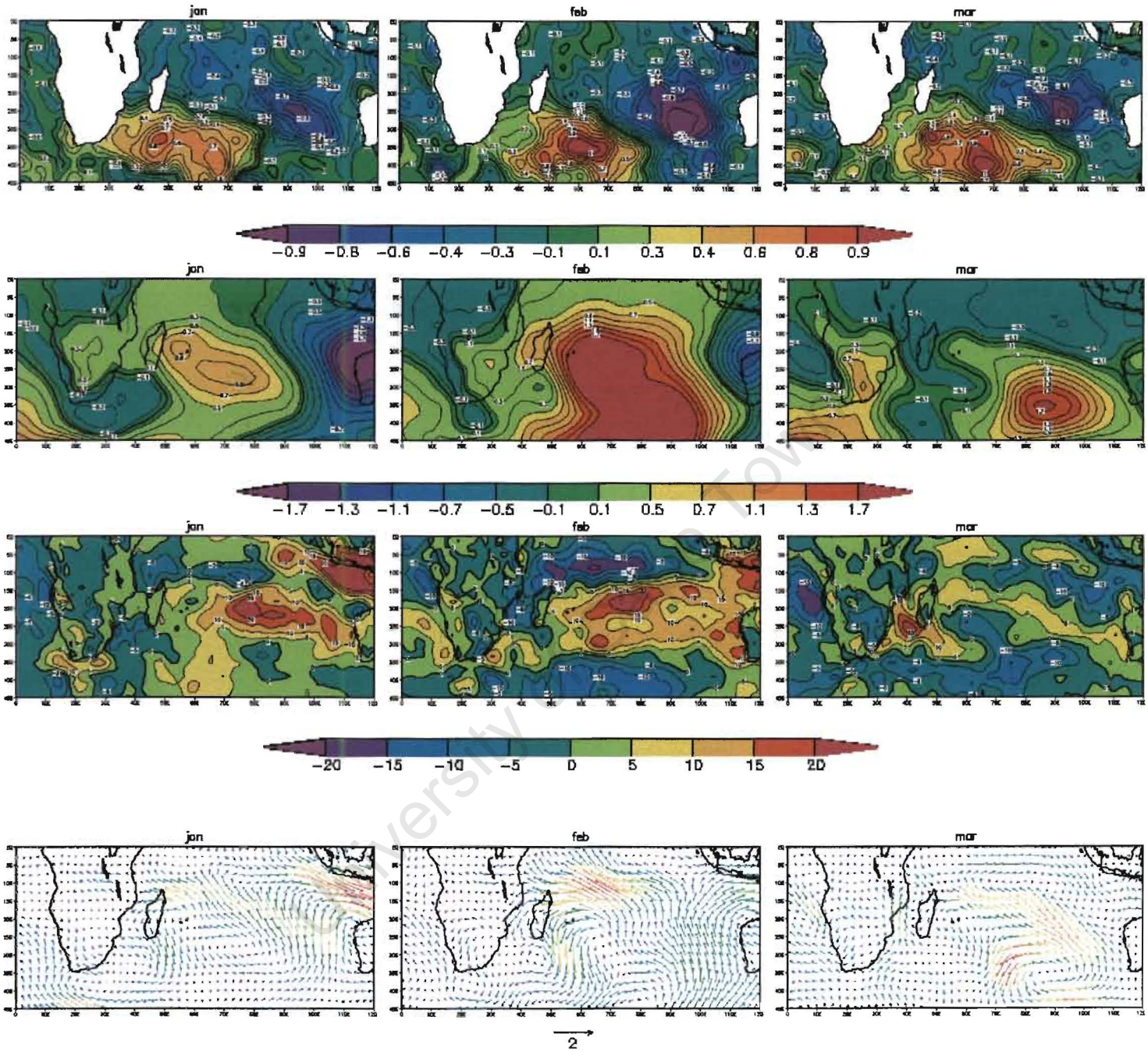

Fig 4.2 *Monthly composites of SST anomalies, SLP anomalies, Latent flux anomalies and surface wind anomalies in Jan, Feb and Mar for nine positive events during 1968, 1974, 1976, 1981, 1982, 1993 and 1999.*

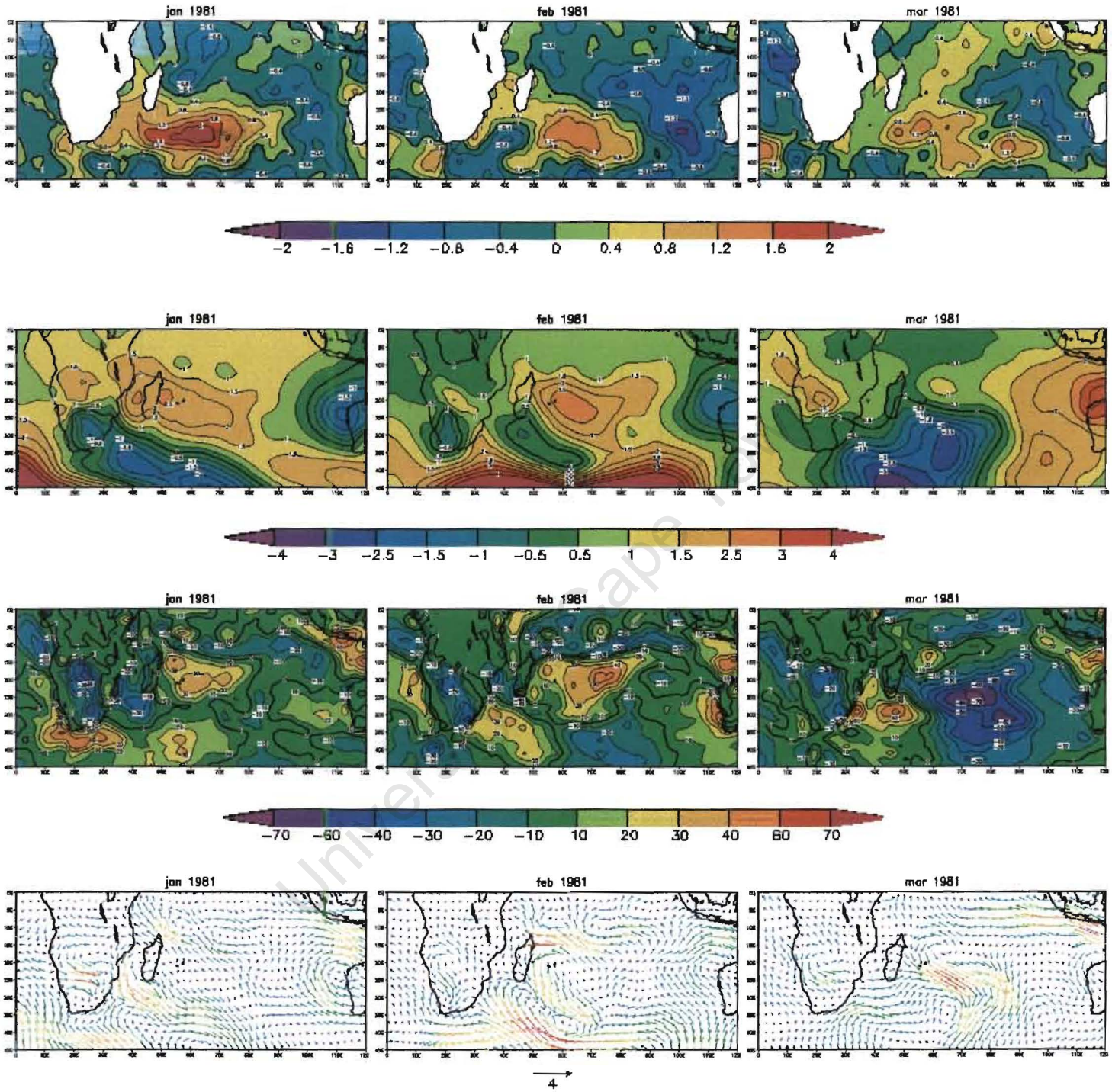

Fig 4.3. *Anomalies of SSTs (first panel), Sea level pressure (second panel), Latent heat flux (third panel) and Surface winds (fourth panel) for the* ***1981*** *positive phase event.*

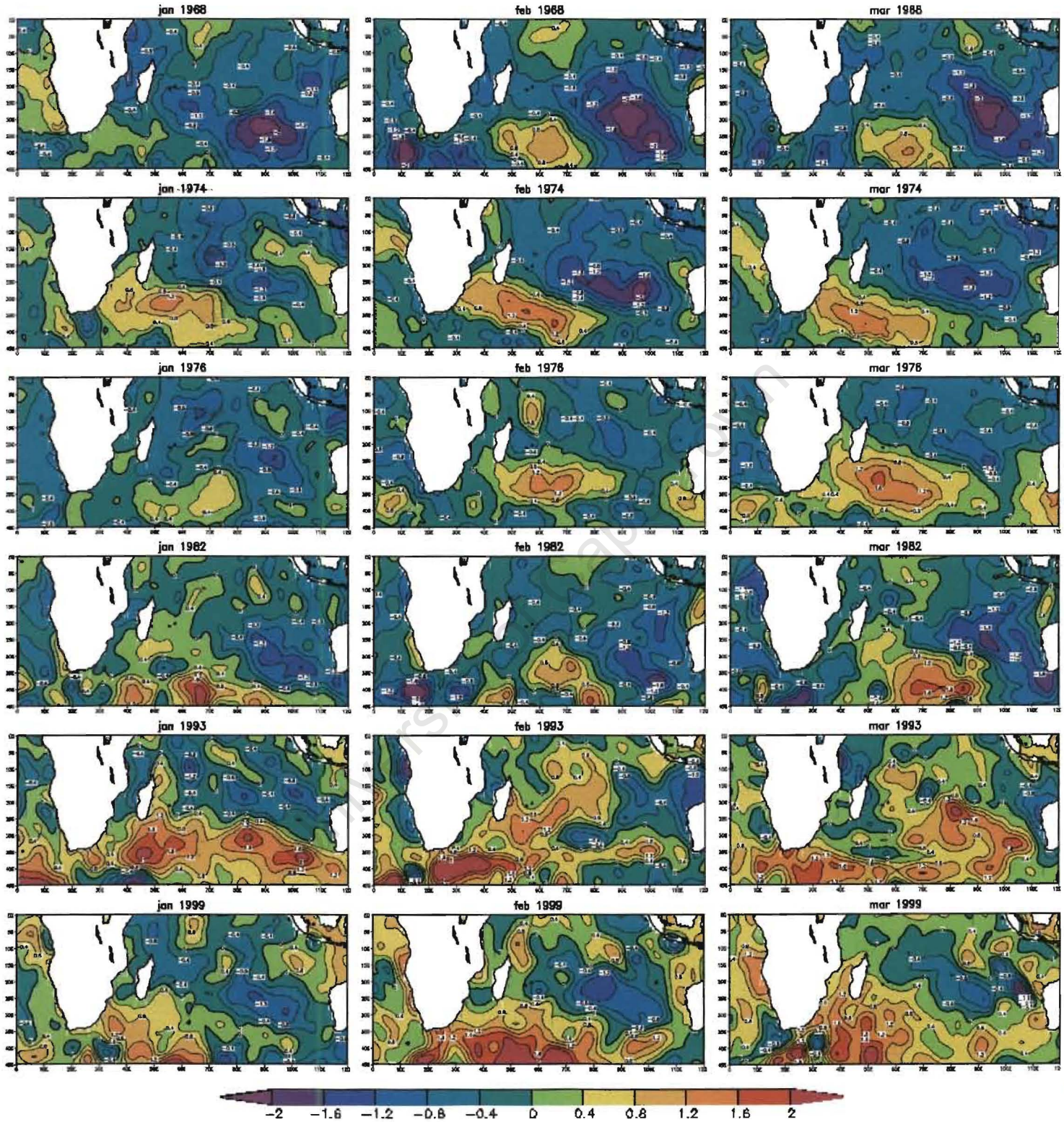

Fig 4.4. *Monthly sea surface temperature anomalies (GISST2.3b dataset) in Jan, Feb and Mar for six strong positive events during 1968, 1974, 1976, 1982, 1993 and 1999. A scale for the anomalies is shown. Contour interval is 0.4°C.*

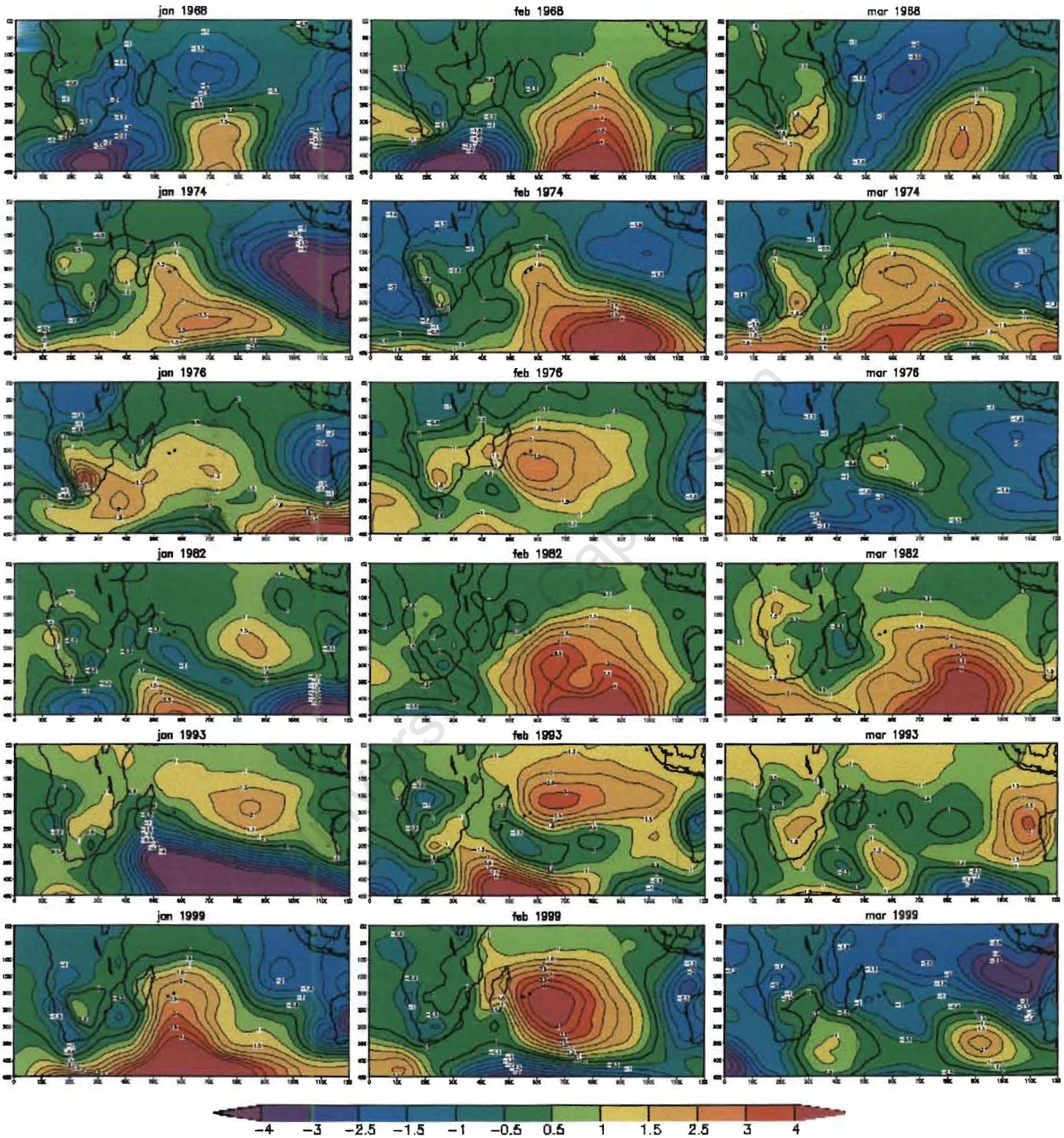

Fig 4.5 *Monthly sea level pressure anomalies in Jan, Feb and Mar for nine strong positive events during 1968, 1974, 1976, 1982, 1993 and 1999. A scale for the anomalies is shown.*

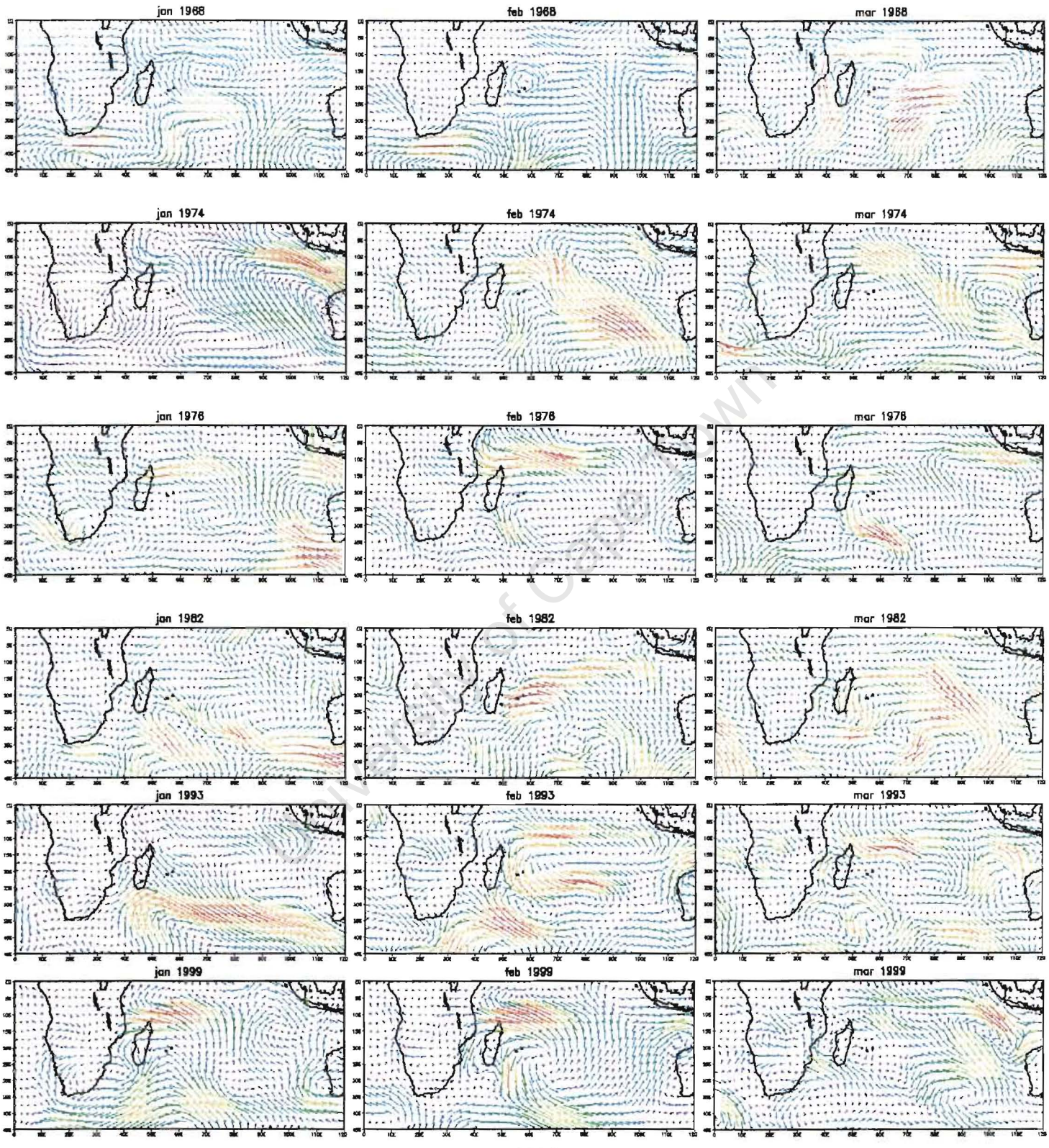

Fig 4.6 *Monthly surface wind anomalies in Jan, Feb and Mar for nine strong positive events during 1968, 1974, 1976, 1982, 1993 and 1999. A scale anomaly vector is shown.*

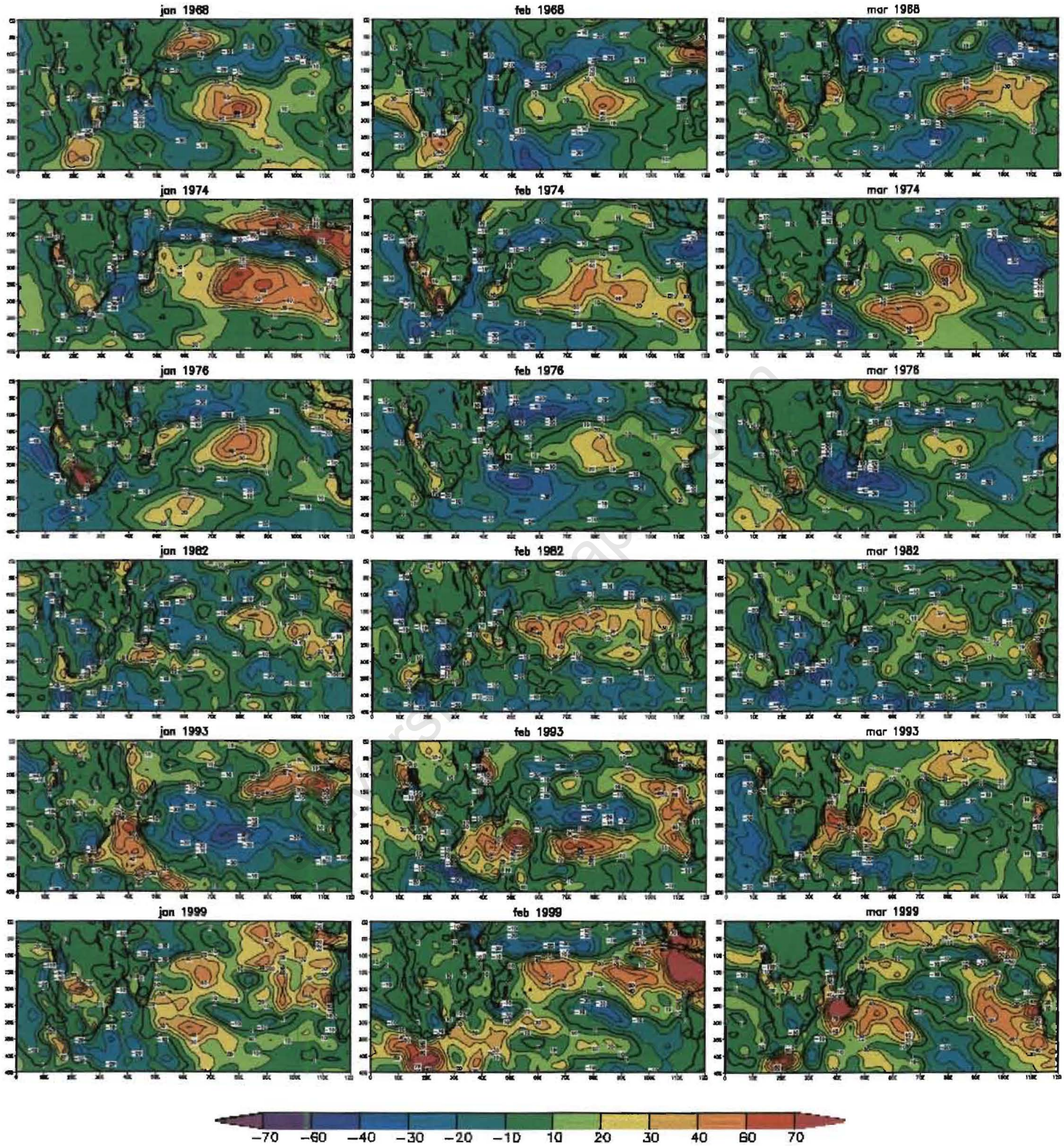

Fig 4.7 *Monthly latent heat flux anomalies in Jan, Feb and Mar for six strong positive events during 1968, 1974, 1976, 1982, 1993 and 1999. A scale for the anomalies is shown.*

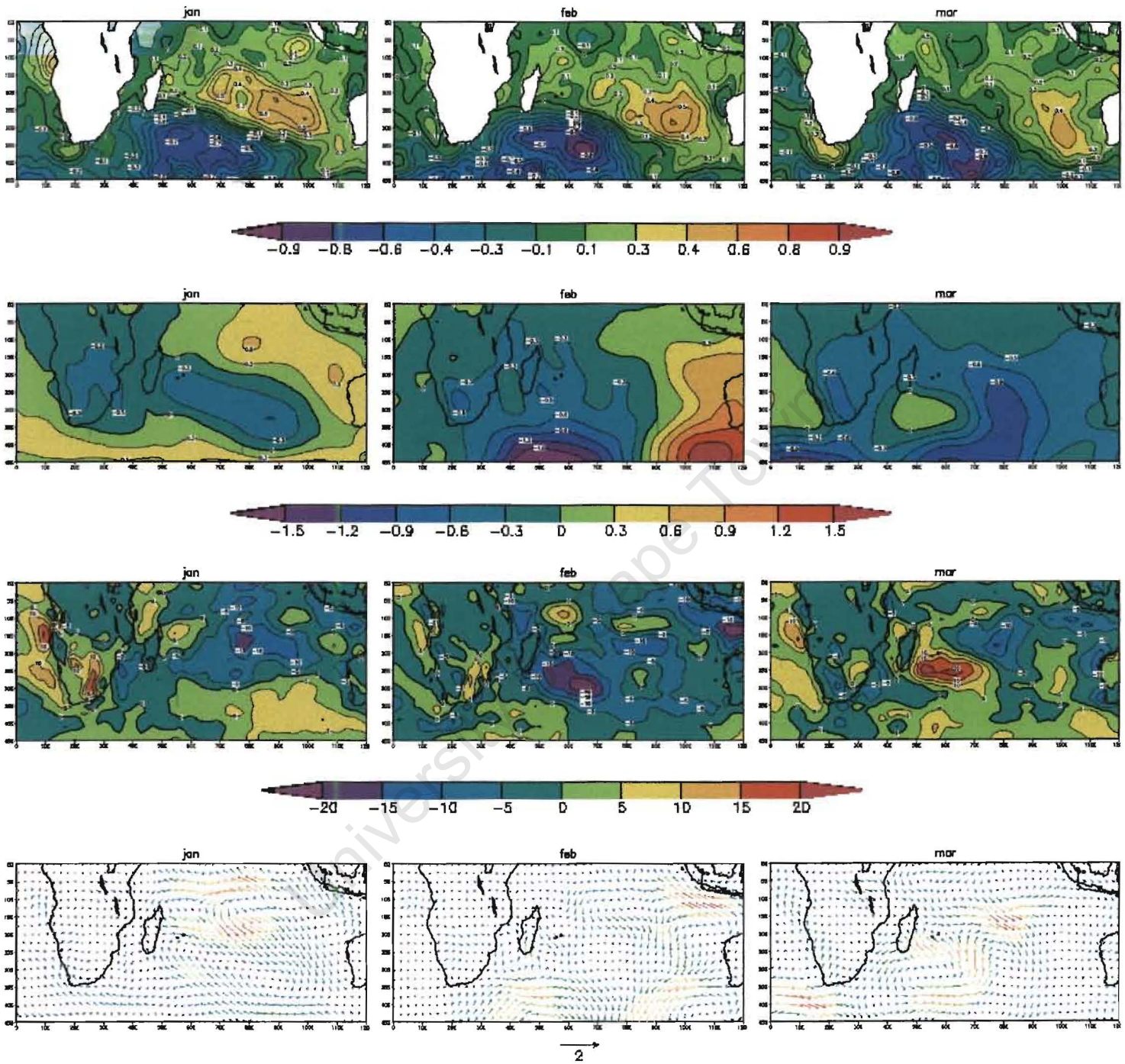

Fig 4.8 *Monthly composites of SST anomalies, SLP anomalies, Latent flux anomalies and surface wind anomalies in Jan, Feb and Mar for nine negative events during 1958, 1959, 1964, 1965, 1967, 1970, 1978, 1984 and 1998.*

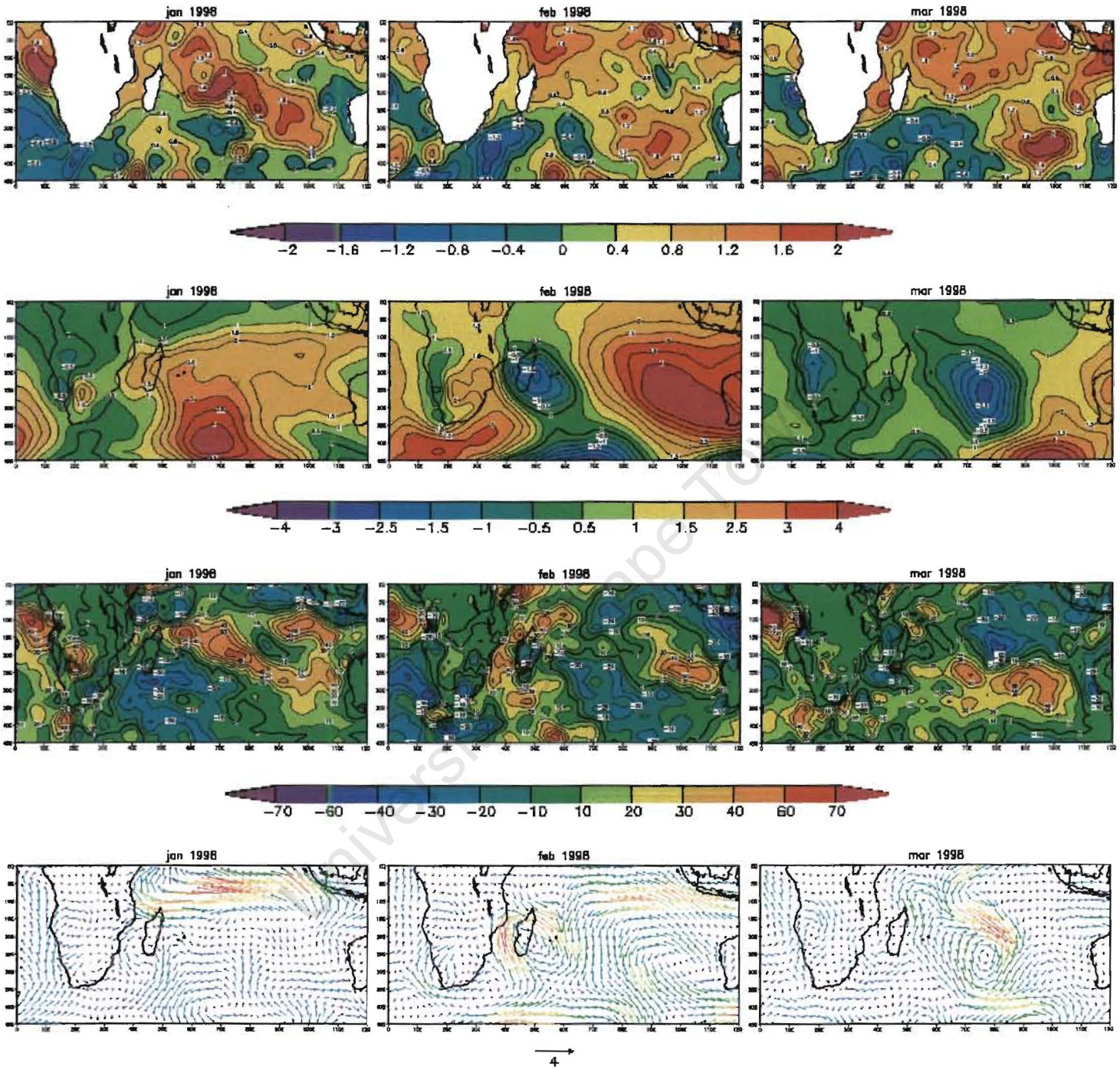

Fig 4.9. *Anomalies of SSTs (first panel), Sea level pressure (second panel), Latent heat flux (third panel) and Surface winds (fourth panel) for the* ***1998*** *positive phase event.*

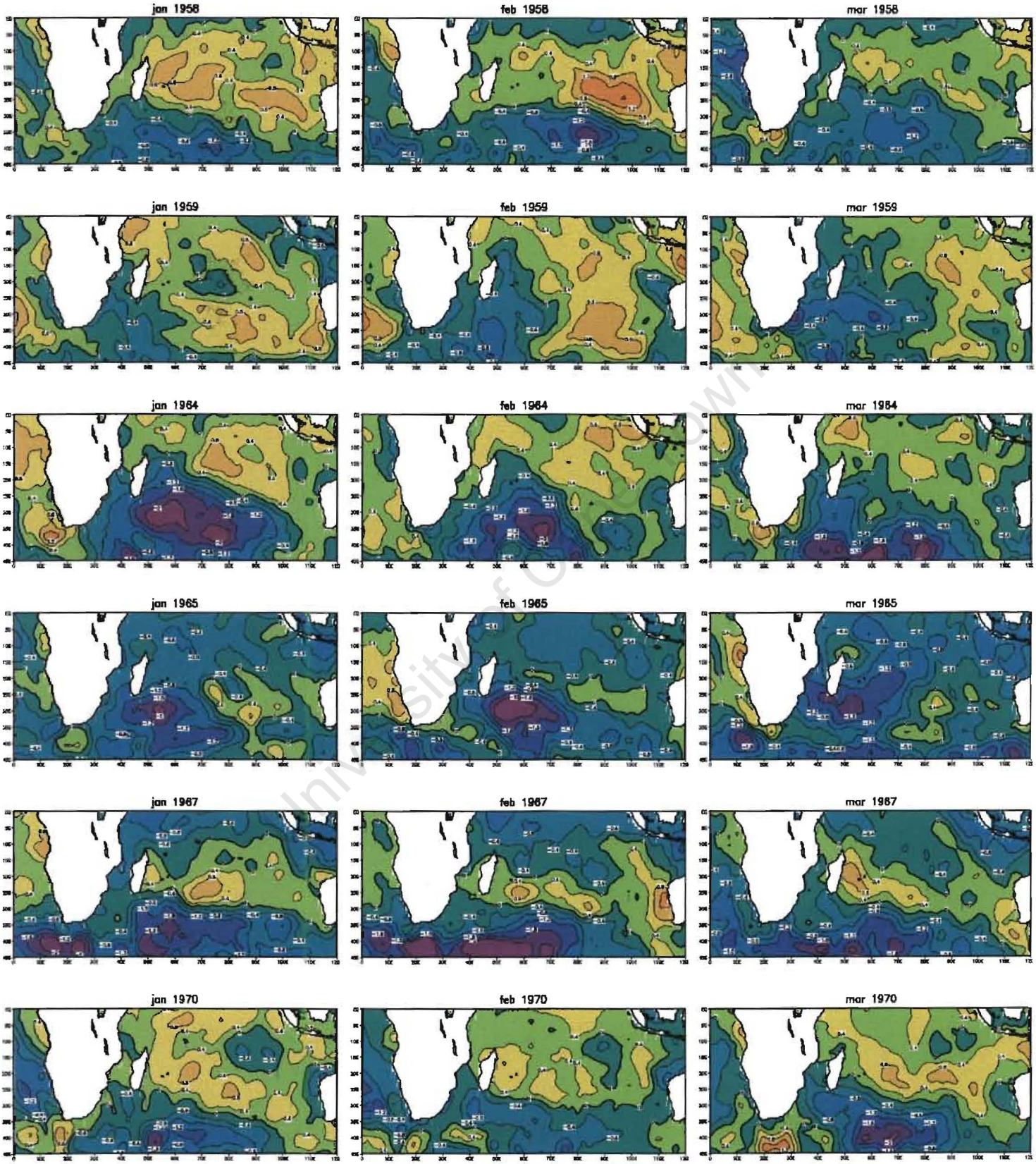
jan 1958
feb 1958
mar 1958
jan 1959
feb 1959
mar 1959
jan 1964
feb 1964
mar 1964
jan 1965
feb 1965
mar 1965
jan 1967
feb 1967
mar 1967
jan 1970
feb 1970
mar 1970

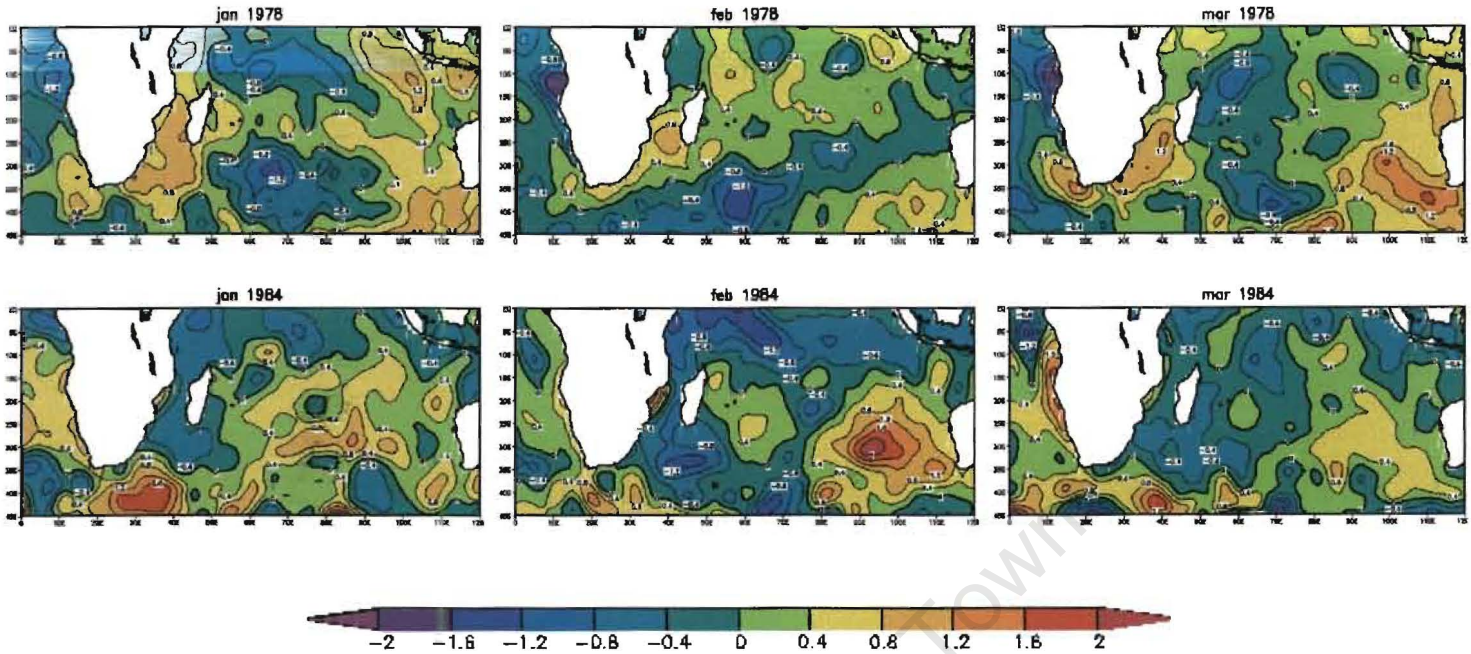

Fig 4.10 *Monthly sea surface temperature anomalies (GISST2.3b dataset) in Jan, Feb and Mar for eight strong negative events during 1958, 1959, 1964, 1965, 1967, 1970, 1978 and 1984. A scale for the anomalies is shown.*

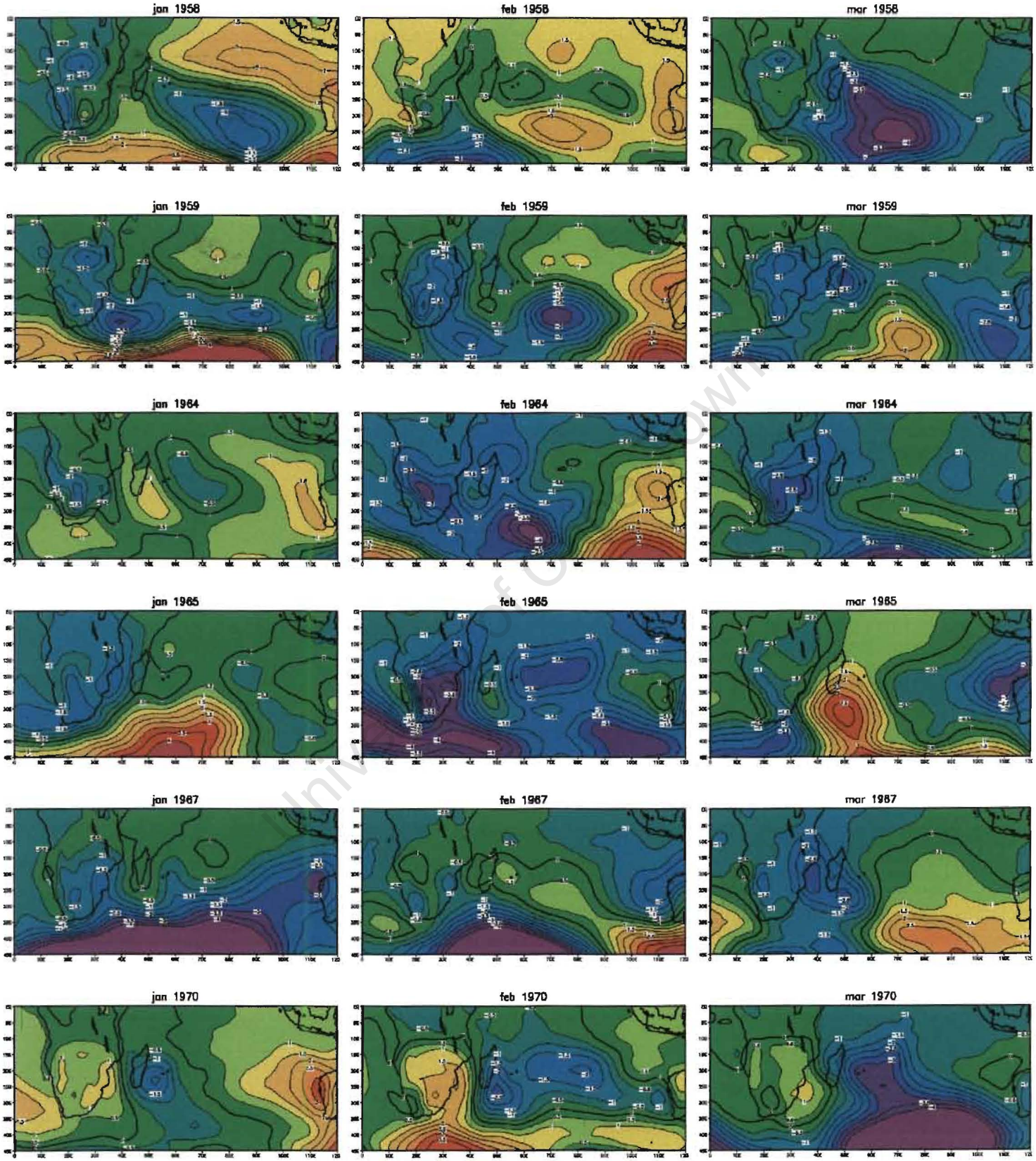
jan 1958
feb 1958
mar 1958
jan 1959
feb 1959
mar 1959
jan 1964
feb 1964
mar 1964
jan 1965
feb 1965
mar 1965
jan 1967
feb 1967
mar 1967
jan 1970
feb 1970
mar 1970

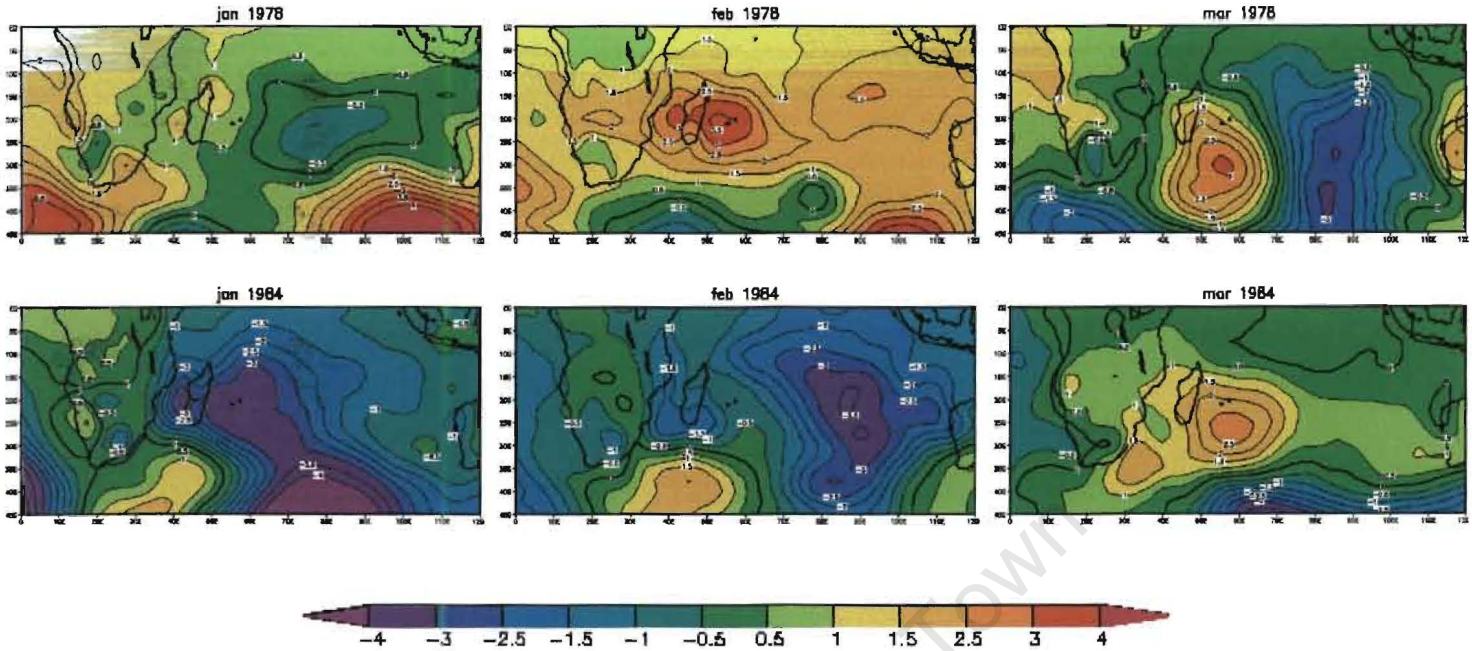

Fig 4.11 *Monthly sea level pressure anomalies in Jan, Feb and Mar for eight strong negative events during 1958, 1959, 1964, 1965, 1967, 1970, 1978 and 1984. A scale for the anomalies is shown.*

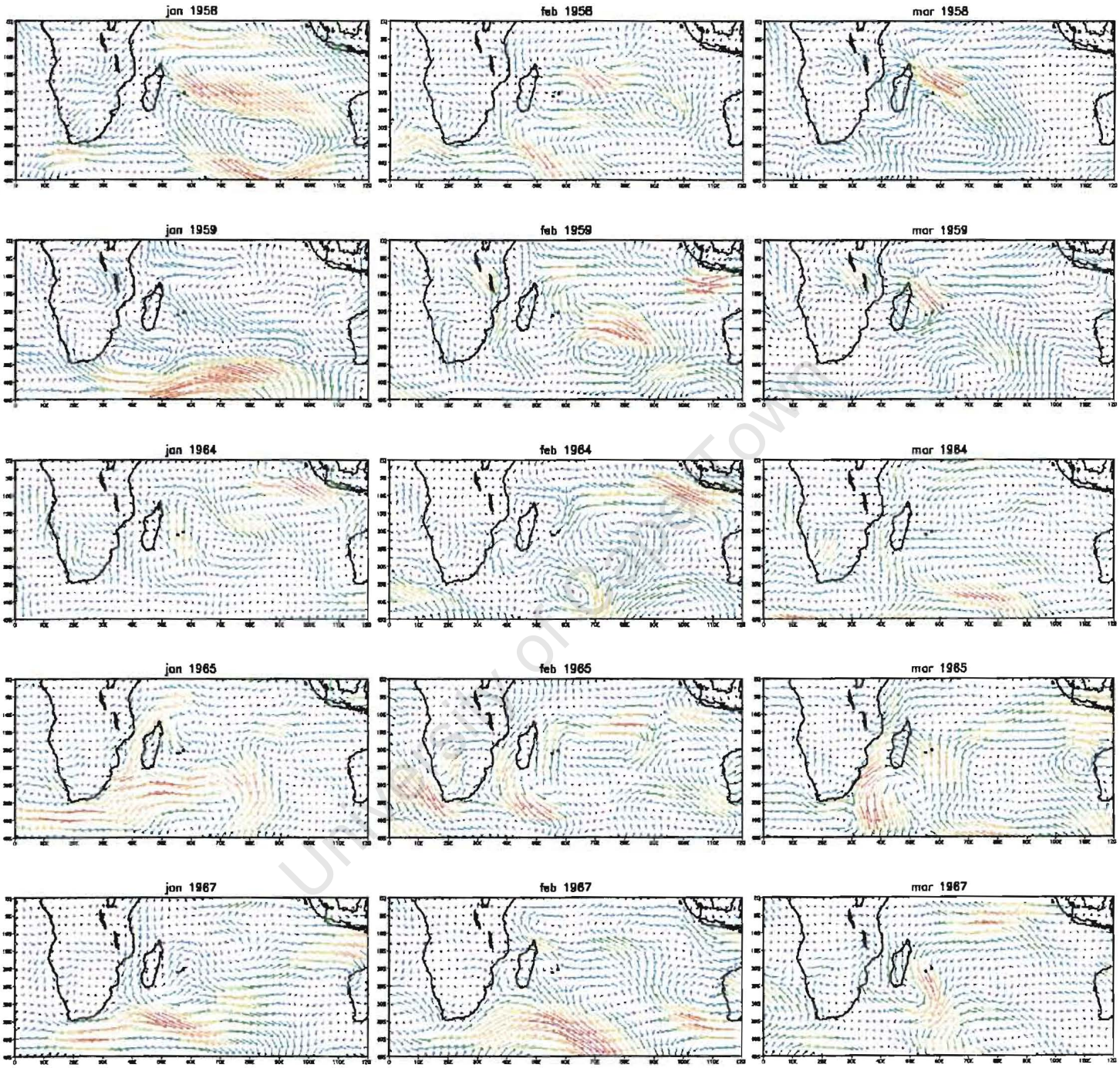

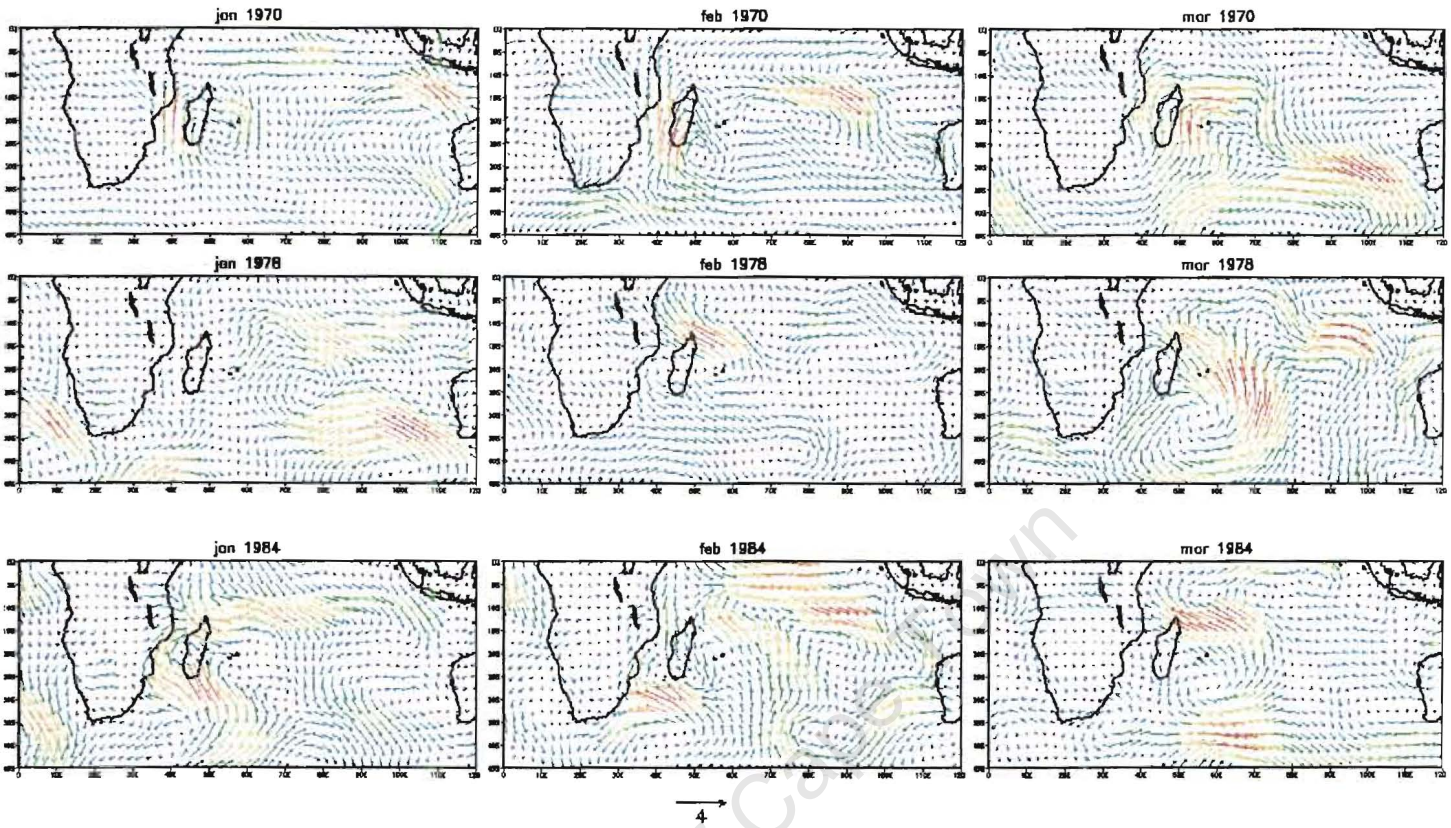

Fig 4.12 *Monthly surface wind anomalies in Jan, Feb and Mar for nine strong negative events during 1958, 1959, 1964, 1965, 1967, 1970, 1978 and 1984. A scale anomaly vector is shown.*

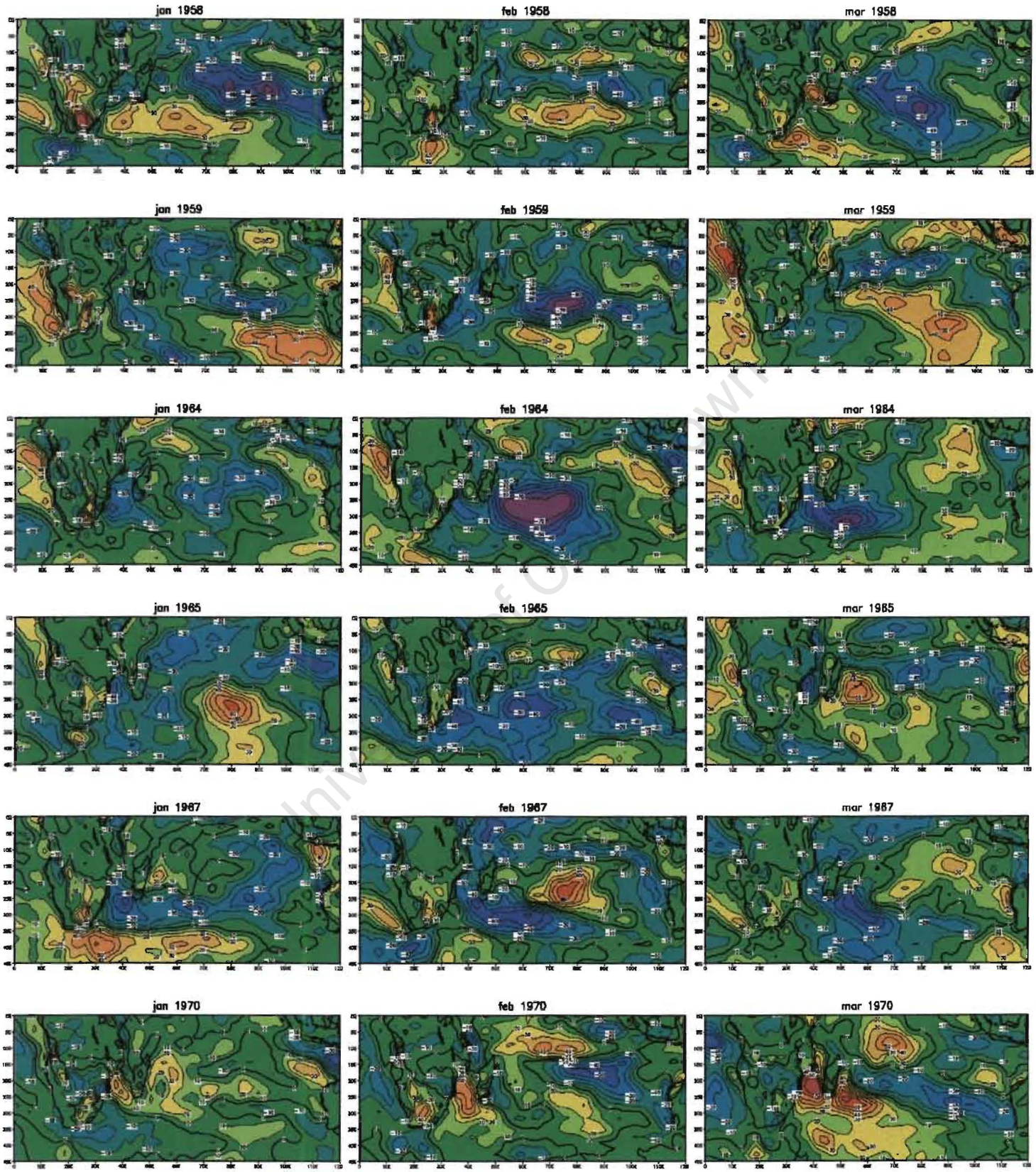
jan 1958
feb 1958
mar 1958
jan 1959
feb 1959
mar 1959
jan 1964
feb 1964
mar 1964
jan 1965
feb 1965
mar 1965
jan 1967
feb 1967
mar 1967
jan 1970
feb 1970
mar 1970

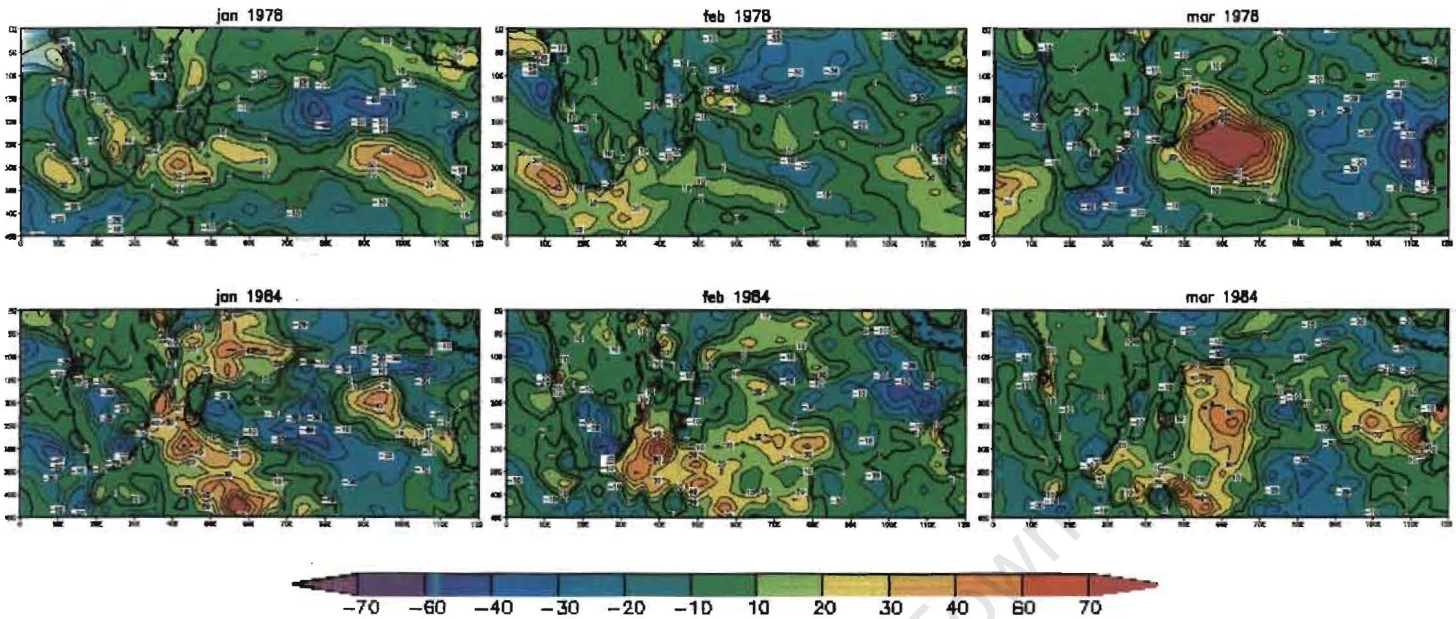

Fig 4.13 *Monthly latent heat flux anomalies in Jan, Feb and Mar for nine strong negative events during 1958, 1959, 1964, 1965, 1967, 1970, 1978 and 1984. A scale for the anomalies is shown.*

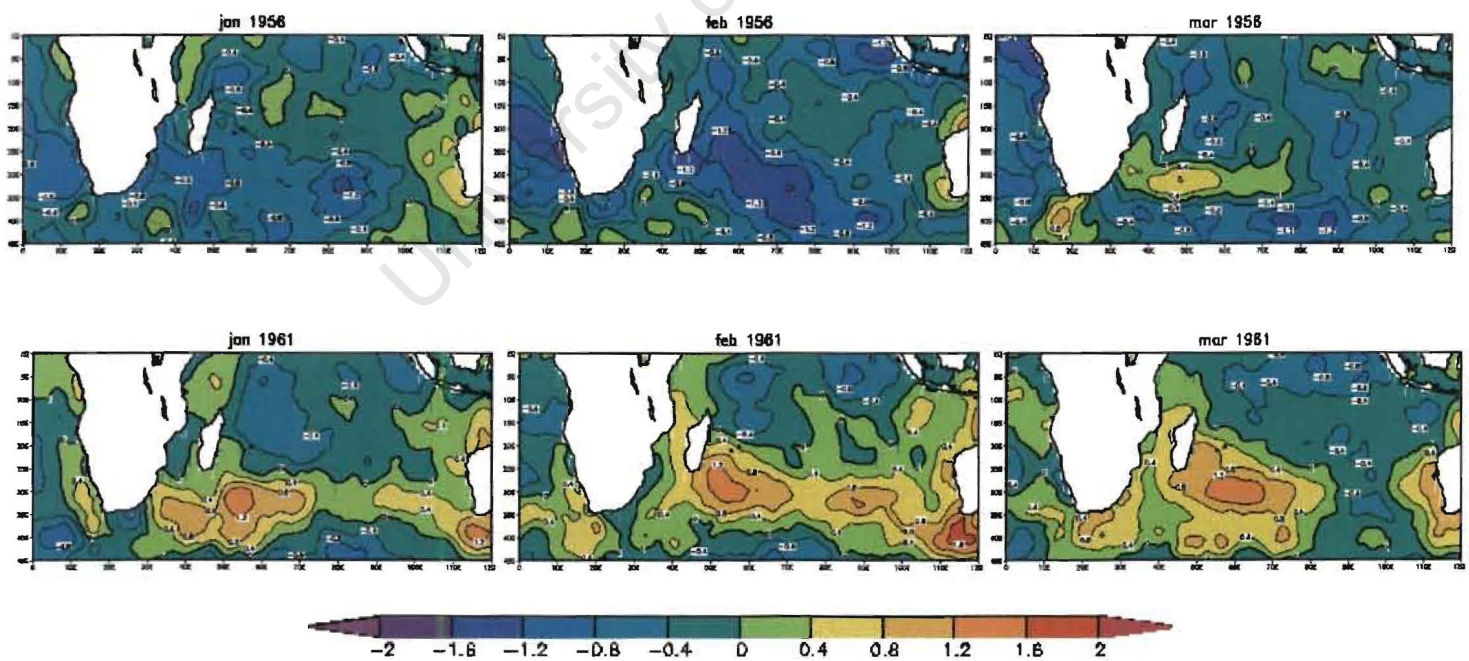

Fig 4.14. *Monthly SST anomalies in Jan, Feb and Mar for two positive events during 1956 and 1961. A scale for the anomalies is shown.*

Chapter 5

Model Results of the 1980/1 And 1997/8 Events

5.1 Introduction

Atmospheric general circulation models (AGCMs) and regional climate models (RCMs) are tools that may be employed in an attempt to simulate the behaviour of the atmosphere (Trenberth 1992; Dabberdt and Schlatter 1996). Different institutions around the world have developed a number of AGCMs and RCMs. These models differ in many ways in how they represent the atmosphere because of differences in the physics, parameterisations and interpolation methods employed by each model. However, the ultimate goal of these models is to realistically represent the atmosphere. Some models represent some regions better than others and therefore it becomes necessary to validate the models over the regions they are run. There are different methods of validating models; for example, this may be as model versus observations or as model versus model. The first method is more reliable than the second one. In this method, the model output of a run over a particular region is compared with observations of that region either via simple visual comparison of various atmospheric fields or with more sophisticated statistical methods. If the outcome of the comparison indicates that the model represents the observations adequately, then the model can be applied over the region with confidence. Additionally, the model run may be compared with the results from a different model run over the same region with the same forcing.

As mentioned in chapter three, little work has been done over southern Africa with MM5, therefore the model's skill in representing southern African circulation is not completely known. This chapter presents the validation of MM5 results using reanalysis data from NCEP because this dataset, which involves the assimilation of all available observations that are compatible with the data assimilation scheme of the AGCM, represents the main Southern African circulation features reasonably well and is essentially the only practical option for validating a RCM like MM5 over the region. But before the model is

validated, a summary of the southern African general circulation and some of the disturbances in the circulation that may lead to wet or dry conditions over the subcontinent are given in the following section.

5.2 Southern African General Circulation

At the mesoscale, which range from a kilometre to a few hundred kilometres, local winds and convective systems may persist for hours to a day or so. However, synoptic circulations, which extend over a thousand kilometres or more, may persist for about a week. The horizontal and vertical circulations, taking place at these temporal and spatial scales, determine weather over conditions southern Africa.

The meridional winds are on order of magnitude weaker than the zonal winds but are significant in transporting water vapour, mass, heat and momentum. Two major meridional cells in each hemisphere are the Hadley and Ferrel cells. The Hadley cell is thermally direct with warm air rising in the tropics and cool air sinking in the subtropics. The Ferrel cell, situated poleward of the Hadley cell, is thermally indirect with cool air rising in the midlatitudes and warm air sinking in the subtropics. During austral summer, a region of maximum subsidence and surface divergence between the descending limbs of the Hadley and Ferrel cells occurs south of 35°S (Hurrell et al., 1998). Another important feature of the general circulation that influences southern Africa is the Walker circulation (Lindesay, 1988). This is a linked series of zonal cells near the equator that has long been known to have important consequences for tropical and subtropical climate. It is the variation in the location of the ascending and descending limbs of the local Walker cell over the Indian Ocean/eastern Africa and the Atlantic Ocean/Southwestern Africa that influence summer rainfall patterns over the subcontinent. Such variation in the location of the limbs may be influenced by variations of sea surface temperatures in both the neighbouring oceans and the Pacific (e.g. Allan et al., 1995; Mason 1995; Mason and Jury 1997; Reason and Mulenga 1999; Reason et al., 2000).

During summer, the NCEP low level tropical easterlies (**Fig 5.1**) are centred near 20°S and expand polewards over the subcontinent. The core of the westerly jet (**Fig 5.1**) shifts poleward during summer. The location and strength of these wind systems is related to the location of the solar maximum with the easterlies strengthening and the westerlies weakening in summer. During summer, the mean meridional flow is markedly asymmetric over the subcontinent, being poleward over eastern parts and equatorward over the western parts as a consequence of the oceanic subtropical high pressure cells (Van Heerden and Taljaard 1998).

At all times, the surface pressure field is characterised by large semi-permanent high pressure cells in the subtropics -the South Atlantic Anticyclone and the South Indian Anticyclone. During summer, pressure tends to lower over the subcontinent as a result of surface heating when the sun is overhead south of the equator. The South Atlantic and Indian Anticyclones vary significantly in position (both longitudinally and latitudinally) throughout the year. However, it is the variation of the South Indian Anticyclone that is particularly important for the weather of southern Africa (Van Heerden and Taljaard 1998).

In summer, the ITCZ (Inter-Tropical Convergence Zone) lies to the south of the equator in the Indian Ocean and southeastern Africa and is more delineated over the ocean than over the subcontinent. This zone is associated with maximum convergence, cloudiness and precipitation. During austral summer, the South Indian Convergence Zone (SICZ), a land-based convergence zone and a region of enhanced precipitation, extends southeastwards from the ITCZ off the southeast coast of southern Africa (Cook, 2000 and 2001). Moisture convergence by transient eddy activity and via advection helps to maintain the SICZ.

The general circulation by itself is not responsible for the observed variations in rainfall patterns over the subcontinent in summer. However, changes in the characteristics of synoptic and mesocale disturbances, which are influenced by interannual and other

variability in the general circulation, may be responsible for wet and dry conditions experienced over the subcontinent during particular years. These disturbances include tropical-temperate troughs, cut-off lows, and easterly and westerly lows and waves. The following subsection discusses some of these disturbances.

5.2.1 Weather Disturbances in the Southern African General Circulation During Summer

Elements affecting the weather of southern Africa owe their origins to subtropical, tropical and midlatitude features of the general circulation (Preston-Whyte and Tyson, 1988, p. 209). Both tropical disturbances (easterly waves and lows) in the easterly flow over the northern parts of the subtropical South Indian Ocean anticyclone and midlatitude disturbances (westerly waves and cut-off lows) may influence summer weather. The easterly waves form in deep easterly currents in the vicinity of an easterly jet and are evident at lower levels (850 hPa and 700 hPa). These waves are barotropic and therefore their axes are not displaced with height. These weather systems peak between December and February and are common over northern South Africa, Zimbabwe and neighbouring regions. Westerly waves are baroclinic, are normally tilted westward with height and tend to only directly affect the south coast of South Africa in summer.

Tropical disturbances are not only influenced by northward-penetrating midlatitude disturbances but also exert a reciprocal influence on the midlatitude circulation. The interaction between tropical lows and the westerly waves to the south of Africa produce the tropical-temperate troughs (Preston-Whyte and Tyson, 1988; Washington and Todd, 1999), which influence cloud distribution and rainfall over southern Africa and define the major cloud bands. These cloud bands are the main rainfall-producing synoptic system over subtropical southern Africa in summer. When the tropical-temperate troughs are confined to land, truncated cloud bands, which terminate at the southeastern coast of the subcontinent, occur.

Although pressure over the land in the southern subtropics is generally low in summer as a result of surface heating, the strength, presence and frequency of tropical and midlatitude disturbances during a particular austral summer season may result in significant pressure differences from one summer to another. Significant pressure differences over the subcontinent and adjacent oceans are evident between wet and dry summers. During wet years, lower than normal pressure occurs over southern Africa, with the reverse in dry years (Rocha and Simmonds, 1997). Although pressure anomalies over the adjacent oceans are not so clear during wet and dry years, high pressure anomalies over the Indian Ocean have been reported during wet years whereas lower than normal pressures have been reported during dry years (Rocha and Simmonds, 1997).

Anomalous high (low) 850 hPa geopotential heights over the central and western interior of the subcontinent are associated with dry (wet) conditions over the region. Anomalous low 850 hPa geopotential heights over central southern Africa, reminiscent of tropical easterly waves at about 15 to 20°S, tend to be associated with wet conditions over land.

5.3 Model Validation

The results of MM5 runs for two summer seasons, dry (1997/8) and wet (1980/1), are analysed in this chapter. The model was run over southern Africa at a spatial resolution of 60km. This resolution is relatively coarse over a region such as Southern Africa with tight topographic and vegetation gradients and so may not represent a particular location very well. However, given the length of the integration period, the need to do a number of ensemble runs, and available computer resources, higher resolution was not feasible. Therefore, comparing the output from this ensemble with observations over a particular station may not yield good results although comparison of trends of various parameters may give insight into the model's validity over the region.

However, a comparison of circulation features between the 60km MM5 model results and the 250km resolution NCEP reanalysis data may be reasonable. Two simulations were

done with the MM5, one for the positive phase of the SST dipole pattern (experiment one-1980/81) and another for the negative phase (experiment two- 1997/98)(see **Table 3.1**). In order to simplify the comparison and because a reasonable length climatology of MM5 over southern Africa was not available, the model difference between the above events (i.e., 1980/1–1997/8) for various fields are compared for MM5 and NCEP. The objective is to compare circulation differences in the two models with a view to assess the robustness of the MM5 simulation. Actual fields for some other variables for MM5 and NCEP are also compared. The output from the two models is on different vertical coordinates, the output from MM5 is on sigma levels whereas the NCEP data made available for this research is on standard pressure surfaces. Given that the top and surface pressure levels used in MM5 are known, the MM5 fields are plotted at the approximate equivalent pressure levels. It is important to compare precipitation between the two events, however MM5 does not simulate rain well at 60km resolution hence variables related to this field are compared instead. Intra-ensemble differences are observed in various fields, sea level pressure in particular, (not shown) for each set of the experiment. Intra and inter-ensemble sea level pressure differences of about 1.0hPa over the subcontinent, 1.5hPa over the tropical Indian Ocean and 0.4hPa over the extratropics are observed in the 1980/1 and 1997/8 experiments. Slight changes in the location of the south Atlantic and Indian Ocean anticyclones are also observed among ensemble members of the two experiments. For brevity, ensemble averages are used in this discussion.

5.3.1 Sea Level Pressure and Geopotential Height

In this study 1981 (positive SST dipole) is considered a wet year and 1998 (negative SST dipole) a dry year over southern Africa (**Fig 5.2**). Monthly mean sea level pressure differences between 1981 and 1998 for January, February and March are shown in **Fig 5.3**. Negative differences are observed over the subcontinent in January and February in MM5 (right panel **Fig 5.3**) and NCEP (left panel) and suggest wetter conditions during the 1981 event than 1998 since negative pressure is favourable for moisture convection

and a strong Angola low, the source for cloud bands. Negative differences over a particular region indicate that the 1980/81 event has lower pressure over that region than the 1997/98 event and positive differences indicate the opposite. Negative and positive differences are observed over the southern and northern parts of the subcontinent respectively in January both in MM5 and NCEP. This suggests that both MM5 and NCEP produced lower sea level pressure values over subtropical southern Africa for the 1980/81 event than the 1997/98 event. The opposite situation is seen over the tropical parts of the subcontinent.

Common in MM5 and NCEP during January are two strong negative sea level pressure difference features, one over South Africa and the other over the midlatitude South Indian Ocean. The negative feature over South Africa is weaker in MM5 and has a magnitude of about –2 hPa while a magnitude of about –3 hPa is observed NCEP. The feature in the South Indian Ocean is of about the same magnitude, over –4 hPa, in MM5 and NCEP. The feature over South Africa coincides with the location of the continental heat low, which is favourable for good rains over this region between October and April (Preston-Whyte and Tyson, 1998, p. 227). The values over this feature may reflect the difference in strength of this heat low during the two events (1981 and 1998), i.e. stronger in 1981 than 1998, consistent with increased rain.

Negative differences over the subtropical South Indian Ocean in January, in MM5 and NCEP, are less favourable for wetter conditions over southern Africa, however (Preston-Whyte and Tyson, 1988; Rocha and Simmonds, 1997) as they suggest reduced easterly flux of moisture to the southwest Indian Ocean. In February, negative differences are observed over the subcontinent in both MM5 and NCEP and positive differences over the subtropical South Indian Ocean in NCEP only. Inconsistencies in the two sets (i.e. MM5 and NCEP) are observed near Madagascar. Positive differences are observed near Madagascar in NCEP, however, negative differences are observed over this region in MM5. This may be due to differences in the models' ability in capturing orographic features. MM5, a high resolution model, should represent more orographic variability than NCEP. In this case, MM5 may be partially capturing the Madagascan mountain

range, which extends from south to north along the eastern region of the island. This mountain range is about 150km wide over central Madagascar and the highest point is about 1.2 km above sea level, as captured by MM5 (**Fig 5.4**). Because NCEP has a coarser resolution, of order 250km, it may not capture this feature properly. However, this inconsistency in the two models may also be as a result of other factors other than differences in resolving orography between models. This thesis, however, focuses on differences over the southern African mainland and it is therefore beyond its scope to determine the exact cause of the differences near Madagascar. Weak positive differences are observed over the western regions of the subcontinent in February in NCEP but not in MM5. These differences strengthen substantially in March in NCEP and MM5 and reflect a substantial weakening of the Angola low, which suggests reduction of cloud band activity and reduced rainfall in March. Negative differences are observed in the southeastern Indian Ocean in both MM5 and NCEP in March.

A comparison of the geopotential height differences at the 850 hPa pressure level (**Fig 5.5**) indicates lower heights in January during the 1981 event than 1998 over most parts of the subcontinent and the subtropical South Indian Ocean. This is more evident in MM5 than in NCEP over the midlatitude ocean and the reverse over South Africa and Botswana. Negative values in NCEP are apparent over the southern parts of subcontinent only. GPCP precipitation anomalies show large wet anomalies, particularly over South Africa and Botswana during January 1981 (Rouault, 2003 pers.comm.).

In February, the difference patterns in the 850 hPa geopotential height are dissimilar between MM5 and NCEP over the eastern half of the domain but are more comparable in the west. Given that MM5 is forced towards NCEP at each boundary, the relatively large differences between MM5 and NCEP east of Madagascar are surprising. Positive differences are seen in March over the western half of the subcontinent (i.e. western South Africa, Namibia and Angola) in MM5 in March. In NCEP, positive differences are seen over Angola and Nambia only. Other similar features in MM5 and NCEP in March are positive differences east of Madagascar and negative differences over the midlatitude South Indian Ocean.

Comparisons of the 500 hPa geopotential differences between MM5 and NCEP (**Fig 5.6**) indicate some similarities in the difference patterns in the two models in all the three months. This may be due to a reduced influence on the 500 hPa circulation of orography and other surface forcing that may differ between the two models. In January, anticyclonic differences over the subtropics extend continuously from the eastern Indian Ocean to the western region of the subcontinent in MM5. This feature is however fragmented in NCEP during this month. Furthermore, this feature is further south in MM5 compared to NCEP. Another feature that is similar in the two sets of January results is strong cyclonic differences in the midlatitudes of the South Indian and Southeast Atlantic Oceans.

In February, negative differences are seen over the subcontinent and the neighbouring oceans both in MM5 and NCEP. Also common in the two models during this month are positive differences in the South Indian Ocean midlatitudes. Strong negative differences over the southwestern coast of the subcontinent extend further inland in MM5 than in NCEP. The region of weak negative differences near Madagascar in NCEP is however further west in MM5.

The MM5 and NCEP difference patterns in March are broadly similar but the feature of strong negative differences south of Madagascar in NCEP is stronger and located slightly further north. Features of positive differences are observed over the southeastern Atlantic and central South Indian Ocean in MM5 and NCEP.

In terms of rainfall influences, the cyclonic differences seen over the midlatitude Southwest Indian Ocean in January and February are favourable for increased westerly wave activity there and the Northwest-Southeast orientation of tropical-temperate troughs over southern Africa.

5.3.2 Precipitation Related Variables

Rainfall is typically not well simulated in either MM5 or NCEP and hence it is better to consider other moisture related parameters such as specific humidity, moisture flux, out-going longwave radiation (OLR), divergence, or latent heat flux. In addition to accessing MM5's ability in simulating southern African circulation during the 1980/1 and 1997/8 events, this section also discusses the above variables in relation to the wet and dry conditions of 1980/1 and 1997/8 events respectively. It should be noted that the above variables, particularly the latent heat and moisture fluxes, fall into the B and C classes (data in these classes is strongly influenced by the model) of the NCEP reanalysis classification and are therefore less reliable (Kalnay *et al.*, 1996). Moreover, the pre-1979 reanalysis appears to be less reliable in the southern hemisphere. Caution should therefore be taken when interpreting the results.

5.3.2.1 Specific humidity, Moisture flux and Latent Heat

Wet summer seasons over Southern Africa are characterised by large specific humidity absolute values, which may be as a result of increased moisture flux over the subcontinent from the surrounding oceans. This moisture from the surrounding oceans may be produced as a result of enhanced evaporation there. Moisture sources can also be local through evaporation over rivers, lakes, vegetation and soils.

A comparison of the 850 hPa specific humidity difference between the 1980/1 and 1997/8 event shows a number of dissimilarities in the three months between MM5 and NCEP (**Fig 5.7**). Generally, NCEP indicates negative differences over most parts of the subcontinent and the South Indian Ocean. In January, negative differences are observed over the central region of the subcontinent in both NCEP and MM5. This indicates that there is more surface moisture over this region during the 1998 event than during the 1981 event. These differences are however, stronger in NCEP than in MM5. Strong, widespread positive differences are observed over the northeastern region of the

subcontinent, indicating more moisture over this region during January 1981, in MM5. Positive differences are observed in the subtropical South Indian Ocean in both MM5 and NCEP. This suggests that low level air masses over the subtropical South Indian Ocean, the source of moisture for South Africa, hold more water vapour during January 1981 than in January 1998.

In February, negative specific humidity differences are still observed over the central regions of the subcontinent in both MM5 and NCEP. These differences however, extend northwestward in MM5 and northwards in NCEP. Positive differences over the eastern parts of the subcontinent are weak in NCEP compared to MM5 in which they are strong and widespread, particularly over Malawi, Mozambique and Tanzania. Both model results indicate availability of more moisture over this region during February 1981 than in February 1998. Major differences between the two models are observed over the tropical South Indian Ocean and western South Africa. MM5 indicates more moisture over these regions during the 1981 event than NCEP.

NCEP indicates less moisture over the subcontinent, except over the northeastern parts, than MM5 during the 1981 event in March. Negative differences are observed over the southeastern parts of the subcontinent, covering large parts of South Africa, in MM5. In MM5, positive differences are observed over the western and northeastern regions of the subcontinent. This indicates availability of more moisture over the Angola low and the tropical region of the tropical temperate trough. However, both MM5 and NCEP show positive difference over the midlatitudes across the domain, helping to strengthen the midlatitude input into the cloud bands. In general, NCEP indicates lower specific humidity over the subcontinent during the 1981 austral summer than in 1998. This is not consistent with observed rainfall (**Fig 5.2**) and may be as result of problems with NCEP in representing moisture-related fields in the low latitudes especially over the continent (Kalnay et al., 1996).

In order to examine the strength of the moisture flux from the surrounding oceans and other sources on the continent during the 1980/1 and 1997/8 events, transects of zonal

and meridional moisture flux at two longitudes and latitudes respectively, are examined. Zonal transects are taken at 40°E and 20°E so as to examine moisture fluxes from the South Indian and Atlantic Oceans during 1980/1 (**Figs 5.8** and **5.9**) and 1997/8 (**Fig 5.10** and **5.11**) in both NCEP and MM5. However the output from these models is on different vertical coordinate systems. As pointed out in **section 5.3**, the output is on sigma levels for MM5 and pressure levels for NCEP. In addition, moisture is minimal above pressure levels of about 300 hPa, hence zonal plots go up to this level.

An inspection of zonal moisture flux transect at 40°E during the 1980/1 event (**Fig 5.8**) suggests that the moisture over the large parts of the subcontinent, from the equator to about 35°S, is mainly from the South Indian Ocean in both MM5 and NCEP. In January, strong easterly moisture fluxes are observed in the tropics. The fluxes are strengthened in February and the ITCZ shifts to the southern most position and weaken in March in both models. The easterly zonal moisture fluxes are observed to extend further south into the midlatitudes in February in NCEP and are also observed to strengthen over the tropics in March in MM5. MM5 generally appears to have stronger moisture fluxes than NCEP.

Fig 5.9 indicates that moisture fluxes from the Atlantic Ocean north of the Angola low are not insignificant during the 1980/1 event. These westerly moisture fluxes advect moisture to western regions of the subcontinent just south of the equator. However, these moisture fluxes are stronger in NCEP than in MM5. Further south, strong and deep easterly moisture fluxes are observed in January, February and March in NCEP. These moisture fluxes are however, weak and shallow in MM5. The examination of these transects and those in **Fig 5.8** suggest that there was convergence of moisture over the region east of 20°E over the northern parts of the subcontinent in February in NCEP.

Stronger moisture fluxes during the 1997/8 (**Fig 5.10**) event than in 1980/1 (**Fig 5.8**) are observed in January, February and March in NCEP and appear to advect much moisture from the Indian Ocean to the subcontinent. Like during the 1980/1 event, the easterly moisture fluxes over the subtropics are observed to strengthen in February and then weaken in March in both MM5 and NCEP. Those in the tropics appear to weaken as the

season progresses in MM5. A prominent difference between MM5 and NCEP is observed in February. Strong westerly moisture fluxes are observed in the tropics, along 40°E between 20°S and 15°S, in NCEP and reflect the recurving of the Northest Monsoon out in the tropical Indian Ocean. MM5 does not show this feature.

Along 20°E, both the equatorial westerly and tropical easterly moisture fluxes, are stronger in all the three months during the 1997/8 event (**Fig 5.11**) than in 1980/1 (**Fig 5.9**) in NCEP. These moisture fluxes are however weak and shallow in MM5. The westerly moisture flux is weakened in March in NCEP. The February equatorial westerly and tropical easterly moisture fluxesin **Fig 5.10** and **Fig 5.11** indicate lack of moisture convergence over the tropical subcontinent during this month in 1998. These fluxes appear to freely traverse the subcontinent in their respective directions with little or no indication of converging between the 20°E and 40°E longitudes. This is not favourable for good rainfall and may explain the dry conditions over the tropical regions of the subcontinent in February the 1998 event. However, there is some indication of weak convergence of these moisture fluxes in January and March in the equatorial region.

Meridional transects at 10°S (**Fig 5.12**) indicate strong northerly moisture flux from about 10°E to 45°E over Africa in January and February during the 1980/1 event in NCEP and reflect the inflow towards the ITCZ. Then northeasterly winds are observed to advect much moisture from the tropical Indian Ocean to the northeastern parts of the subcontinent. They are also the major source of rainfall over East Africa, Tanzania in particular. The northerly moisture flux dies down in March in NCEP. MM5 fails to capture this flow or does so very weakly in the three months. Southerly moisture fluxes are observed further west from about 10°E to 0°. This flow is from the South Atlantic Ocean anticyclone and generally along-shore and weaker at this latitude. MM5 captures this flow and appears to be stronger than in NCEP in February and March.

Through 20°S, the northerly flux is weaker and is shifted eastward particularly in February 1981 in NCEP (**Fig 5.13**). This flow weakens further in March 1981. At this latitude, the northerly flux reflects the South Indian anticyclone, hence it is more

pronounced over the Southwest Indian Ocean between 40 and 50°E.Such northerly flux is less evident in MM5. The southerly moisture fluxes, further to the west, are however strengthened in NCEP in the three months and remain unchanged in MM5 at this latitude compared to those through 10°S (**Fig 5.12**). As mentioned above, this flow is as a result of the South Atlantic Ocean anticyclone and is stronger at this latitude. However, it may not result in much rain over the western subcontinent due the relatively stable atmosphere there.

During the 1997/8 event, the northerly moisture fluxes are observed to have generally strengthened in NCEP in January, February and March at 10°S (**Fig 5.14**) compared to the 1980/1 event (**Fig 5.12**). This flow is weak in MM5 and moisture fluxes in this model are mainly southerly. In February, the northerly flow is strong and widespread during the 1997/8 event in NCEP. This suggests enhanced moisture advection by the monsoons in this month compared to January and March. The southerly moisture flux over the Atlantic Ocean also appears to strengthen during this event. The strengthening of both the southerly and northerly moisture fluxes suggests there is increased moisture over the subcontinent during the 1997/8 event compared in 1980/1.

The northerly moisture fluxes are reduced in extent at 20°S in January, February and March in NCEP during the 1997/8 event (**Fig 5.15**). The extent of the southerly fluxes is however increased. This suggests that there is reduced moisture advection around the tropical margin of the South Indian Ocean anticyclone by the monsoon wind and increased moisture advection from the Atlantic Ocean. The extent of the northerly moisture fluxes appears to be increased and the southerly fluxes reduced at this latitude in all three months in MM5.

Latent heat flux differences between the 1980/1 and 1997/8 events (**Fig 5.16**) indicate enhanced evaporation over the South Indian Ocean in January during the 1980/1 event in NCEP. During January, increased latent heat flux is observed over the subtropical and midlatitude South Indian Ocean, in particular, and to the south of South Africa in both models. Increased latent heat flux south of South Africa suggests strengthening of the

midlatitude input into the cloud bands during 1981 relative to 1998. This moisture increase southeast of South Africa may be advected to the subcontinent by predominant southeasterlies in the subtropical Indian Ocean (see above and **section 5.3.3** below). Over the land, increased latent heat is observed over Southeastern Africa. The area of increased latent heat flux appears to decrease both over the land and the subtropical South Indian Ocean in February and March. In March, increased latent heat is observed to the south of Madagascar and in the Mozambique Channel suggest increased moisture available to be advected towards the land by the easterlies in 1981 compared to 1998.

MM5 shows increased latent heat both over the land and the subtropical South Indian Ocean in all the three months compared to NCEP. Areas of reduced latent heat over the central parts of the subcontinent are not seen in January, February and March in MM5. However, MM5 appears to capture the trend of latent heat difference changes over the Atlantic Ocean observed in NCEP i.e. reduced latent heat in January and March and increased latent heat in February.

5.3.2.2 Divergence and OLR

The availability of moisture over a region does not guarantee rainfall there. Conditions necessary for this moisture to be uplifted and fall as rain later, via the dissipation of clouds, are required. In order for this moisture to be lifted up, processes like low level convergence, convection and upper level divergence should occur. Areas of increased convergence are indicated by negative values in the divergence field and areas of increased cloud cover by negative OLR anomalies.

Increased cloud cover over a region may be as a result of convective or convergence processes at the surface, and imply increased rainfall. Conversely, positive OLR anomalies suggest clear skies and dry conditions. However, areas of increased convection or convergence, at the surface, do not coincide sometimes with areas of increased cloud cover. Due to a model climatology not being avaliable, as mentioned above, the

differences of this variable between 1980/1 and 1997/8 events are presented instead of anomalies. If the difference (1981-1998) is negative over a particular region, this suggests that the 1980/1 event has less OLR (cloudy) over that region compared to the 1997/8 event and positive differences may suggest the opposite. However for divergence, because the actual field of this variable has both negative and positive values, the difference of this variable between 1981 and 1998 may be ambiguous, and therefore the 1000 hPa actual field for the events is compared and presented. Note that the negative values are shaded.

During the 1980/1 event (**Fig 5.17**), convergence of air is observed over the southern parts of the subcontinent and the tropical South Indian Ocean in NCEP. In January, strongest convergence occurs over land and is observed to be orientated in the northwest-southeast direction consistent with a typical cloud band location, which is observed to be associated with increased rainfall over southern Africa. Enhanced convergence is also observed over southeastern South Africa and is favourable for increased rainfall over this region. Increased divergence, indicating dry conditions, is observed over Botswana, Zimbabwe and western Zambia. A similar, but noisier pattern of low level convergence is seen in MM5.

The region of increased convergence shifts westward in February in both models. Both NCEP and MM5 show low level convergence strengthening over northern Namibia and Angola. The area of increased divergence extends further northwest in NCEP and northwest in MM5. Areas of enhanced convergence weaken further in March consistent with the dieing down of the dipole and areas of enhanced divergence are observed over the central parts of the subcontinent in both models. Both MM5 and NCEP show low level divergence of air over the Atlantic Ocean and subtropical South Indian Ocean, this reflects the subsidence associated with the ancticyclones.

Areas of increased convergence are slightly further to the west in January and February during the 1998 event (**Fig 5.18**) than 1981 in NCEP and to less extent in MM5. Furthermore, convergence over these areas, particularly in the south, is weaker than in

1980/1 (**Fig 5.17**). This suggests reduced rainfall over the southern part at least during 1998 relative to 1981 in these months. In March, the western areas of convergence are similar to 1981 but the central area of divergence is smaller. Stronger divergence is observed over the eastern parts of the subcontinent in January, February and March in MM5 than in NCEP. As for the1980/1 event, increased divergence is observed over the Atlantic Ocean in both MM5 and NCEP in all the three months during the 1997/8 event. Comparison of OLR difference patterns (**Fig 5.19**) reveals some similarities between MM5 and NCEP. Negative differences are observed over the northern and southwestern parts of the subcontinent in January in NCEP and to some extent MM5, suggesting more cloud cover and rainfall here during the 1981 than in 1998. Positive differences over the central parts of the subcontinent in both models suggest less cloudy skies and drier conditions over this area during the 1981 than in 1998. The area of more negative OLR difference is increased in February and March in NCEP suggesting more cloud and rainfall in 1981. The feature of positive OLR differences in NCEP weakens in February and vanishes in March. Regions of reduced OLR over the southwestern parts of the subcontinent, during January – March 1981, coincides with areas of enhanced convergence in **Fig 5.17** in NCEP. Regions of positive OLR differences coincide with regions of negative specific humidity differences (**Fig 5.7**) over the central parts of the subcontinent in NCEP. This relationship is evident in January and February. In MM5, relative enhanced cloud cover (i.e. reduced OLR) is observed over the northern and southern parts of the subcontinent in January 1981. In February, strong negative OLR differences are observed over South Africa and to the northeast of Madagascar in MM5. Most parts of the subcontinent are characterised by negative OLR difference during February 1981 relative to 1998 in MM5. In March MM5 shows large positive OLR differences over South Africa unlike NCEP.

Dissimilarities in OLR differences in the two models are seen over the subtropical South Indian Ocean in January. A negative difference feature is observed over this region in MM5 while a positive feature is observed in NCEP. This implies more convection during the 1981 event than during the 1998 event over this region and southeastern South Africa in MM5. Also strong negative OLR differences are observed over the tropical Indian

Ocean in MM5 during both January and February. These dissimilarities in the two models may be due to MM5's weakness in resolving precipitation properly. However, both models generally indicate negative OLR differences over the region, suggesting more rain in 1981 than in 1998.

5.3.3 Zonal Wind

The general circulation of southern Africa is characterised by low and middle level tropical easterlies and middle to upper level midlatitude westerlies. An analysis of the transect of MM5's zonal winds over this region may give insight into the model's ability in representing this region's atmospheric circulation. Transects are taken at three different longitudes; at 10°E, 20°E and 40°E (i.e. just offshore of the west coast, through the western part of the subcontinent and through the Mozambique channel). The actual zonal wind field and not differences for the two events is discussed because differences of this parameter are less easy to interpret. However for the sake of comparing patterns between MM5 and NCEP, the differences plots are given in the appendix. The transects are also examined to find out areas of convergence over the region during the 1981 and 1998 event. Change in sign of the zonal wind (from easterly to westerly and vice versa) from one longitude to another indicates convergence over this region bound by these longitudes. The levels of the zonal wind are in sigma (σ) coordinates in MM5 and hectopascals (hPa) in NCEP. The surface sigma level ($\sigma = 1$) corresponds to the surface and at the topmost level ($\sigma = 0$) to 100 hPa. MM5 has 23 pressure levels while NCEP has 17. Differences in wind speed between the upper and lower levels represents wind shear, which is essential for baroclinic westerly disturbances, which contribute to the formation of cloud bands over southern Africa. These clouds are major rain-producing features over the subcontinent. In order to investigate wind shear, we take the difference between of the 200 and 850 hPa zonal winds.

A transect of zonal winds along 10°E west of the subcontinent in the Atlantic Ocean during 1981 (**Fig 5.20**) indicates that westerlies dominate the midlatitude areas south of

35°S from January to March at all levels. In both MM5 and NCEP, a low level easterly flow is observed north of 35°S to about 15°S. This flow appears to be an extension of the tropospheric tropical easterly flow in NCEP (left panel) while it is separated from this by a westerly flow in MM5 (right panel). Nonetheless, this flow indicates that the easterlies supply moist air to the central regions across the subcontinent from the Indian Ocean. Strengthened easterlies in this region may also play an important role in the southeast-northwest orientation of the tropical temperate trough. Both models show a low level westerly flow south of the equator to about 15°S, which reflects the cyclonic circulation north of the Angola low into the ITCZ. The differences in the zonal wind at this longitude between the two models may be as a result of differences in the vertical resolution of the models. Because of the many pressure levels in MM5, this model may capture small changes in zonal winds with height. The low level equatorial westerly flow mentioned above is weak in both MM5 and NCEP. This indicates weak moist air advection from the Atlantic Ocean to the tropical regions of the subcontinent. Common to both MM5 and NCEP is a westerly flow feature embedded in the upper level tropical easterly flow. This feature extends downward more in MM5 than in NCEP in January and February and may represent the occurrence of an anomaly in the amplitude of the quasi-biennial oscillation (Logan *et al.*, 2003). An easterly flow in the midlatitudes above the 100 hPa level is only observed in NCEP. Note however that MM5's top most level is set at 100 hPa, and therefore it is unable to pick up features beyond this level. Upper level easterlies are stronger in NCEP than in MM5 in January and February 1981. In addition, a comparison of the low level subtropical easterlies indicates a stronger flow in NCEP in January and weaker in March than MM5. The subtropical easterly flow is further south in February in MM5. This may strengthen the tropical and midlatitude link, which is favourable for the formation of the tropical temperate trough.

A transect along 20°E during 1981 indicates that the upper level midlatitude westerly flow extends further north throughout the three months in MM5 than in NCEP (**Fig 5.21**). Common to both MM5 and NCEP, is a low level tropical westerly flow extending from the equator to about 10°S. This flow appears to be weaker in MM5 than in NCEP. Easterlies extend south of this latitude to 20-25°S in NCEP and to near 35°S in MM5.

This suggests that more moisture may be advected from the Indian Ocean over the South Africa in MM5 than NCEP. As mentioned above, the easterly flow over this region supplies moist air from the Indian Ocean. This moist air is important for the formation of cloud bands associated with the tropical-temperate trough and the Angola low. Moist air may be forced to ascend over the region of the tropical-temperate trough via convergence or surface heating, for example. However, strengthened and deep easterlies may push the cloud bands associated with the these features further west, leading to wet conditions over the western regions of the subcontinent and drier conditions over the eastern parts during summer.

The flow through 40°E is simpler (**Fig 5.22**), essentially consisting of easterlies north of about 30° - 35°S and westerlies further south in both models. The former is slightly stronger in MM5 again suggesting more moisture advection from southwest Indian Ocean towards South Africa. The upper level midlatitude westerlies are weaker in MM5 than NCEP suggesting reduced shear and less cyclonic systems Southeast of Africa.

Inspection of zonal winds through 10°E (**Fig 5.20**) and 20°E (**Fig 5.21**) in MM5 and NCEP reveals no evidence of convergence over the region between the two longitudes. However, weak convergence is observed over the subtropical western region between latitude 30°S and 20°S in NCEP in all the three months of the season as seen in **Fig 5.17**. This suggests favourable conditions for moisture ascent over the southwestern region of the subcontinent during the 1981 event. Indeed, January and February 1981 showed large positive anomalies in rainfall over western South Africa and Namibia. The flow through 20°E (**Fig 5.21**) and 40°E (**Fig 5.22**) indicates weak convergence from the equator to about 15°S and 10°S in MM5 and NCEP.

A transect of the 1998 zonal winds along 10°E indicates that the upper level midlatitude westerly flow extends further north in MM5 than in NCEP from January to March (**Fig 5.23**). Low level monsoonal westerlies are observed in the tropics from the equator to about 15°S during the season in particularly in NCEP. This flow is related to the cyclonic circulation around the Angola low and helps to advect moist air from the Atlantic Ocean.

An easterly low level flow is observed in the subtropical region during this season but appears to be weaker in NCEP and to lesser extent MM5 than in 1981 consistent with 1998 being a drier season than in 1981.

As for 1981, a transect along 20°E during 1998 (**Fig 5.24**) may indicate differences in the ability of MM5 to represent orography compared to NCEP. This is reflected in the undulating pattern of the zero zonal wind contour from 35°S to 25°S in each month in MM5. Weaker low level monsoonal westerlies are observed south of the equator during the season. This flow however, is much stronger and extends considerably higher in NCEP compared to MM5. This flow coupled with an easterly flow to the south reflects the Angola low and ITCZ to the east and is important for tropical temperate trough formation and rainfall. Significant differences between the models are the extent and strength of the low level tropical easterlies and the upper level easterly jet near 5°S.

A transect along 40°E shows a transition in both models in the direction of the low level zonal flow from easterlies to westerlies around 35°S (**Fig 5.25**). The easterly flow strengthens near 10°S, particularly in MM5. In NCEP, this easterly flow interrupted by low level westerlies between 20°S and 10°S in February. The upper level westerly jet appears to be stronger in NCEP than in MM5 throughout the season. This feature with the generally stronger low level shear over subtropical southern Africa in NCEP suggests that the latter may be more likely to generate significant rainfall than MM5.

The difference between the 850 and 200 hPa zonal winds (shear) (**Figs 5.26** and **5.27**) clearly shows the easterly (negative) and westerly (positive) waves over the tropical and midlatitude regions respectively and their location is also evident as the season progresses. It is these waves that are responsible for the formation of the cloud bands, the main rain-producing feature over southern Africa (Preston-Whyte and Tyson, 1988). In the westerly wave, regions of maximum shear or baroclinic disturbances are characterised by large values and are associated with frontal disturbances.

In January during the 1980/1 event (**Fig 5.26**), the strongest westerly shear is located near the region 30 – 40°E, 35 – 40°S (i.e. southeast of South Africa) and has a northwest-southeast orientation, consistent with the orientation of the cloud band, in NCEP. Therefore, baroclinic westerly disturbances, associated with wet conditions, are anticipated over this region during this event. Indeed, GCPC precipitation anomalies (**Fig 5.2**) show all of South Africa (particularly the southwest), Botswana and Zimbabwe very wet in this month. MM5 has a similar maximum in the westerly shear but located near the South African continent and weaker in magnitude. In NCEP, the maximum shear is greater than $30ms^{-1}$, while in MM5 it is only about $26ms^{-1}$.

The region of maximum shear appears to weaken and split into two in February, one over the Indian Ocean, south of Madagascar, and the other over southeast Atlantic Ocean (0 – 20°E, 26 –35°S), in NCEP. The split may be due to the splitting of the midlatitude westerly jet. The shear over the Atlantic Ocean is stronger than that over the Indian Ocean, therefore particularly wet conditions are expected west of the subcontinent as observations indeed show in February. The westerly wave also shifts northward in February. Though MM5 captures this split, it locates the westerly wave further north compared to NCEP. In MM5, the shear over the Atlantic appears like a cut-off and that in the Indian Ocean is further east.

In March, the shear weakens further and shifts north. The weakening of the shear indicates reduced baroclinc disturbances and hence reduced rainfall over Southern Africa. GPCP rainfall anomalies show smaller positive anomalies in March 1981 than earlier in the season. The shear maximum over the Atlantic Ocean shifts further west while that in the Indian Ocean is to the southeast of Madagascar, in NCEP. These regions of shear are weak and further north in MM5 over the SouthEast Atlantic and east of Madagascar respectively.

During January 1981, the NCEP region of maximum shear is again southeast of South Africa with a weaker maximum over northern South Africa (**Fig 5.27**). The southwest Indian Ocean maximum is however, weaker compared to that during 1980/1 and is

further south suggesting weaker cloud bands and drier conditions. In MM5, a weaker maximum is evident southern of South Africa near 40°S. Another region of maximum shear is observed to the southeast of Madagascar in MM5. The magnitude of the shear over these regions is about $20ms^{-1}$ compared to $24ms^{-1}$ in NCEP.

In February, the NCEP area of maximum shear in the westerly wave shifts northeastward to lie just South of Cape Town with another maximum south of Madagascar. This implies that baroclinic disturbances intensify southwest of South Africa, which is unfavourable for cloud bands across southern Africa. Indeed almost all of Southern Africa shows dry conditions in February 1998. In MM5, the westerly shear maximum is further west than NCEP (over the South Atlantic) and is weaker.

In March, NCEP shows a westerly shear maximum just off the South coast whereas MM5 does not show any clear feature here. Consistent with this NCEP shear maximum, March 1998 shows positive precipitation anomalies over southeastern South Africa.

5.4 Conclusion.

With the advent of fast and large computational resources, a number of general and regional circulation models, developed by different institutions around the world, are now available. These models differ from one another because of the different physics, parameterisation and interpolation methods employed. Furthermore, some models represent some regions better than others. Therefore, it becomes necessary to validate these models over the regions they are run.

MM5, a regional climate model used in this thesis, was validated over southern Africa using the model versus model method with the NCEP model, which assimilates all available observations into its integration. Monthly (January, February, and March) sea level pressure differences, 850 hPa and 500 hPa geopotential height differences for 1981 and 1998 MM5 simulations and NCEP were compared in order to validate the former.

Transects of monthly zonal winds and moisture fluxes, at different longitude (10°E, 20°E, and 40°E) and latitudes (10°S and 20°S), were also compared. Other rainfall related variables, such as specific humidity, latent heat, divergence and out-going longwave radiation for the two models were compared.

The comparisons between the two models showed similarities in the difference patterns, particularly the 500 hPa geopotential differences. Common features in NCEP and MM5 sea level pressure and 850 hPa geopotential differences were also observed. An examination of rainfall related variables indicated more moisture and convergence processes over the southern Africa in 1981 than 1998. An analysis of zonal wind transects for the models indicated similarities but also some significant differences in zonal components of the midlatitude westerlies and tropical easterlies. Both models showed increasing zonal wind speed with height in both events. Wind shear clearly indicates wetter conditions in January and February 1981 than in 1998.

There are some significant differences between MM5 and NCEP fields, and therefore one needs to interpret the MM5 results with caution. In the next chapter, an experiment similar to the 1980/1 dipole event is carried out but using an idealisation of the observed 1980/1 SST over south Indian Ocean. The purpose of this is to hopefully isolate the atmospheric response over southern Africa more clearly and also to compare with previous AGCM experiments with idealised SST forcing.

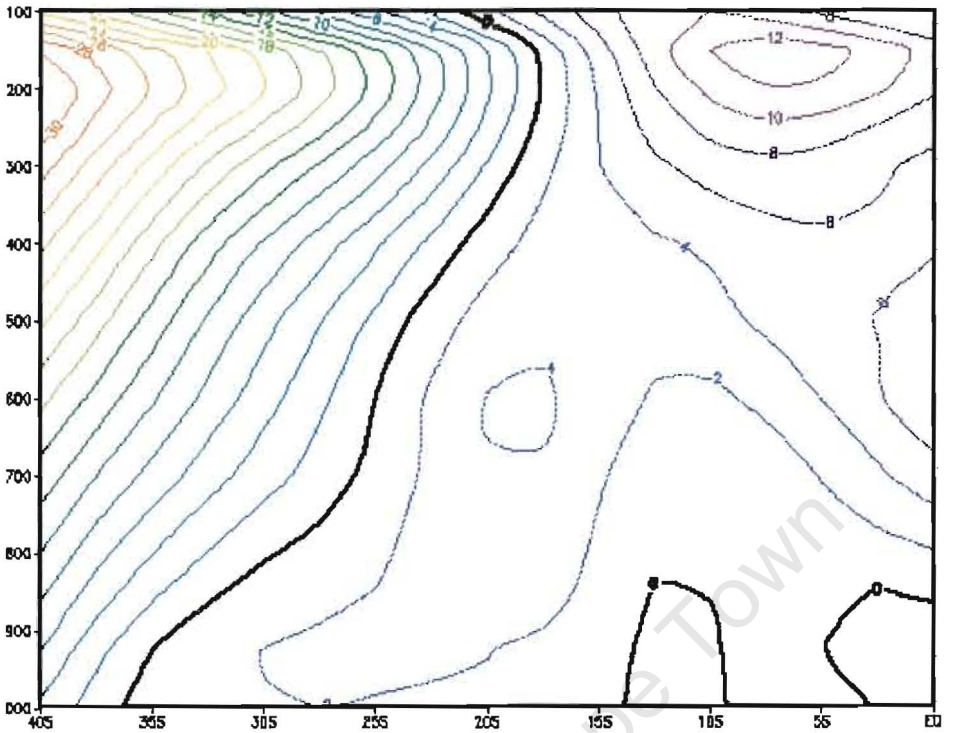

Fig 5.1 *JFM 1970-1999 Zonal wind climatologoy averaged over 10-40°E. Contour interval is 2ms^{-1}.*

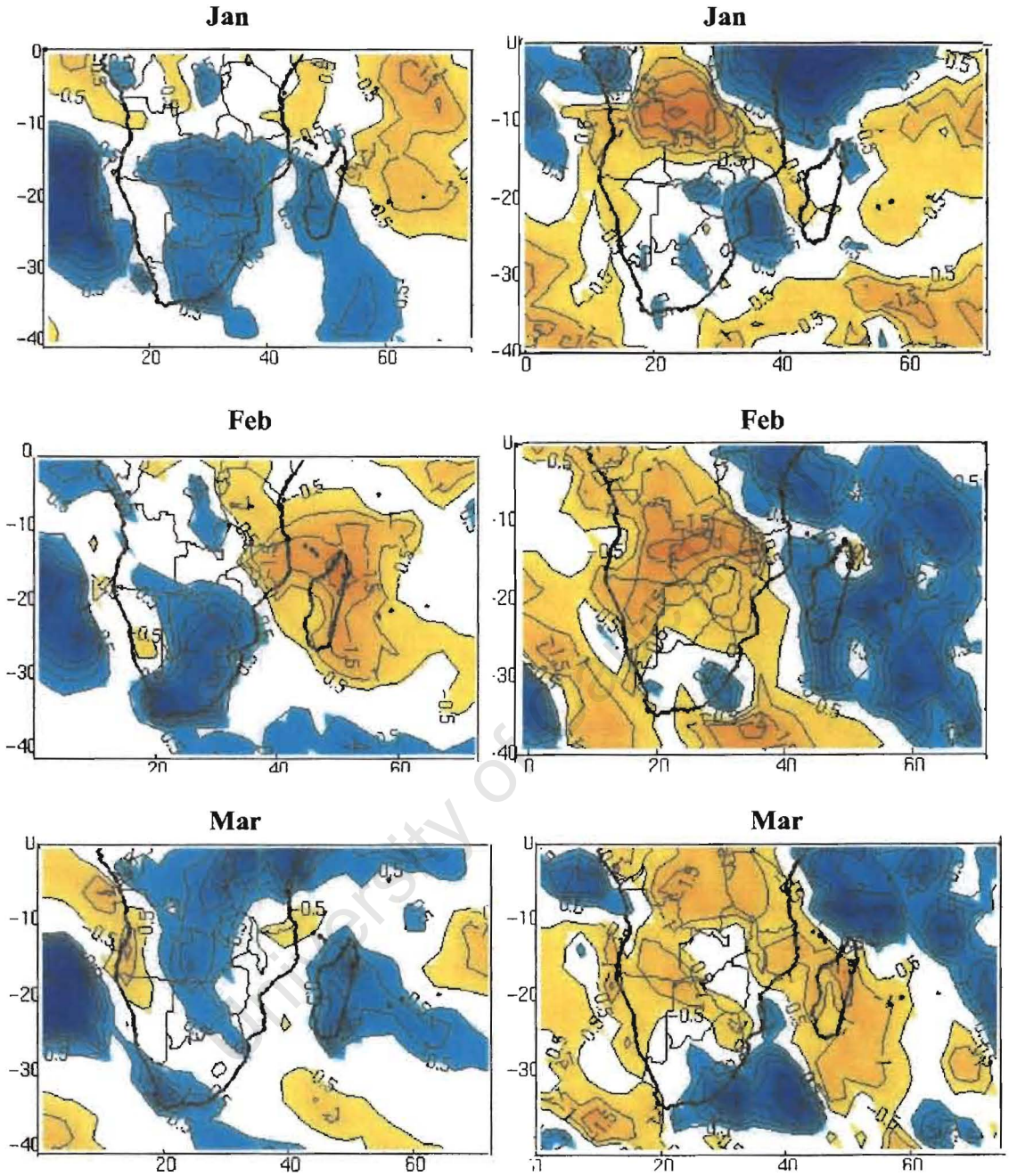

Fig 5.2 *1981 (left panel) and 1998 (right panel) Jan, Feb and Mar monthly mean GPCP normalised rainfall anomalies obtained from www.egs.uct.ac.za/~rouault/. Yellow indicates negative anomalies and blue indicates positive anomalies. Contour interaval is 0.5 standard deviation.*

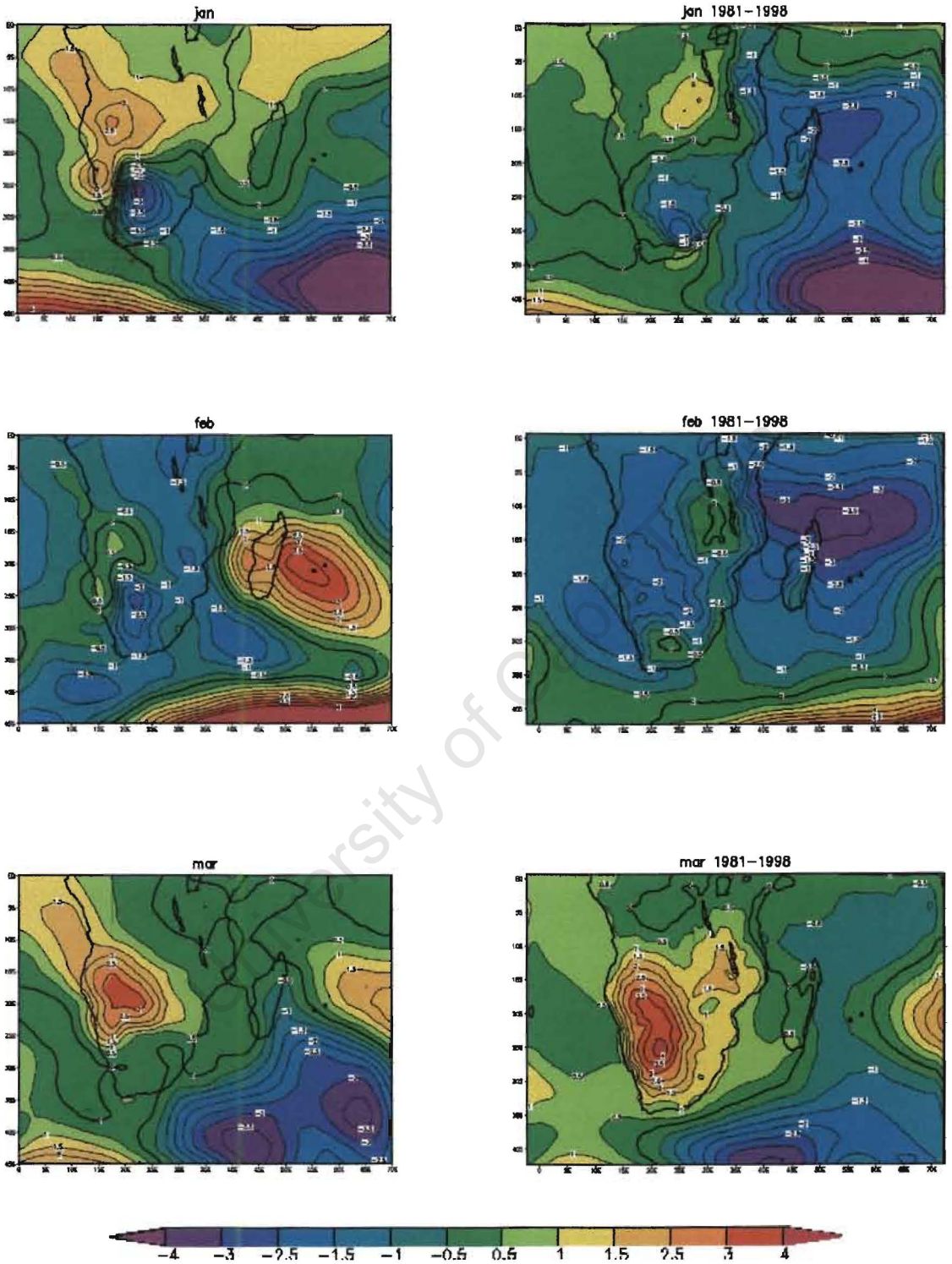

Fig 5.3 *Monthly Sea level pressure differences (1981-1998) Jan, Feb and Mar NCEP (left panel) and MM5 (right panel). Contour interval 0.5hPa.*

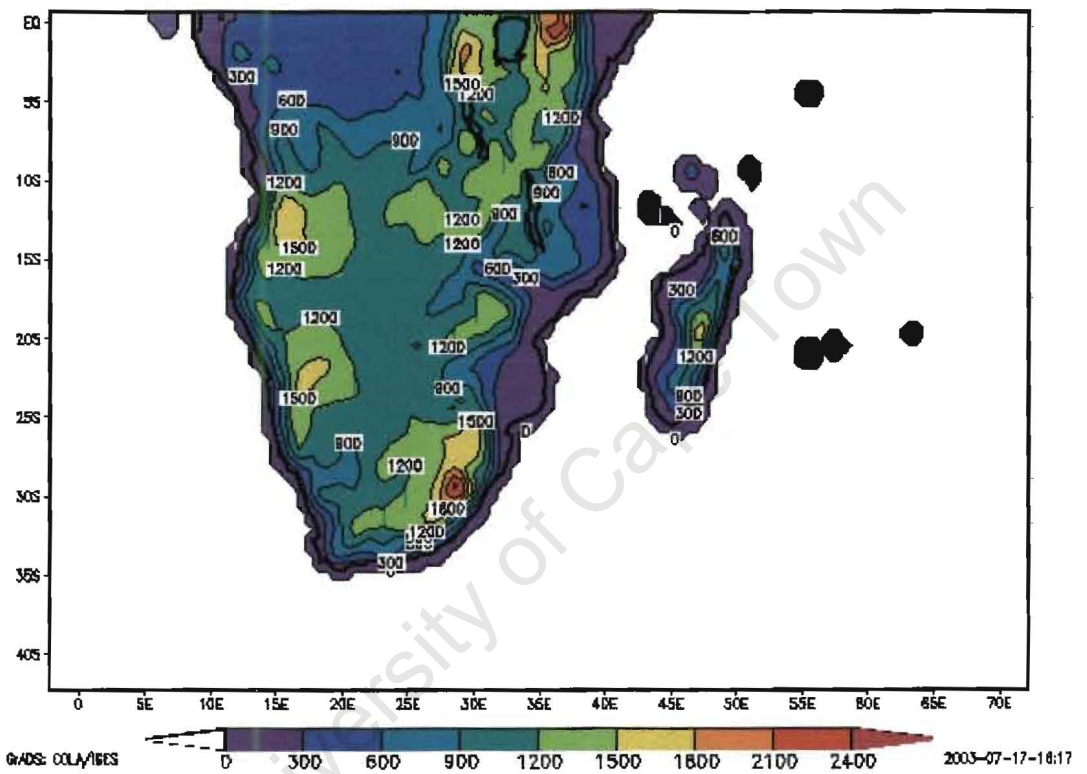

Fig 5.4 *MM5 terrain height in meters. Contour interval is 300m.*

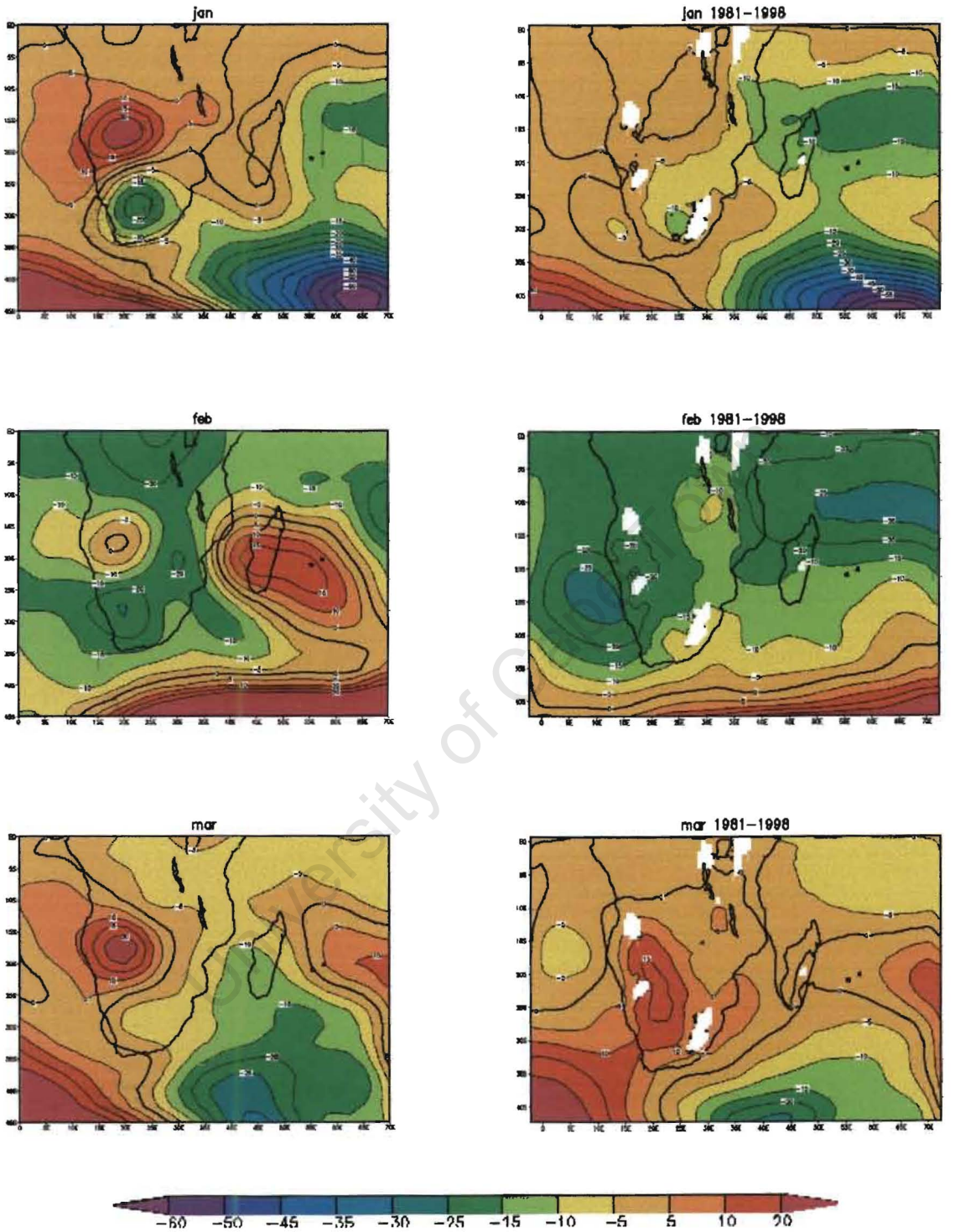

***Fig 5.5** same as **Fig 5.3** except geopotential height at 850 hPa. Contour interval 5m.*

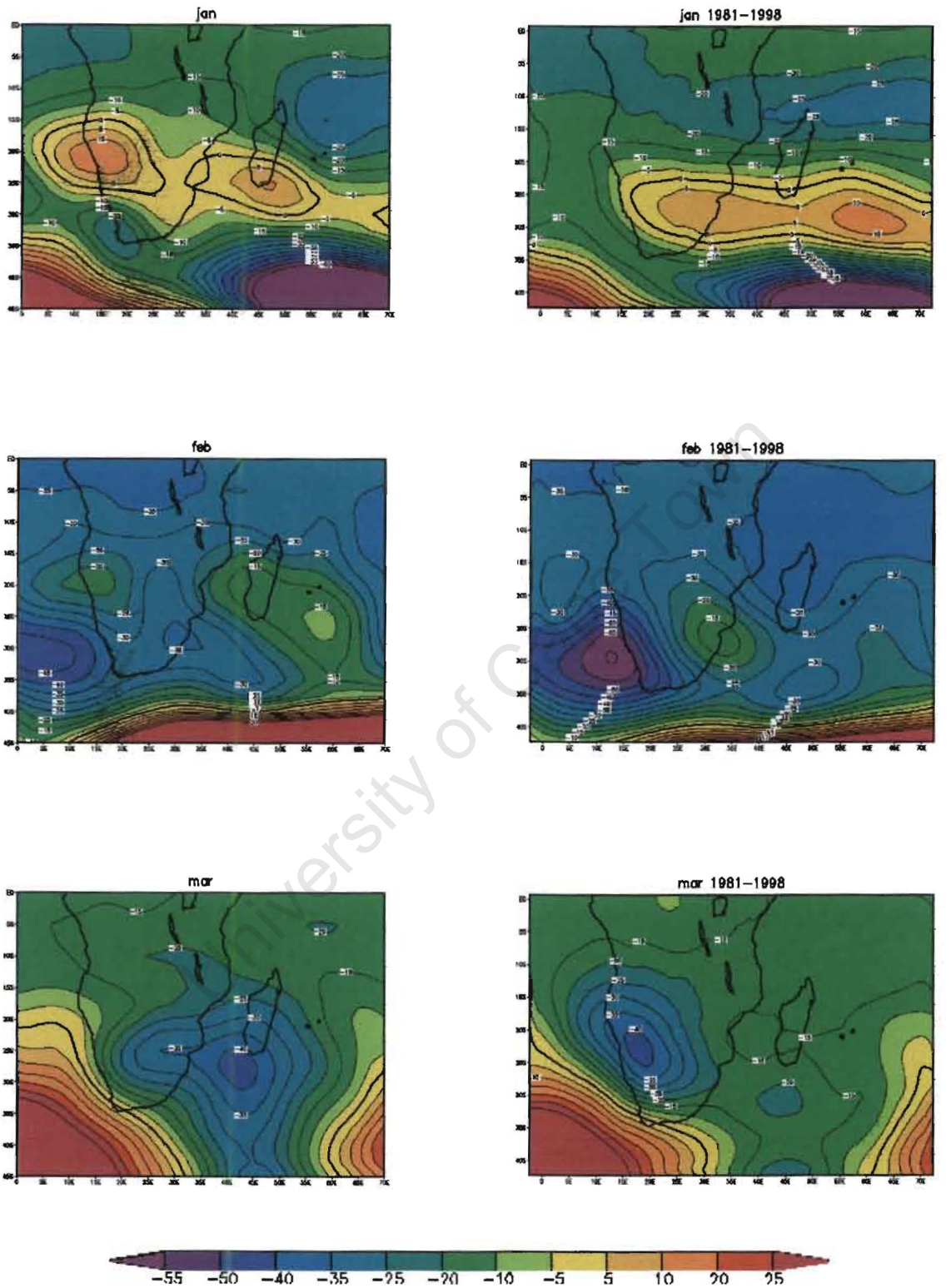

***Fig 5.6** same as **Fig 5.3** except at 500 hPa. Contour interval 5m.*

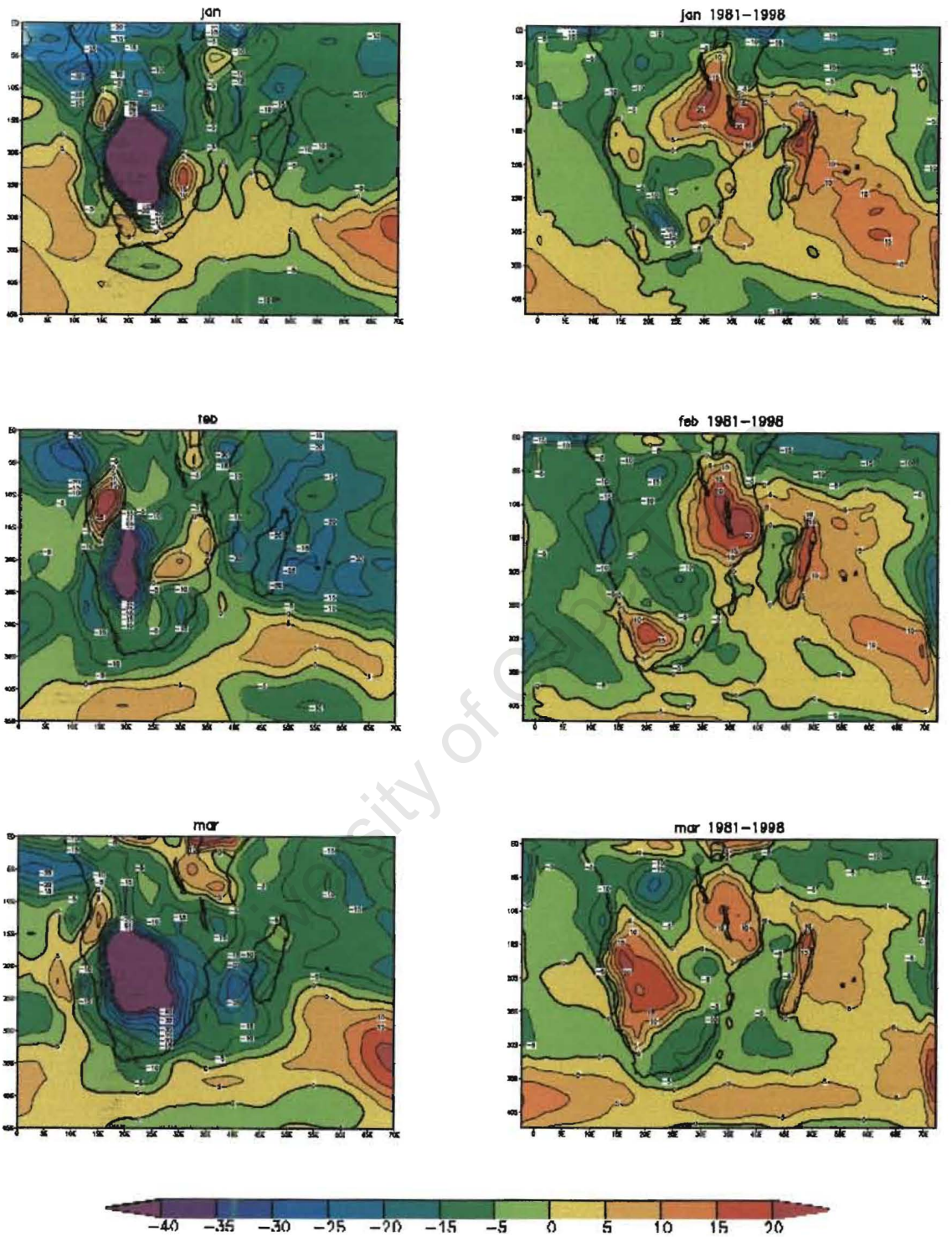

Fig 5.7 *Same as* ***Fig 5.3*** *except for specific humidity at 850 hPa. Contour interval is* $5x10^{-04}$.

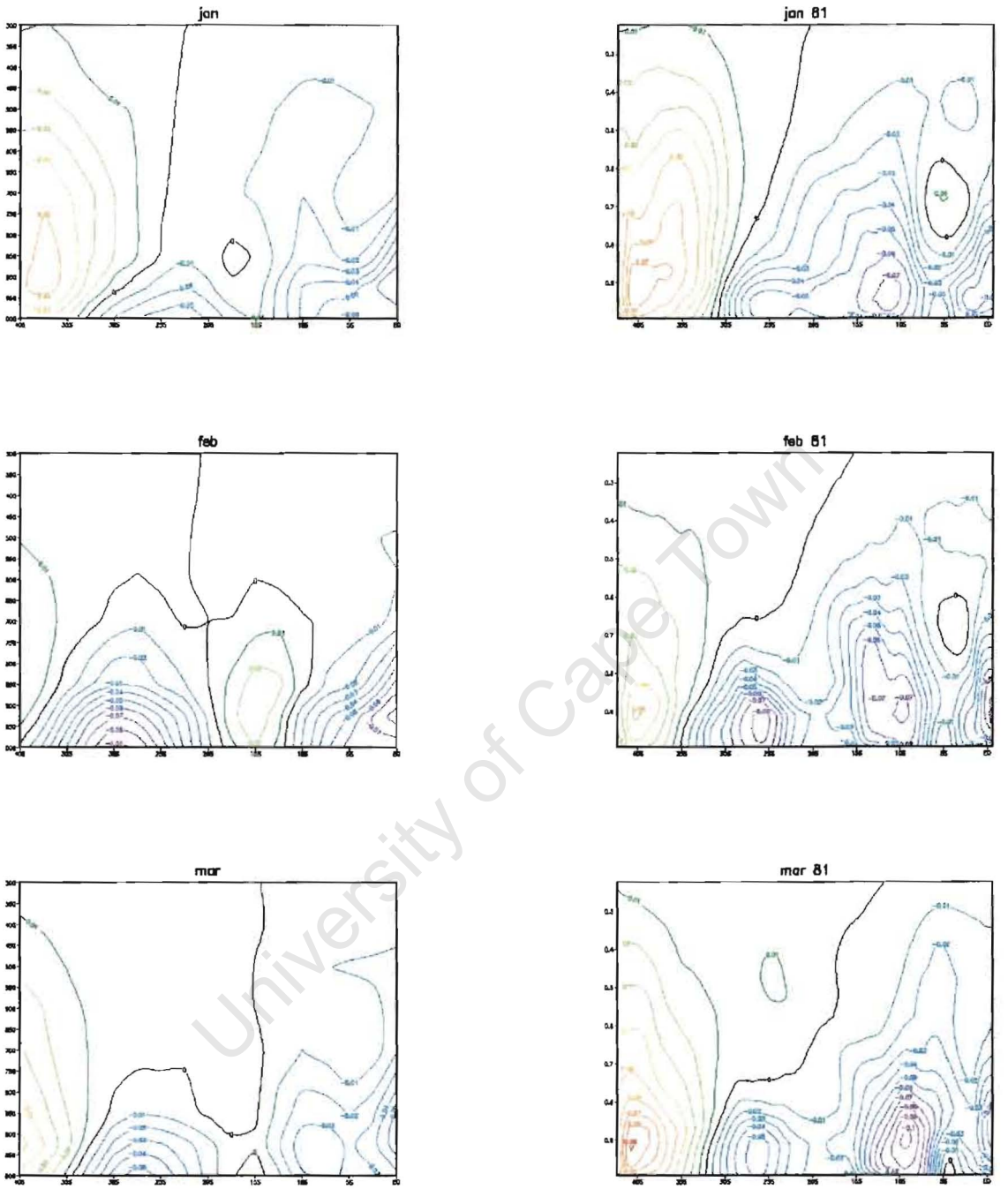

Fig 5.8 *Zonal moisture flux transect along 40°E during 1981 for NCEP (Left panel) and MM5 (Right panel). Contour interval is* $0.01ms^{-1}.kg^{-kg}$.

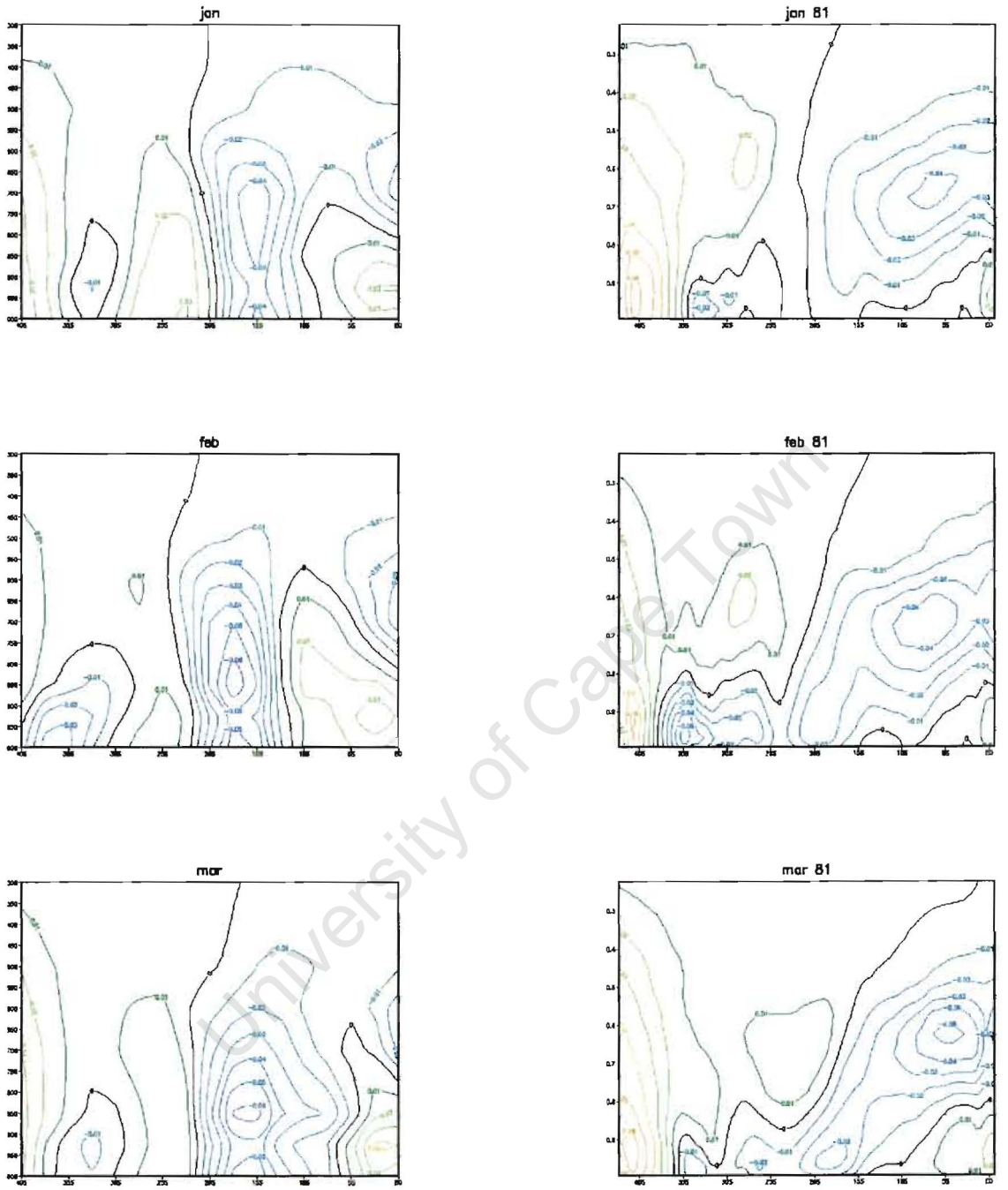

Fig 5.9 *Zonal moisture flux transect along 20°E during 1981 for NCEP (Left panel) and MM5 (Right panel). Contour interval is* $0.01 ms^{-1}.kg^{-kg}$.

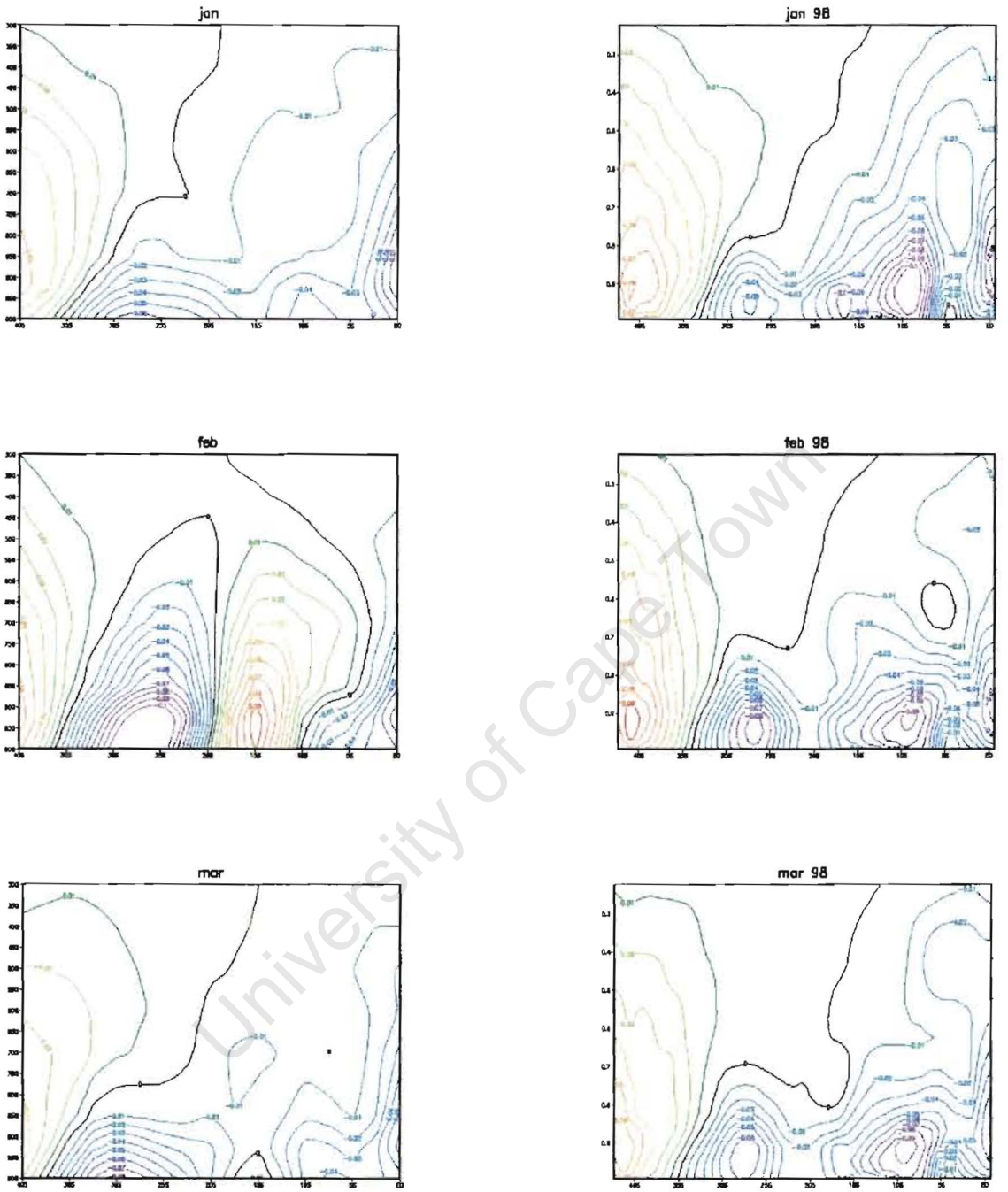

Fig 5.10 *Zonal moisture flux transect along 40°E during 1998 for NCEP (Left panel) and MM5 (Right panel). Contour interval is* $0.01ms^{-1}.kg^{-kg}$.

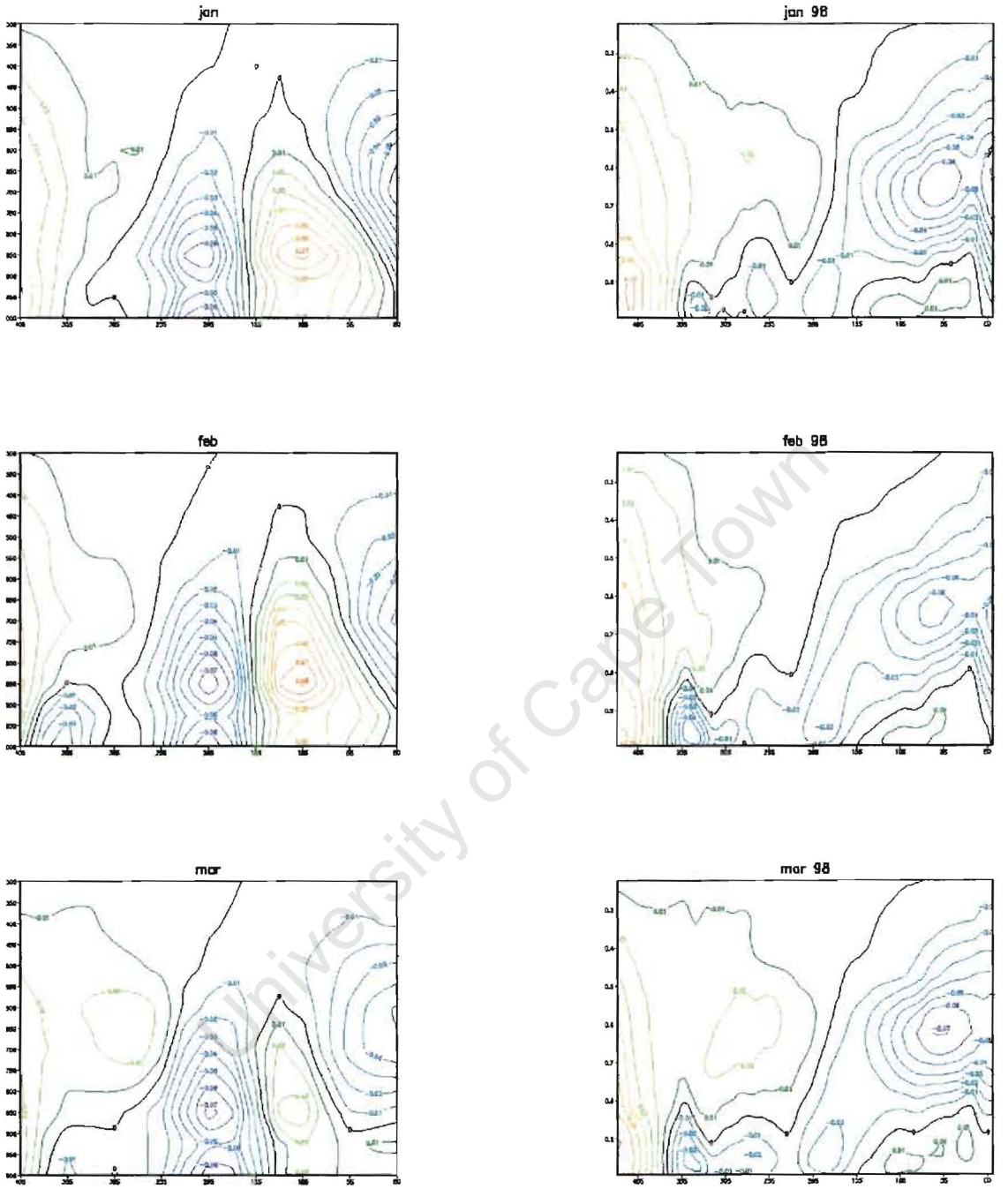

Fig 5.11 *Zonal moisture flux transect along 20°E during 1998 for NCEP (Left panel) and MM5 (Right panel). Contour interval is* $0.01 ms^{-1}.kg^{-kg}$.

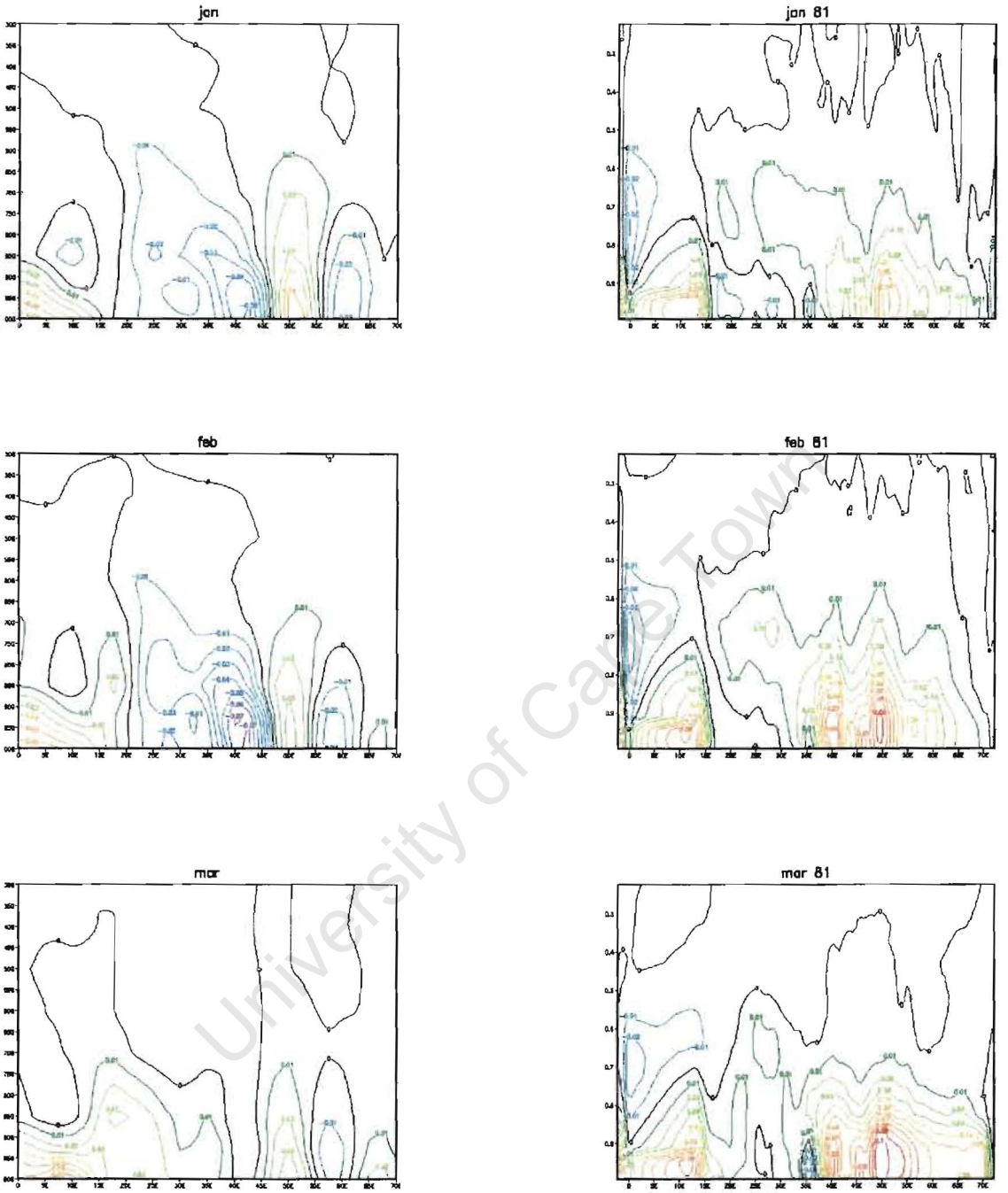

Fig 5.12 *Meridional moisture flux transect along 10°S during 1981 for NCEP (Left panel) and MM5 (Right panel). Contour interval is* $0.01 ms^{-1}.kg^{-kg}$.

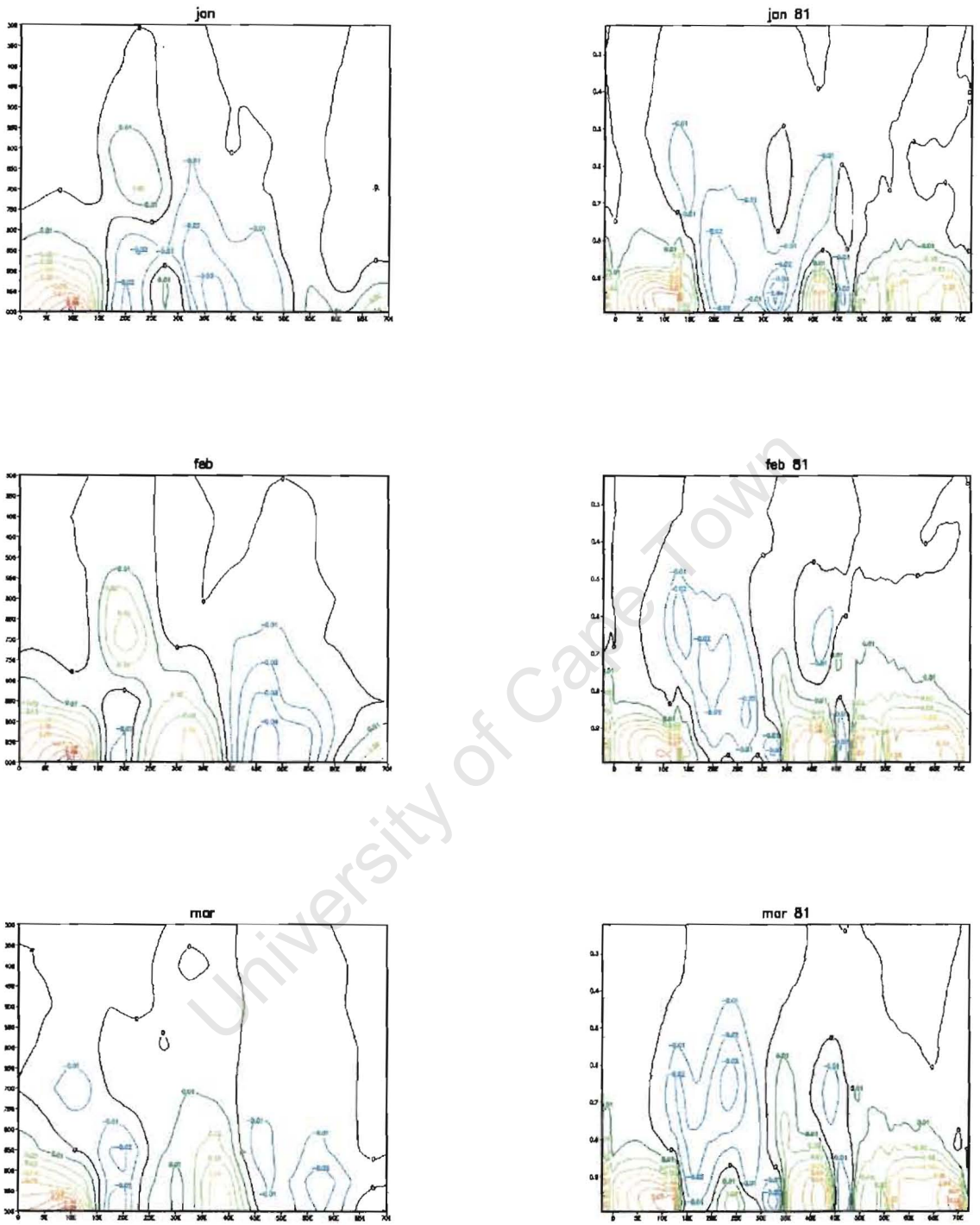

Fig 5.13 *Meridional moisture flux transect along 20°S during 1981 for NCEP (Left panel) and MM5 (Right panel). Contour interval is* $0.01ms^{-1}.kg^{-kg}$.

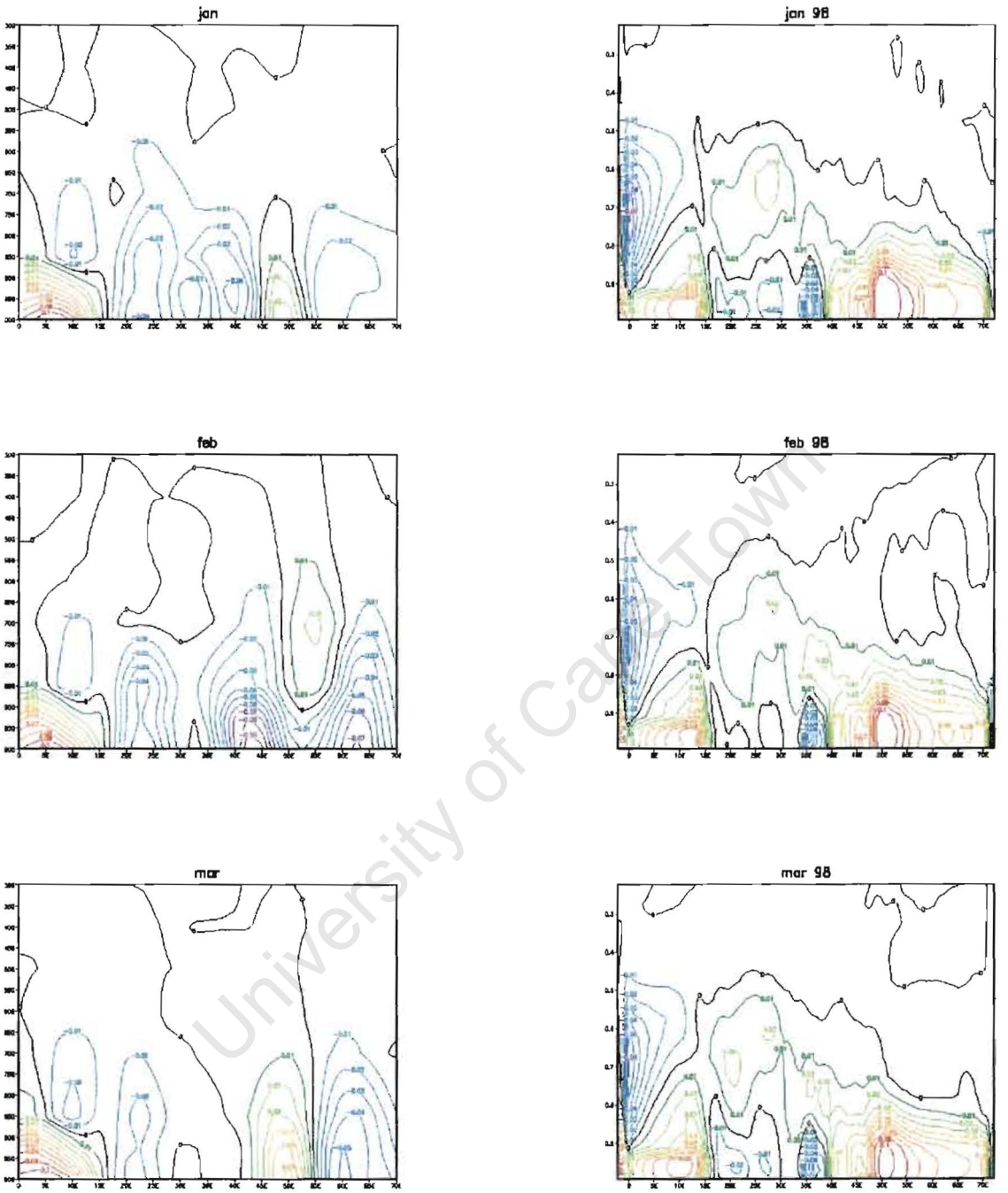

Fig 5.14 *Meridional moisture flux transect along 10°S during 1998 for NCEP (Left panel) and MM5 (Right panel). Contour interval is* $0.01 ms^{-1}.kg^{-kg}$.

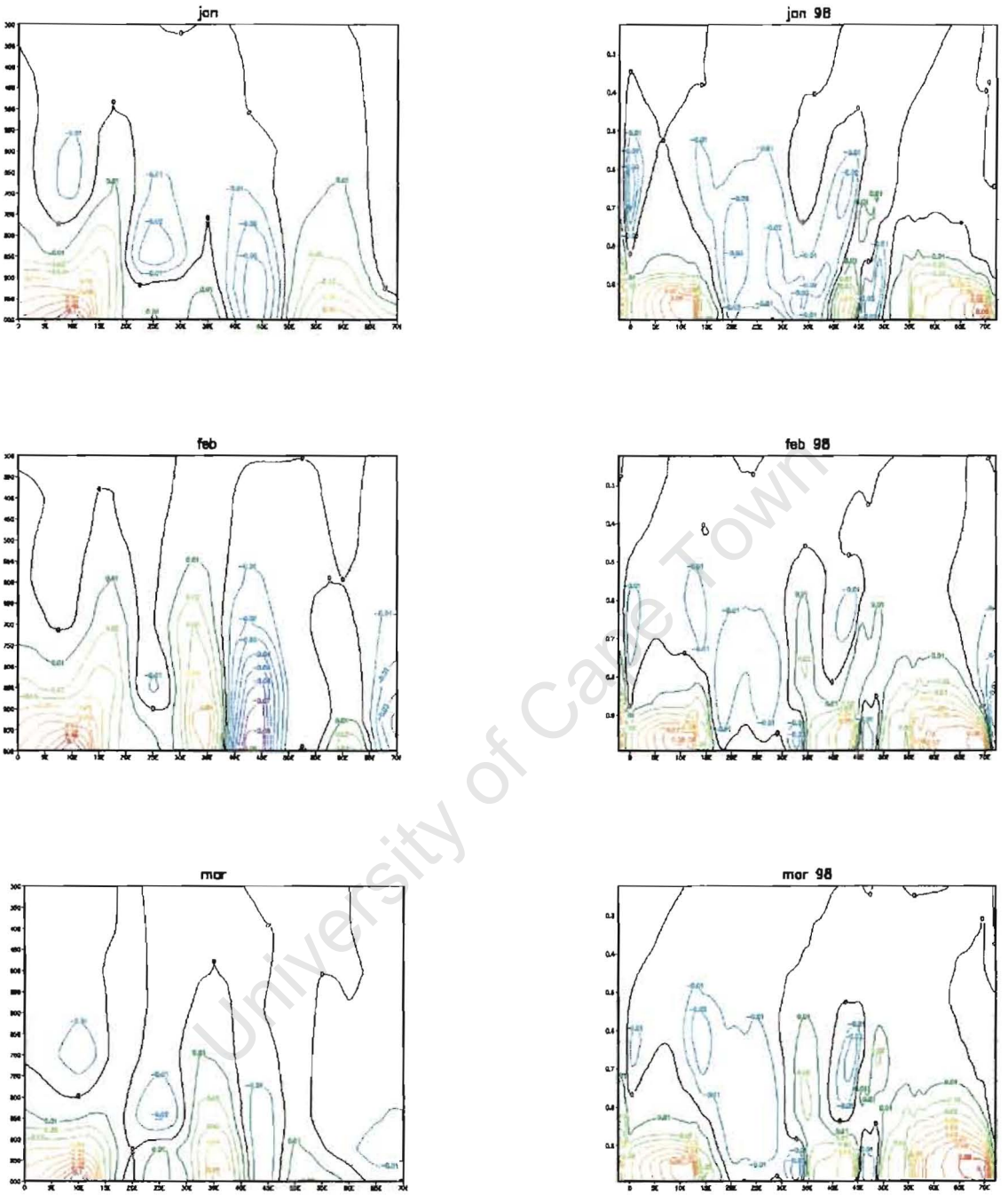

Fig 5.15 *Meridional moisture flux transect along 20°S during 1998 for NCEP (Left panel) and MM5 (Right panel). Contour interval is* $0.01 ms^{-1}.kg^{-kg}$.

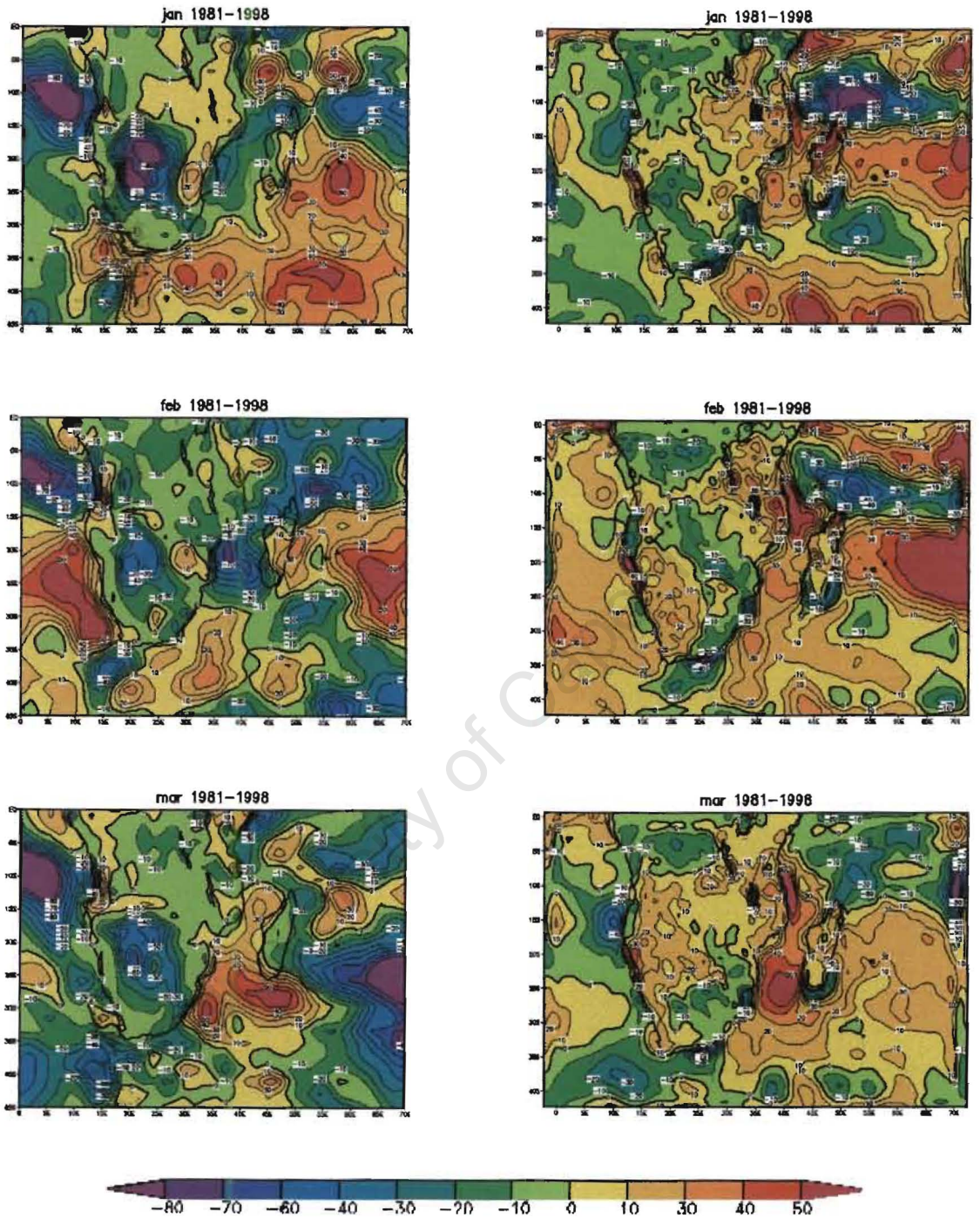

Fig 5.16. *Latent heat flux difference for 1981 and 1998 for NCEP (Left panel) and MM5 (Right panel) Scale is shown and contour interval is 10Wm^{-2}*

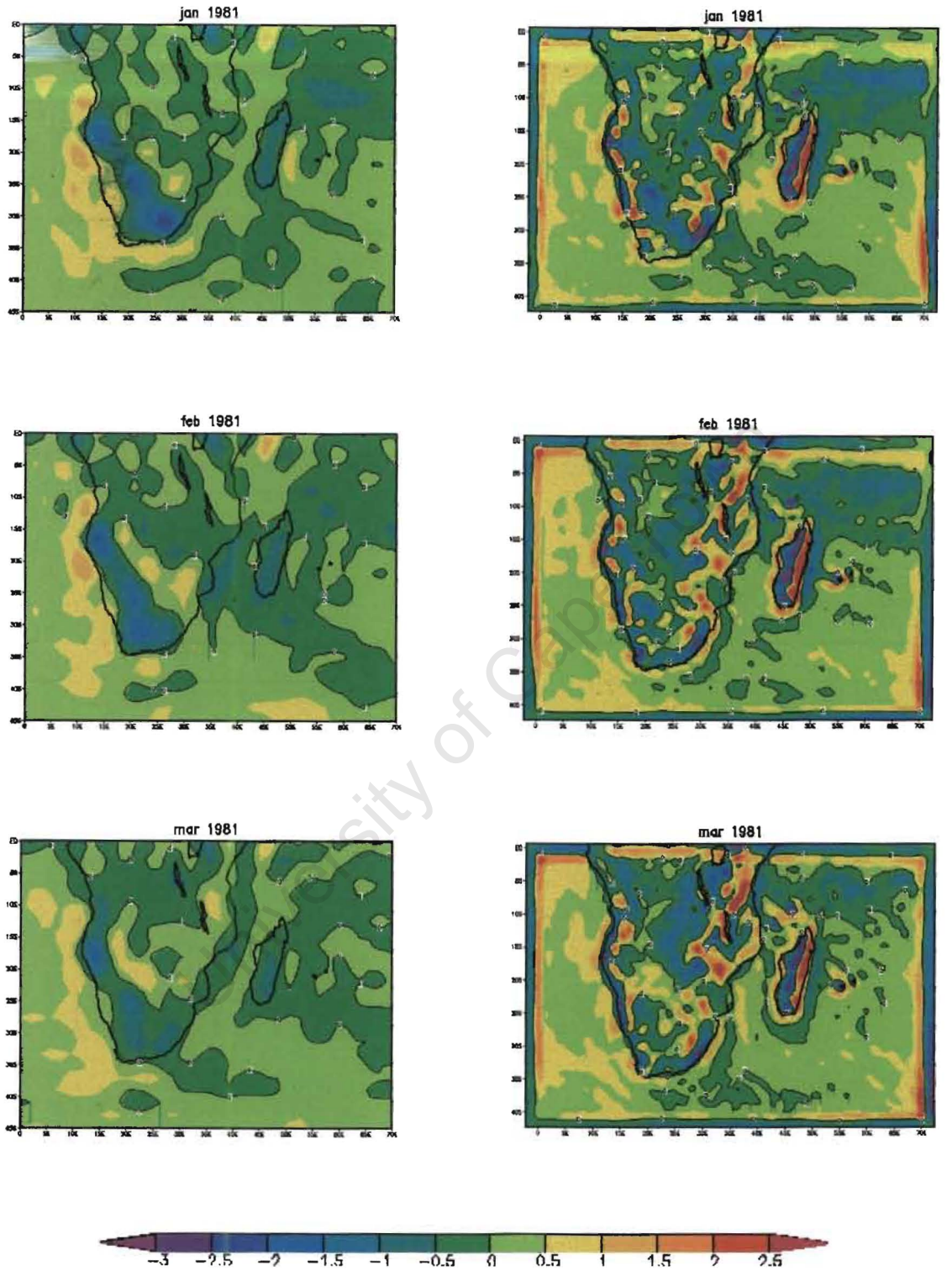

Fig 5.17. *Surface divergence during 1981 for NCEP (Left panel) and MM5 (Right panel). The scale is shown and interval is 0.5 x* 10^{-05}.

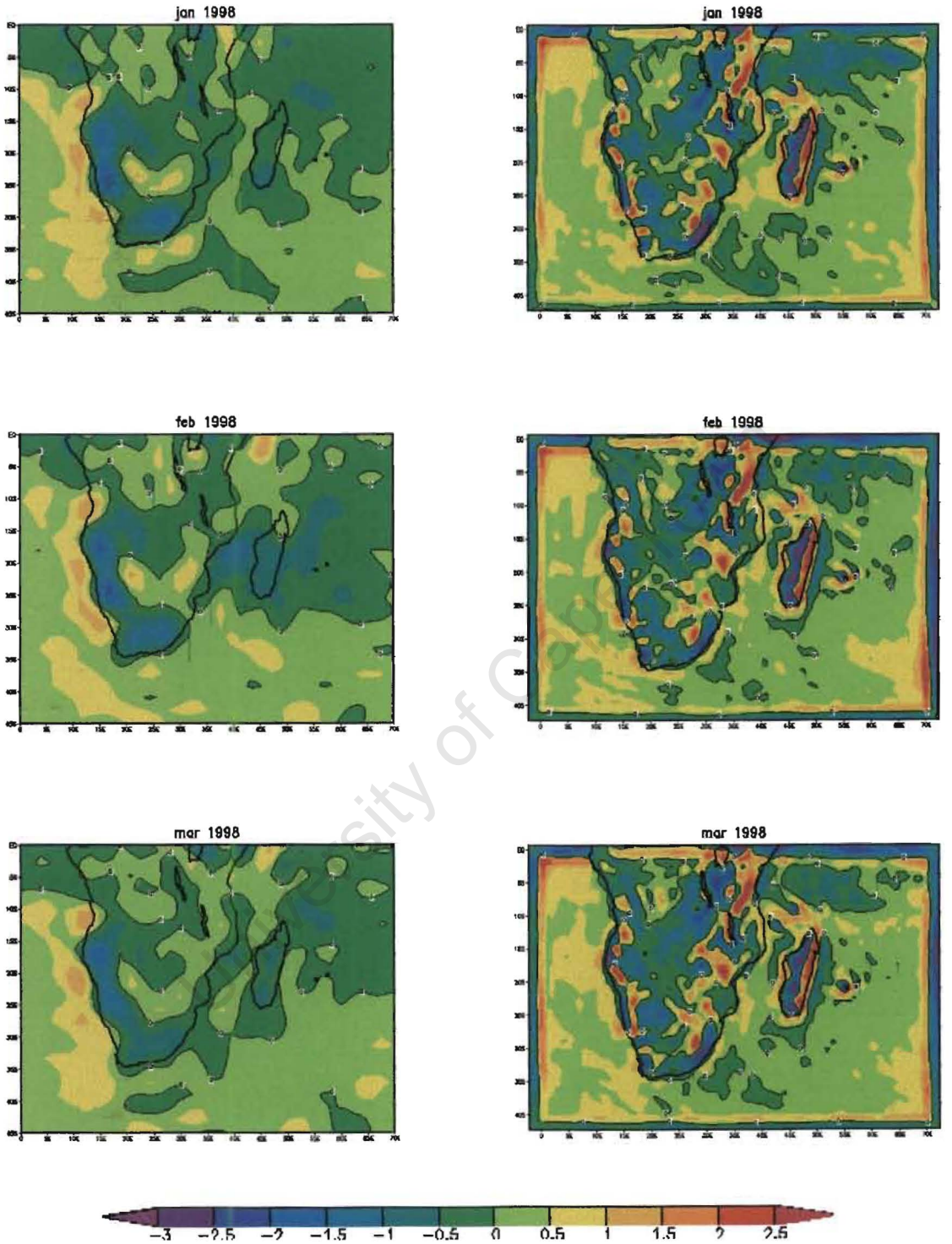

Fig 5.18. *Surface divergence during 1981 for NCEP (Left panel) and MM5 (Right panel). The scale is shown and interval is 0.5 x* 10^{-05}.

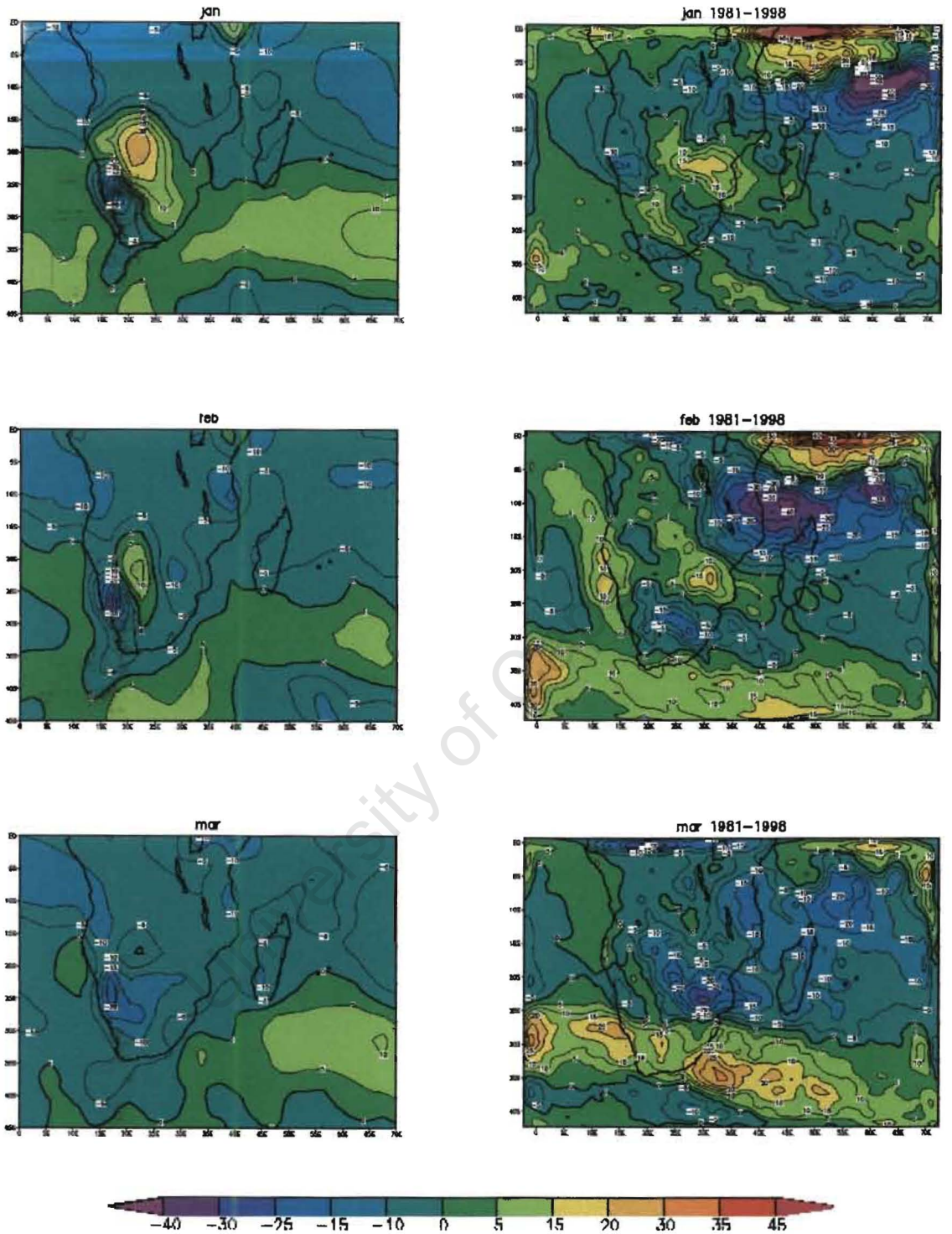

Fig 5.19 *Same as* ***Fig 5.3*** *except for Out-going Long-wave Radiation. Contour is interval is* $5Wm^{-2}$

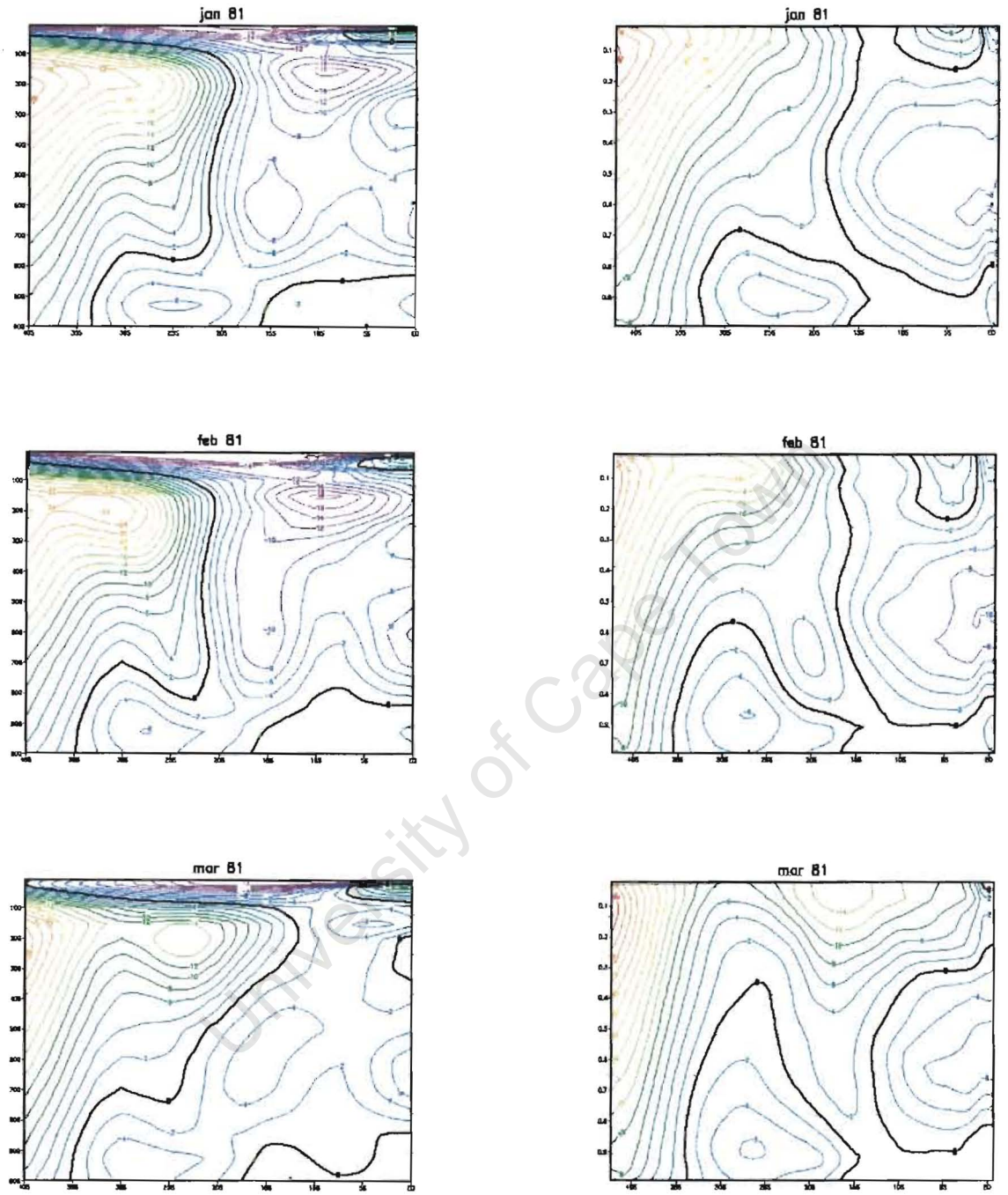

Fig 5.20 *A transect of zonal winds for 1981; taken along* ***10°E****. MM5: Right panel and NCEP: Left panel. Contour interval is* $2ms^{-1}$.

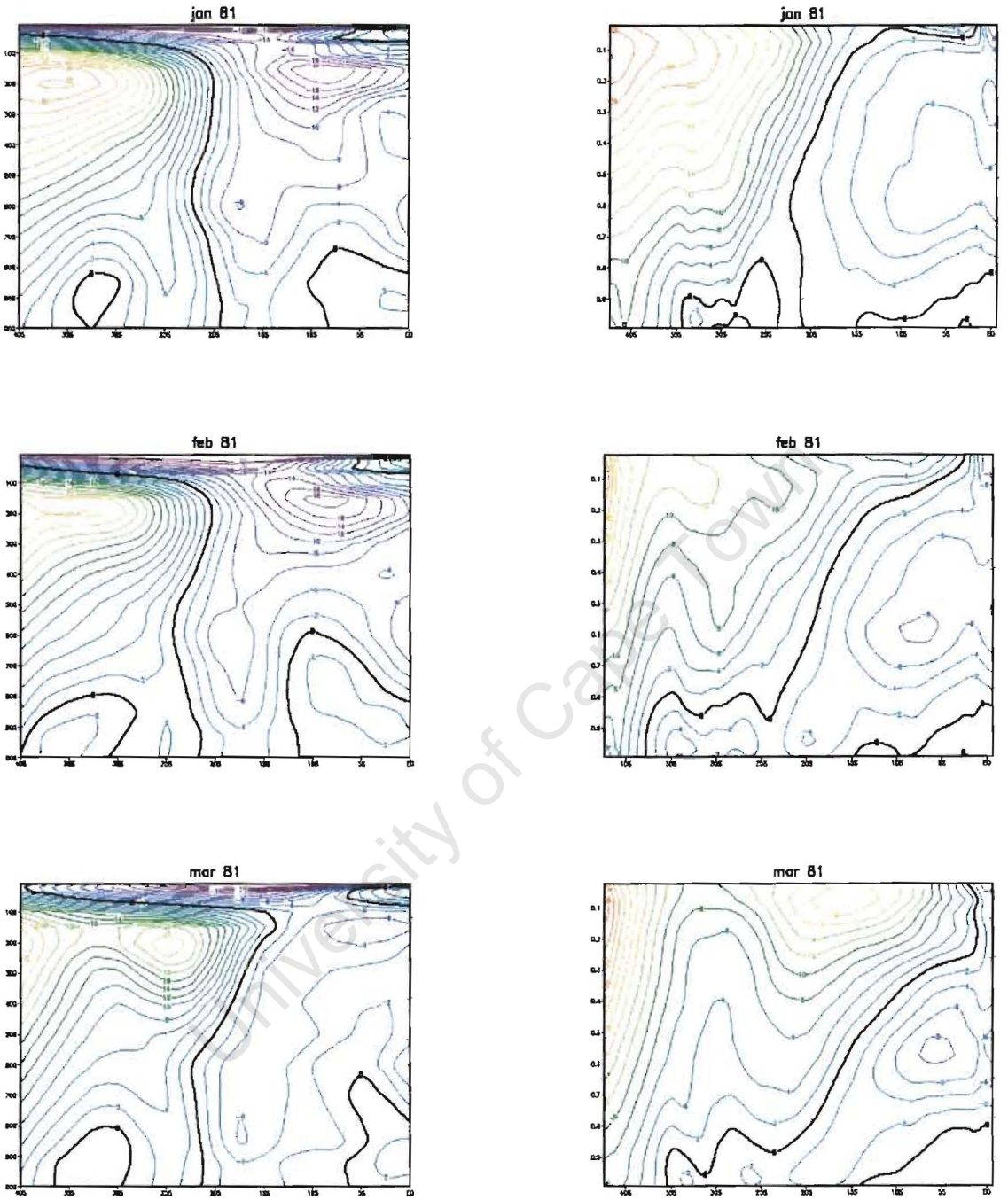

Fig 5.21 *A transect of zonal winds for 1981; taken along* ***20°E****. MM5: Right panel and NCEP: Left panel. Contour interval is* $2ms^{-1}$.

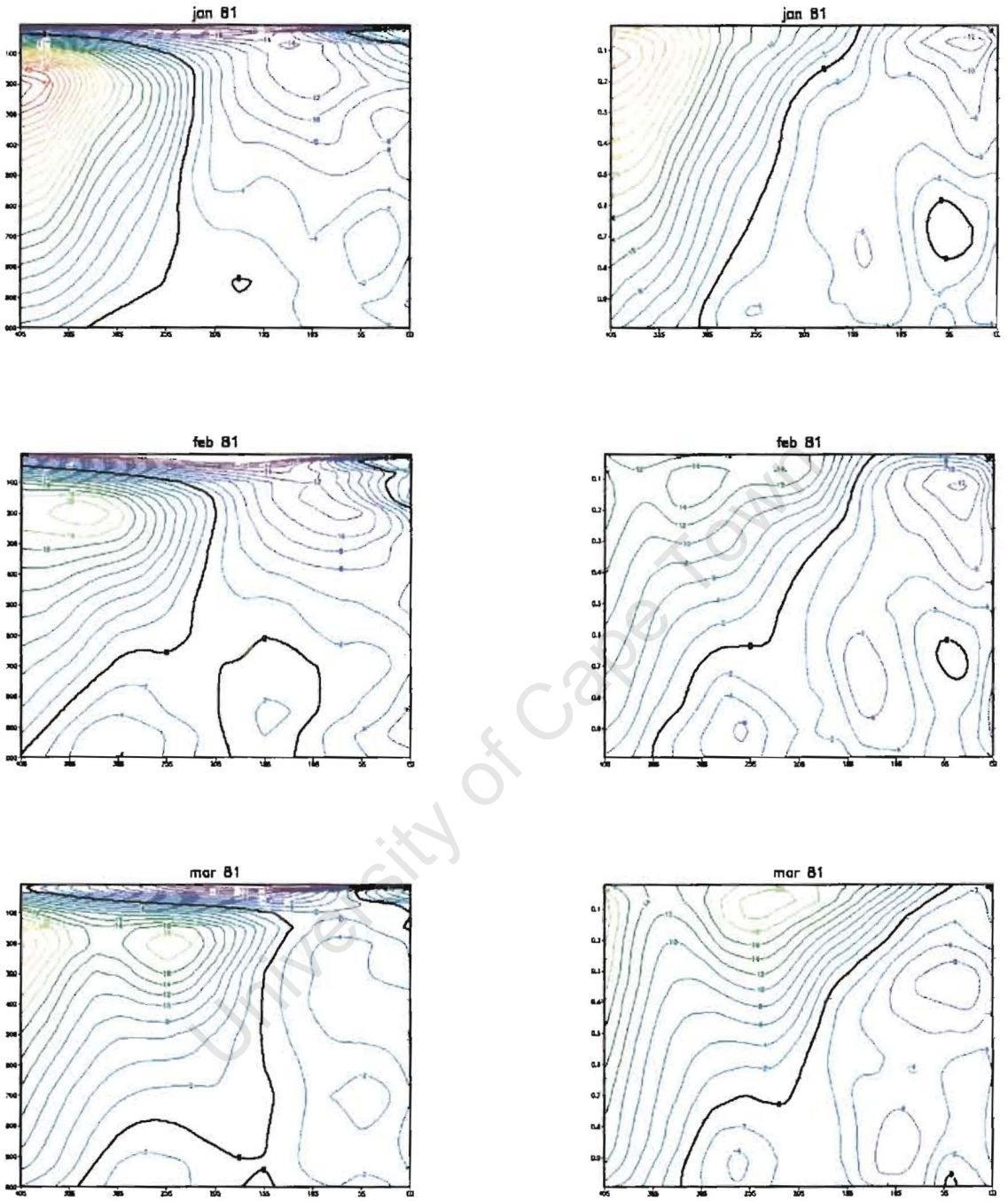

Fig 5.22 *A transect of zonal winds for 1981; taken along* ***40°E****. MM5: Right panel and NCEP: Left panel. Contour interval is* $2ms^{-1}$.

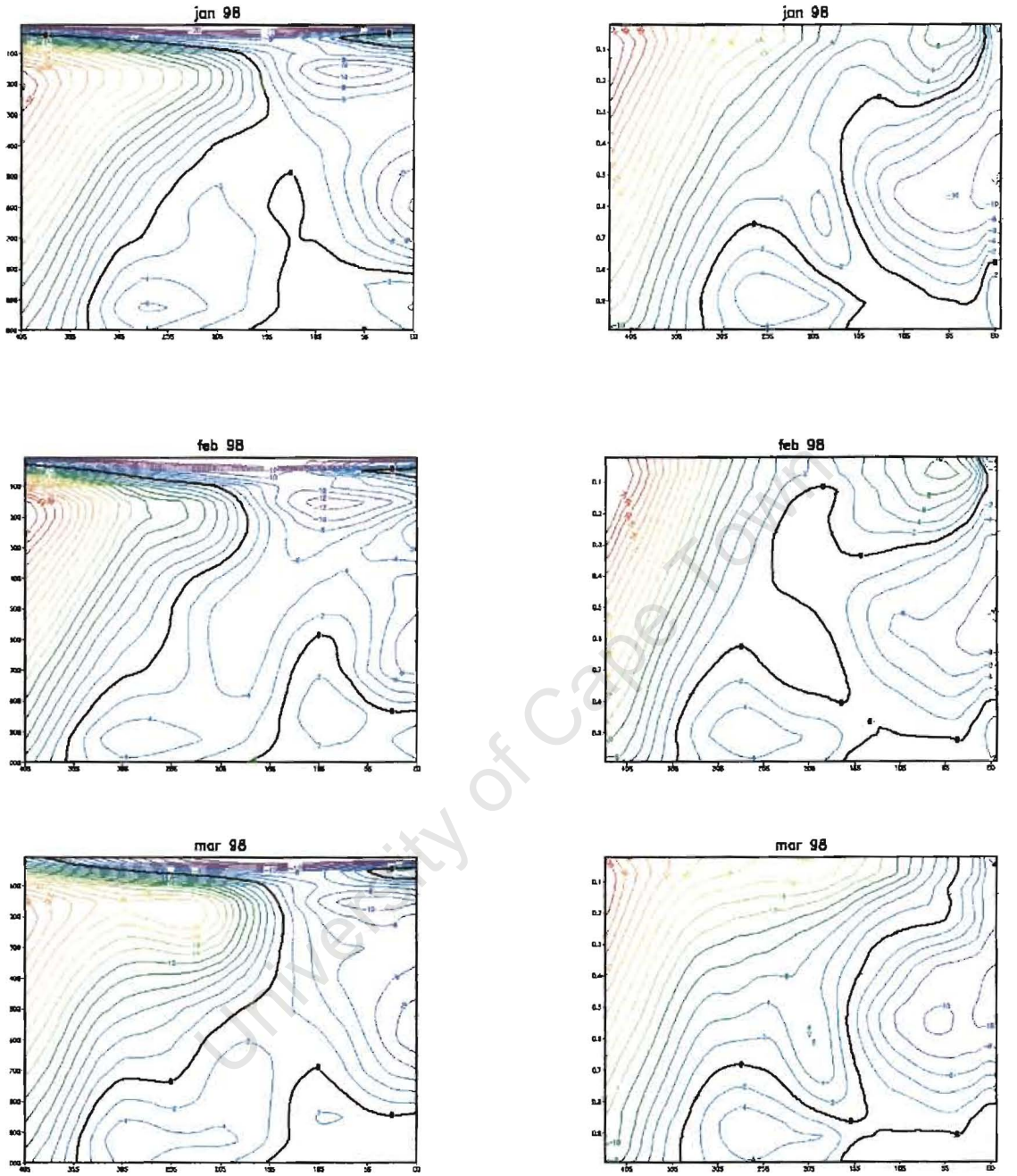

Fig 5.23 *A transect of zonal winds for 1998; taken along* ***10°E****. MM5: Right panel and NCEP: Left panel. Contour interval is* $2ms^{-1}$.

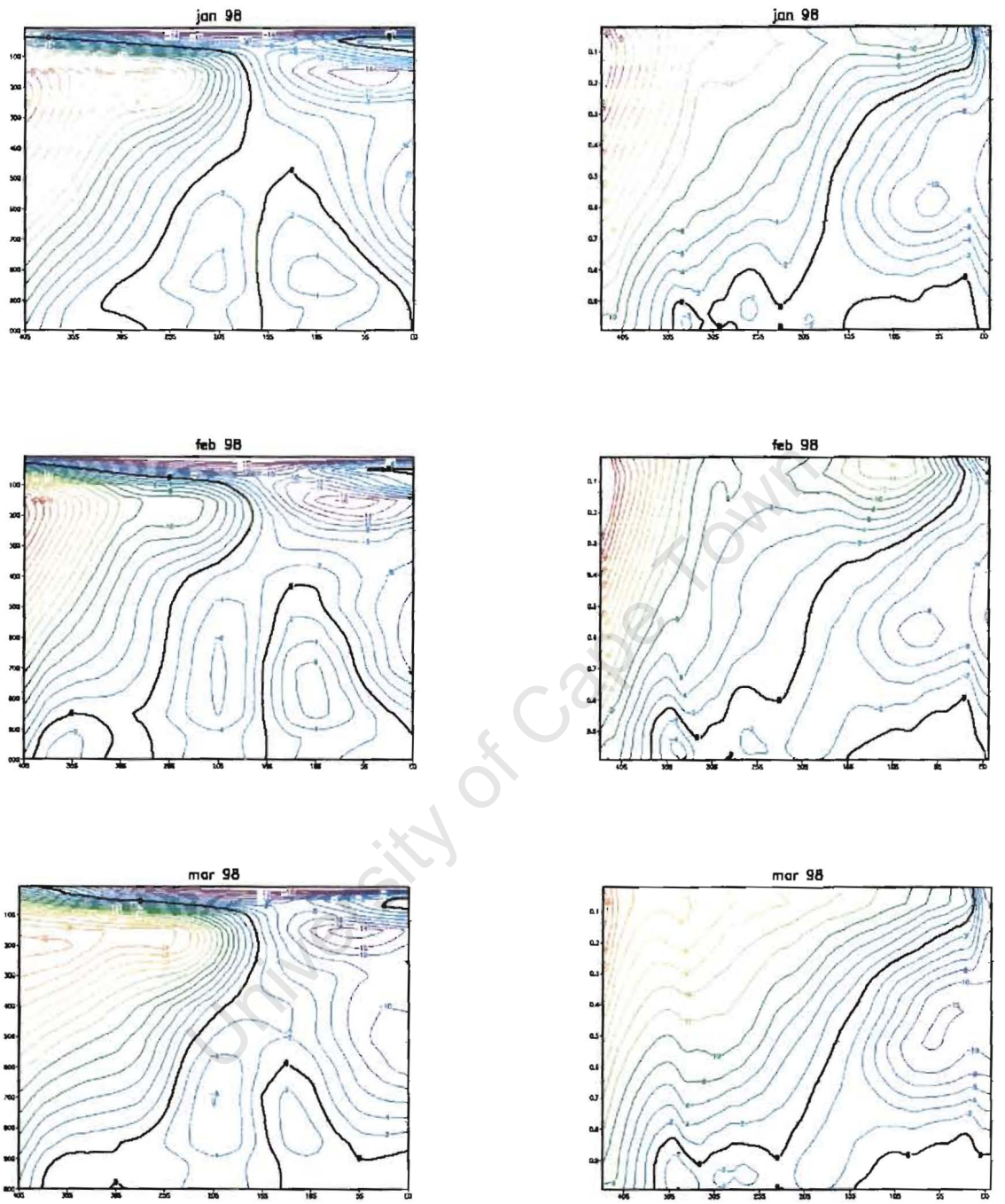

Fig 5.24 *A transect of zonal winds for 1998; taken along* ***20°E****. MM5: Right panel and NCEP: Left panel. Contour interval is* $2ms^{-1}$.

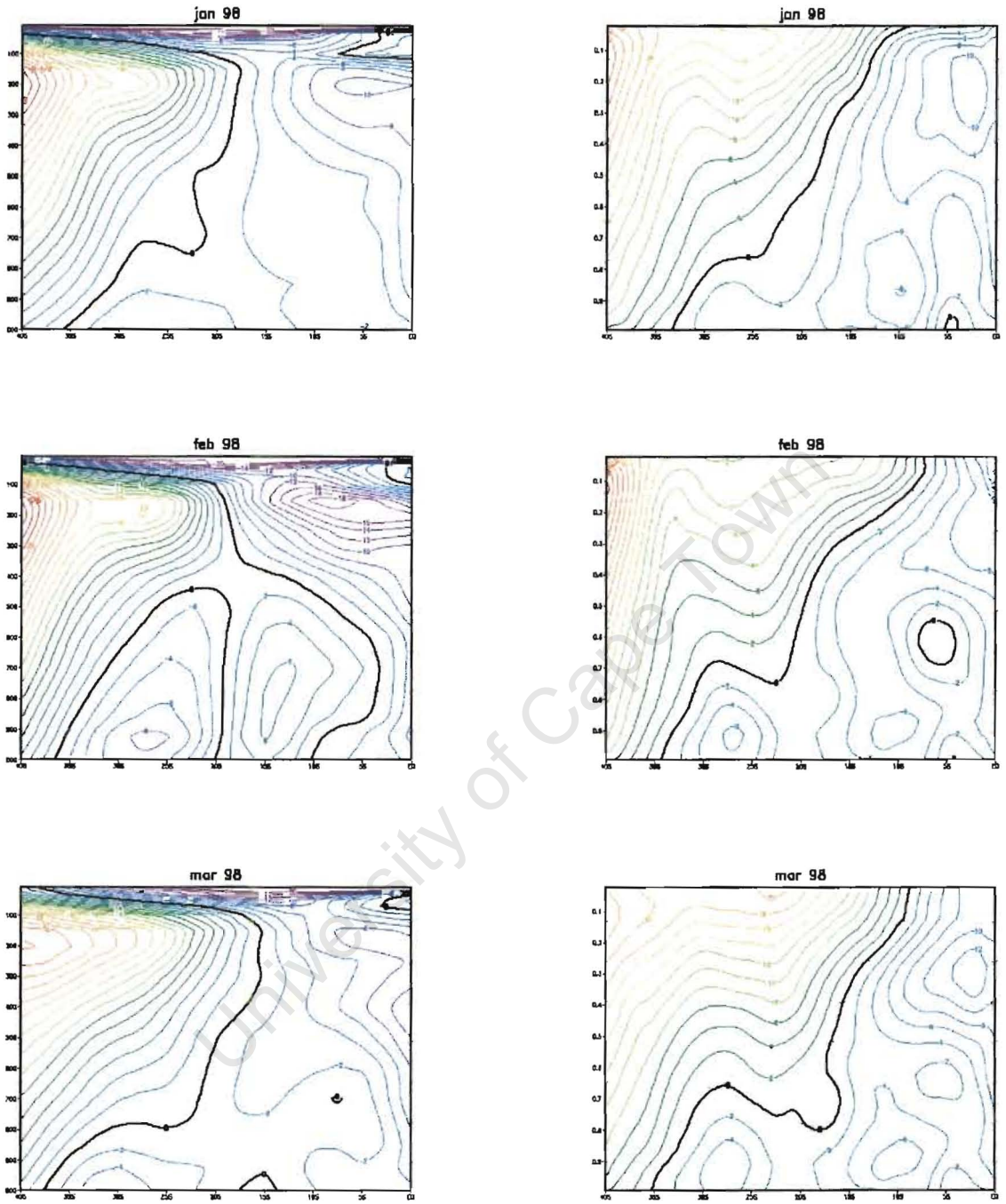

Fig 5.25 *A transect of zonal winds for 1998; taken along* ***40°E****. MM5: Right panel and NCEP: Left panel. Contour interval is* $2ms^{-1}$.

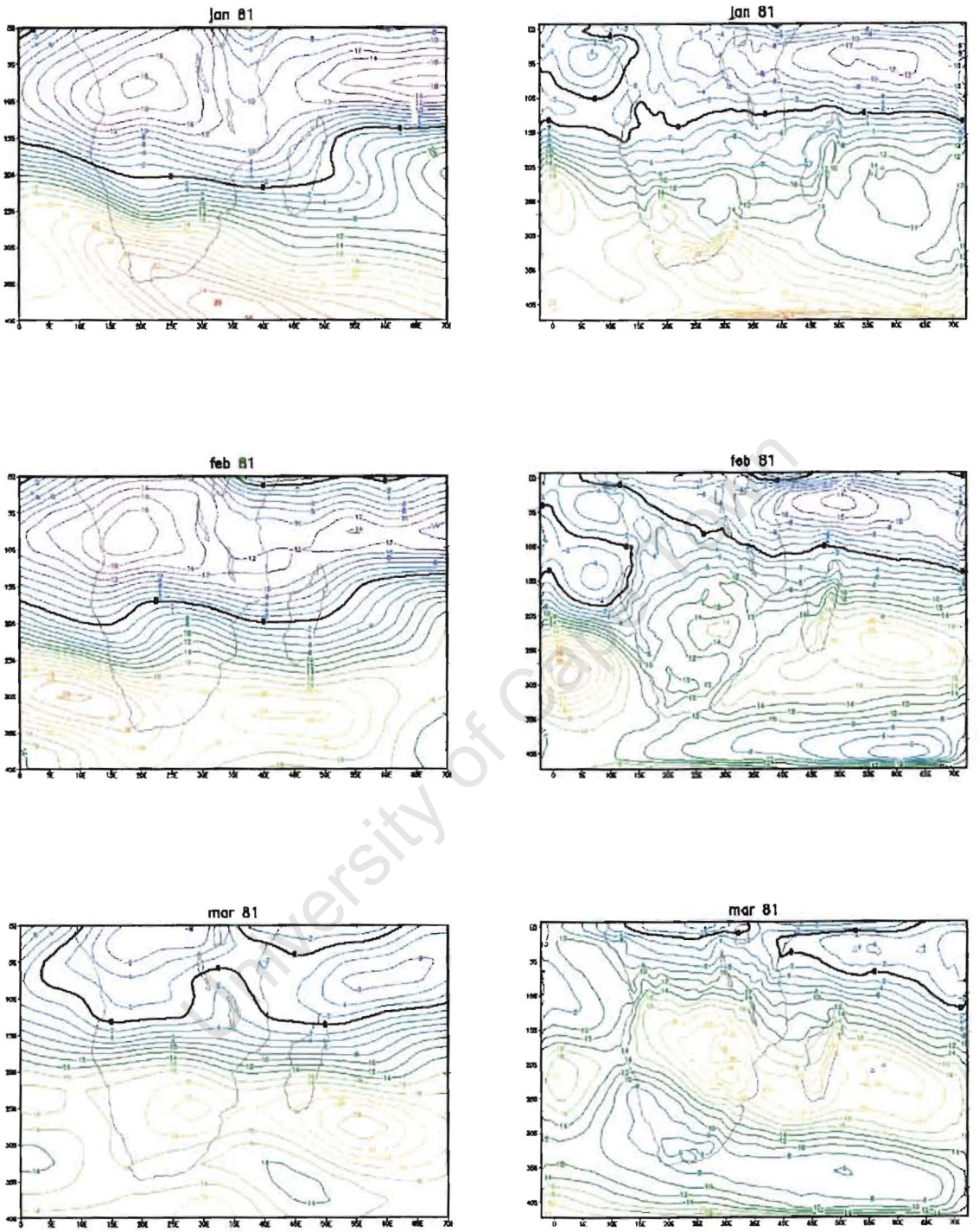

Fig 5.26. *Zonal wind shear (200-850 hPa) for 1981. MM5: Right panel, NCEP: Left panel. Contour interval is* $2ms^{-1}$.

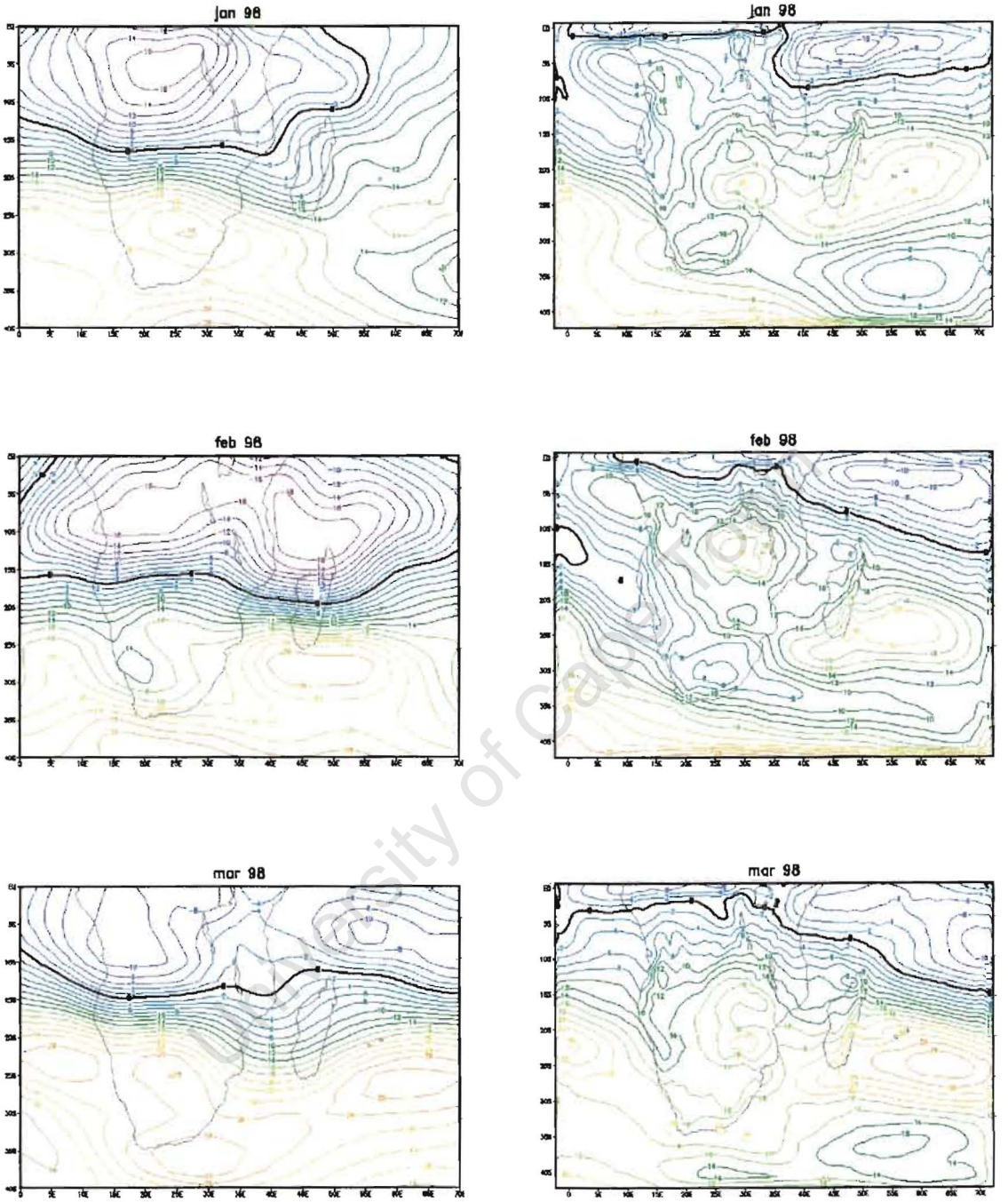

Fig 5.27. Zonal wind shear (200-850 hPa) for 1998. Contour interval is 2ms^{-1}.

Chapter 6

The Observed and Idealised Experiments

6.1 Introduction

Using a general circulation model, Reason and Mulenga (1999) and Reason (2001b) have shown that atmospheric circulation over southern Africa is sensitive to SST anomalies in the southwest Indian Ocean, particularly when the region of warm SSTs is close to the eastern coast of subcontinent. Furthermore, Reason (2001) has suggested that the response over southeastern Africa is stronger if the warm pole of the subtropical SST dipole pattern is located closer to the subcontinent than when it is further to the east. Such perturbation experiments with numerical atmospheric models forced by observed SST anomalies may be one method of examining and understanding the atmospheric response over southern Africa to anomalous ocean conditions. This chapter presents the results of the model response over southern Africa to an idealized warm SST (Skin temperature and SST are used interchangeably here) forcing that resembles the warm pole of the 1980/1 positive event (experiment four). As indicated in chapter three, the domain size is such that the signal from the lateral boundary conditions is unlikely to have a significant influence on the response over Southern Africa. Results presented here are monthly differences from the regional model climatology obtained by running the model with climatological SST while maintaining the 1980/81 conditions for the other parameters (experiment three). These results are then compared with the anomalies of the 1980/1 simulation where the model was run with observed SSTs (experiment one), obtained from the same climatology as above. In order to examine the atmospheric response, particularly circulation changes, to SST forcing in experiment four, the sea level pressure, geopotential height winds and latent heat flux differences from climatology are examined. Like in the previous chapter ensemble averages, with each ensemble consisting of five integrations, are used in this analysis

6.2 Observed and Idealised SST Forcing

Fig 6.1 shows the observed and idealized SKT anomaly forcing for the 1980/1 dipole event. In the observed case, the location of the warm pole is further east, southeast of Madagascar compared to the idealised case in which the warm pole is to the south of Madagascar. As mentioned in **chapter 3**, the forcing in the idealised case is close to the subcontinent so as to make the response stronger. As can be seen from **Fig 6.1** the magnitude of the SST anomaly over the observed warm pole forcing is varying (left panel). In January, the anomaly is about 1.8°C, about 1.3°C in February and about 1.0°C in March. The location of the centre of the observed warm pole appears to shift eastward slightly from January to March. However, the magnitude and centre of the idealised warm pole forcing (right panel) is constant at 2.0°C and 40°E, 30°S throughout the simulation period.

6.3 The Model's Response

Linear quasi-geostrophic theory (Gill, 1982; Fandry and Leslie, 1984) suggests that a low pressure anomaly which decays with height is generated over and downstream of a warm SST anomaly. This theory suggests a baroclinic response to surface heating, which is characterized by a low level trough and an upper level ridge (Peng et al, 1997). Consistent with this theory a low pressure anomaly is generated over the warm pole in the three months in the idealized experiment as shown in **Fig 6.2** (right panel). Note that the anomalies in this case are obtained from the run with climatological SSTs (i.e. Experiment three. See **chapter three**). The strength of the low surface pressure anomaly varies in the three months. These variations may not be directly attributed to the warm pole forcing because the forcing is constant both in time and location although we might expect strongest response in March after the forcing has been imposed for the longest. However, these variations in January, February and March in the idealized experiment may also be due to variations in the NCEP boundary conditions imposed at the edges of the domain. The low pressure anomaly is observed to peak in February in the idealised

case. Examination of the 850 hPa geopotential height of the idealized and observed experiments indicates that the low pressure anomaly weakens and tilts west in the lower 1.5km of the atmosphere with height (**Fig 6.3**). Inspection of the geopotential height at 500 hPa (**Fig 6.4**) shows that the weakening only occurs in January at 500 hPa with a reverse in sign of the anomaly over the southwest Indian Ocean in the idealised experiment in February and March.

6.4 Circulation Changes.

Consistent with the quasi-geostrophic theory (Gill, 1982; Fandrey and Leslie, 1984), a low sea level pressure anomaly is generated over the warm pole in the idealised and observed experiments. In the idealised experiment, the low pressure anomalies extend to the eastern and southern parts of the subcontinent in February and only the eastern parts in March (**Fig 6.2** right panel). The anomalies are weaker in January compared to February and March. The sea level pressure anomalies are less pronounced over the subcontinent in the idealised experiment compared to the observed. This suggests that convergence of low level moist air from the surrounding oceans over the subcontinent is less favoured in the idealised compared to the observed. This may suggest that the response over the subcontinent may also be sensitive to SST anomalies elsewhere in the domain beside that south of Madagascar.

In the observed SST experiment there is some evidence of an eastward shift in the surface low pressure response between February and March in conjunction with the shifting SST forcing. In the idealized SST case, the surface cyclonic anomaly remains near the fixed SST forcing (**Fig 6.1** right panel) or even shifts west slightly as a result of advection by the prevailing southeasterlies. In the observed SST case, strong negative surface pressure anomalies are observed over the eastern and western parts of southern Africa in January, over central and northeastern southern Africa in February and only over northeastern southern Africa in March (**Fig 6.2** left panel). This may suggest increased low level convergence of moist air and hence rainfall over these regions (**Fig 6.5**). However, there

is reduced low level convergence over the subcontinent in the idealised experiment (**Fig 6.5** right panel) as a result of the forcing suggesting reduced rainfall. Weakened divergence is also observed over the subcontinent in the idealised experiment.

Examination of the surface winds indicates that a cyclonic wind anomaly is generated over the warm pole (**Fig 6.6**). This is in association with the cyclonic sea level pressure anomaly generated over the SST warm pole forcing (**Fig 6.1**, right panel). The circulation extends further to the east in January compared to February and March in the idealised case. The circulation anomaly is observed to be along the southeastern coast of South Africa in the three months in the idealised experiment. In the observed case (not shown), only the western part of the cyclonic circulation is seen. This is because the centre has shifted further west as a result of the location of the warm SST pole in the observed SST case (**Fig 6.1** left panel). The cyclonic wind anomaly over the warm pole in the idealised experiment (**Fig 6.6**) shows enhanced evaporation (**Fig 6.7**), over the warm pole. This is supported by anomalous 850 hPa specific humidity values over the warm pole forcing (**Fig 6.8**). However, these values over the southwest Indian Ocean are weaker than in the observed SST case in January and February. Due to the location and spatial extent of the cyclonic anomaly (**Fig 6.6**), there is little indication of more moist air being advected over the eastern region of the subcontinent as suggested by GCM results (Reason 2001).

The moisture flux transects through 40°E (**Fig 6.9**) indicates no significant change in the idealised experiment from the observed experiment in moisture advection to the southeastern regions of the subcontinent in February and March. There is however significant decrease in moisture advection towards the southeastern part of the subcontinent in January in the idealised case. This is consistent with the strong southeasterly wind anomaly in this month (**Fig 6.6**). Climatological low level wind indicate an easterly flow just to the north of the 35°S in the subtropical South Indian Ocean. This flow may be responsible for advecting moist air to the southeastern parts of the subcontinent. However, establishment of a cyclonic wind anomaly in the southwest subtropical Indian Ocean, like in the idealised forcing experiment, would weaken the mainly southeasterly flow. This may result in reduced advection of moist air to the

subcontinent. Therefore, the cyclonic wind anomaly generated by idealised SST forcing reduces the advection of moist air from the warm pole to the subcontinent. On the other hand, a cyclonic sea level pressure anomaly may enhance convergence over the warm pole and vertical uplift of moist air may occur. This moisture can find its way to the subcontinent (west of the SST forcing) if baroclinic conditions over the warm pole prevail. This is however not evident from the above results.

Inspection of out-going longwave radiation (OLR) (**Fig 6.10**) suggests that there is anomalous cloud cover in the idealised experiment (right panel) compared to the observed case (left panel). Negative OLR anomalies are observed over the western parts of the subcontinent in January, the eastern parts in February and over the central regions across the subcontinent in March in the idealised experiment. Positive OLR anomalies, indicating less cloudy skies, are observed over most parts of the subcontinent during the season in the observed experiment, particularly the northern and southern extremes. The northeast-southwest band of negative anomalies across the southern parts of the subcontinent, and out into the subtropical south Indian Ocean, may represent the cloud bands, which are associated with increased rainfall over southern Africa, in January. This appears to be weaker over the Indian Ocean in the idealised experiment. Strong negative anomalies are evident over South Africa and the northern end of the Mozambique channel in February in the observed. Anomalous positive OLR in western parts of Southern Africa extending into the interior of the subcontinent, indicate clearer skies over these regions. These anomalies are however, weak in the idealised experiment. Negative OLR anomalies, which may be associated with cloud bands, are observed in March in the observed experiment unlike in the ideaslised experiment. The above observations suggest enhanced rainfall in the observed experiment but less obviously in the idealised.

Changes in zonal winds through 10°E (**Fig 6.11**) are observed in the low level westerlies north of the Angola low and the low level easterlies to the south in the three months. These flows are enhanced in the idealised and may indicate the strengthening of the Angola low as seen to some extent in the 850 hPa anomalies (**Fig 6.3**). The enhanced

circulation around this low may advect more moisture from the tropical southeast Atlantic Ocean into the western parts of the subcontinent.

Zonal winds through 40°E (**Fig 6.12**) indicate similar wind distribution in the two experiments except that the low level easterlies are slightly stronger in the idealised case. The upper level westerly jet in the midlatitudes strengthens in each case during three months, suggesting enhanced zonal wind shear. This field (**Fig 6.13**) indicates maximum shear off the southeastern coast of South Africa in both experiments in January. In general the westerly shear in the two experiment s is similar indicating that this parameter is less sensitive to SST forcing outside the Southwest Indian Ocean unlike some of the other fields discussed.

6.5 Conclusion

A low pressure anomaly is generated over the warm pole forcing, in agreement with AGCM experiments (Reason 2001 and 2002). Inspection of the 850 hPa indicates that the low pressure decays and tilts west with height in the lowest 1.5km above the surface expected from the quasi-geostrophic theory (Gill, 1982; Fandry and Leslie, 1984). The response at 500 hPa is less indicative of this type of response however. However there is no clear indication of the low shifting downstream with height as suggest by previous research (Reason 2002). Whether this is as a result of the lateral boundary conditions constraining the shifts, requires further investigation beyond the scope of this thesis.

A cyclonic wind anomaly generated over the warm pole, in association with the low pressure, suggests that the predominantly southeastly winds in the southwest Indian Ocean, are weakened in the idealised experiment. This weakening of the southeasterlies suggests reduced moisture advection to the southeastern parts of the subcontinent and hence reduced rainfall. Consistent with this, the OLR and specific humidity anomalies in the idealised experiment show less pronounced changes than for the observed SST experiment.

In summary, although the model results are broadly consistent with GCM experiments this is not to say that other factors and SST anomalies elsewhere in the Indian Ocean or soil moisture and vegetation anomalies may not contribute to MM5 response over the subcontinent. This needs to be confirmed in runs with higher resolution and using diagnostics based on long term model climatology for one to be confident that they are robust. The current MM5 configuration at 60km resolution only partially resolves important local SST (e.g. Agulhas Current), topography (e.g Drakensberg), soil and vegetation gradients and hence the results presented in this chapter must be viewed with caution.

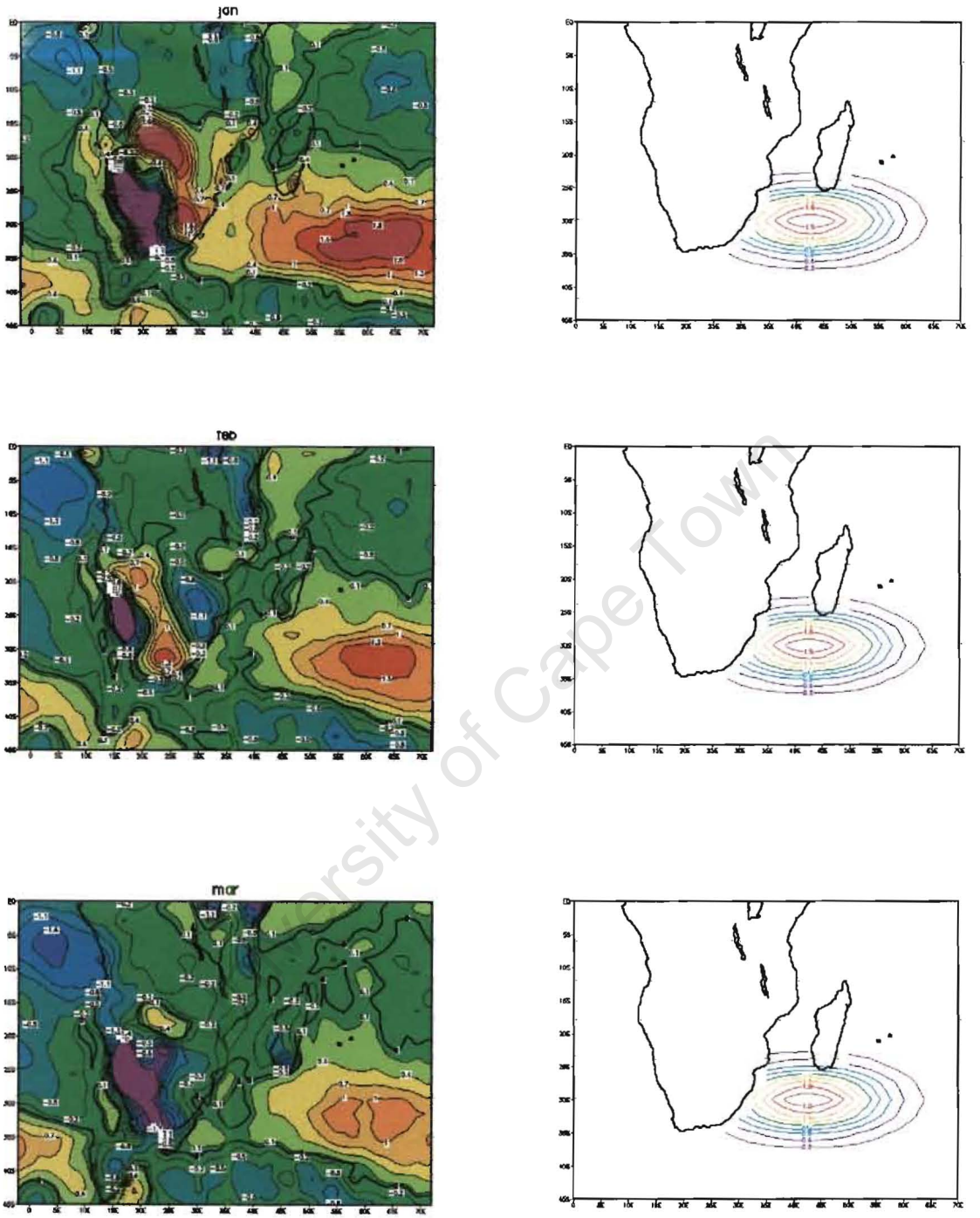

Fig 6.1 *1981 observed (left panel) and idealised (right panel) SST anomaly pattern.*

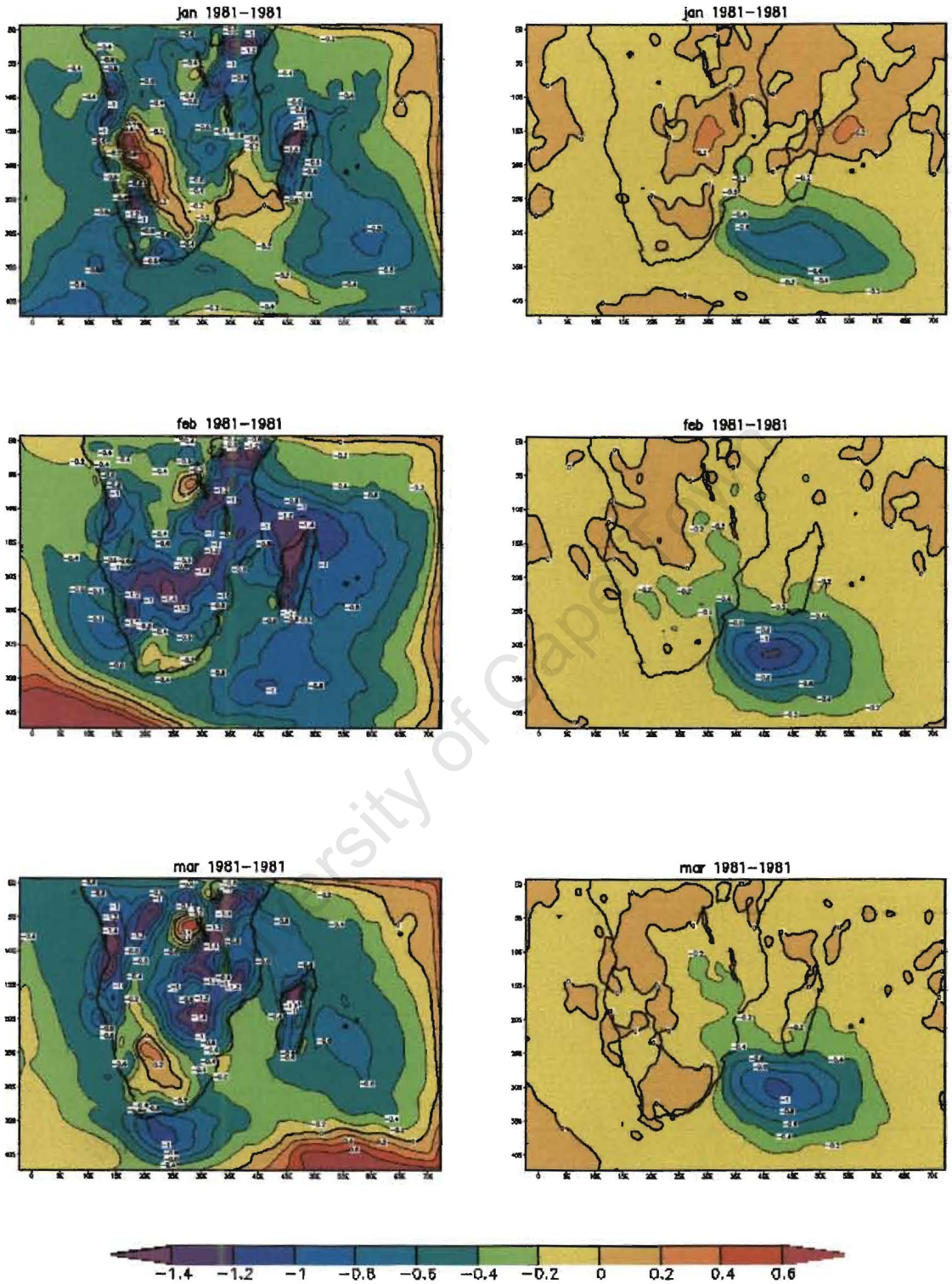

Fig 6.2 *Sea level pressure anomalies for observed (Left panel) and idealised (Right panel) SST anomaly experiments. The scale is shown and contour interval is 0.1hPa.*

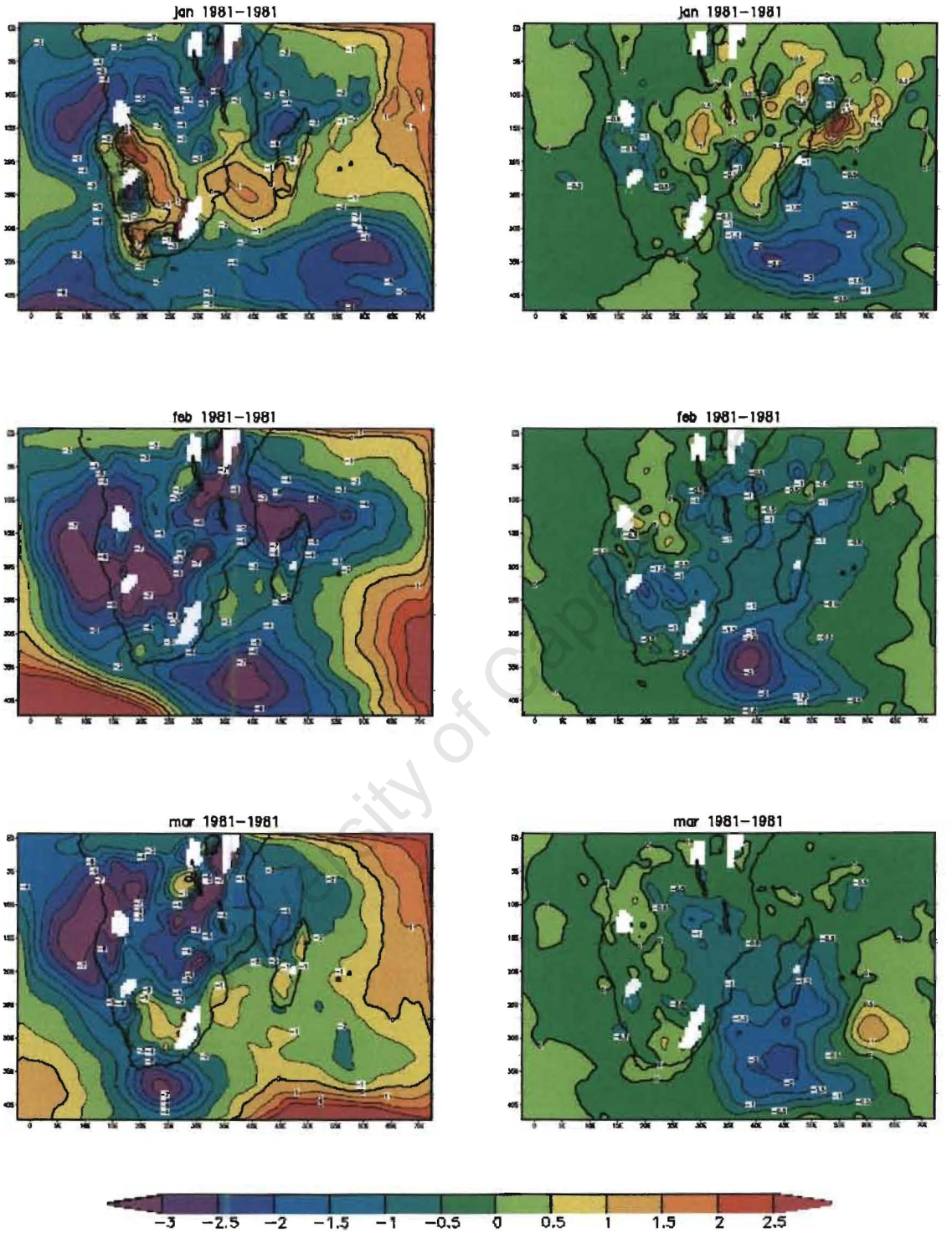

Fig 6.3 *850hPa geopotential height anomalies for observed (Left panel) and idealised (Right panel) SST anomaly experiments. The scale is shown and contour interval is 0.1m*

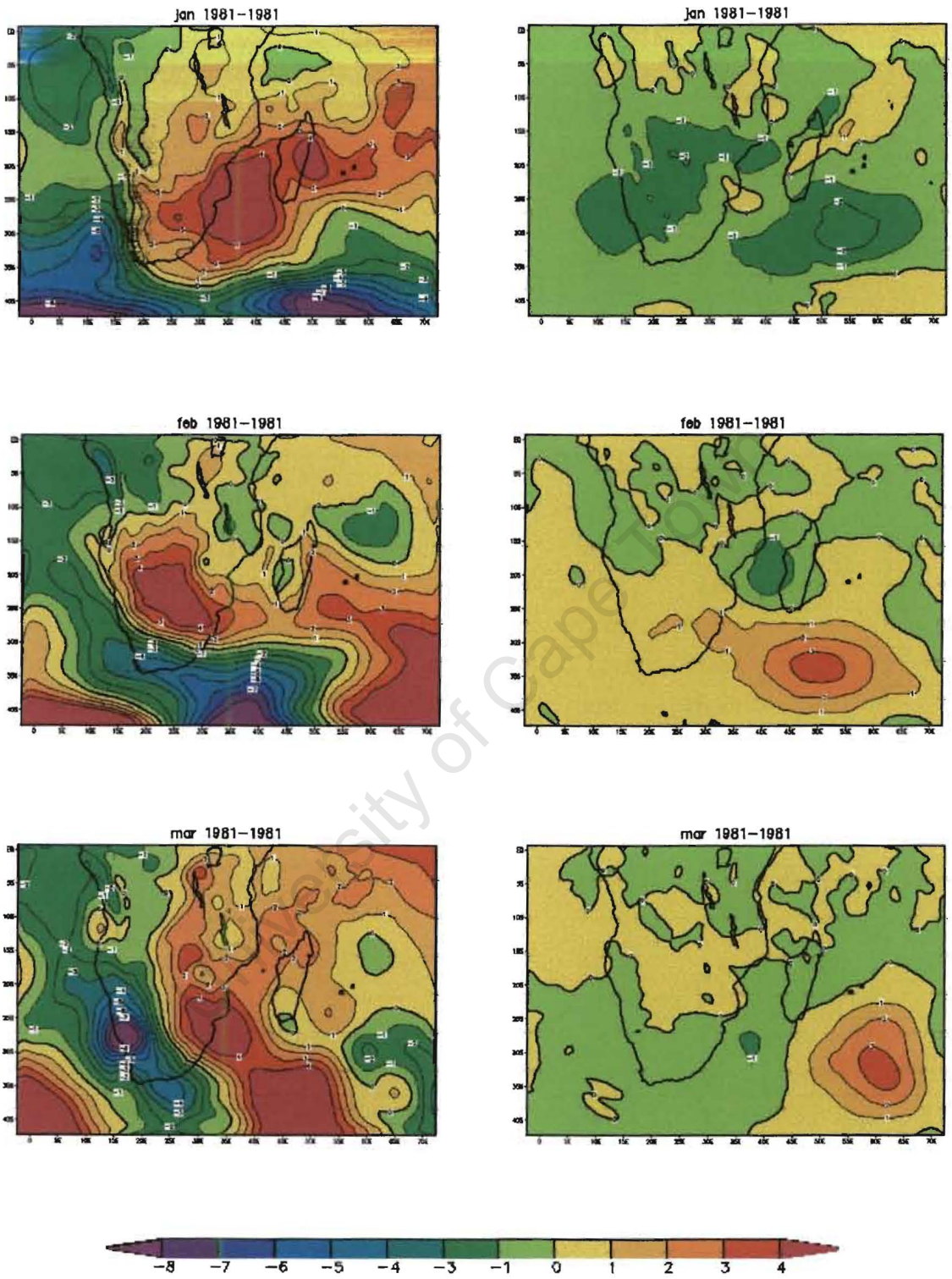

Fig 6.4 *500hPa geopotential height anomalies for observed (Left panel) and idealised (Right panel) SST anomaly experiments. The scale is shown and contour interval is 0.1m.*

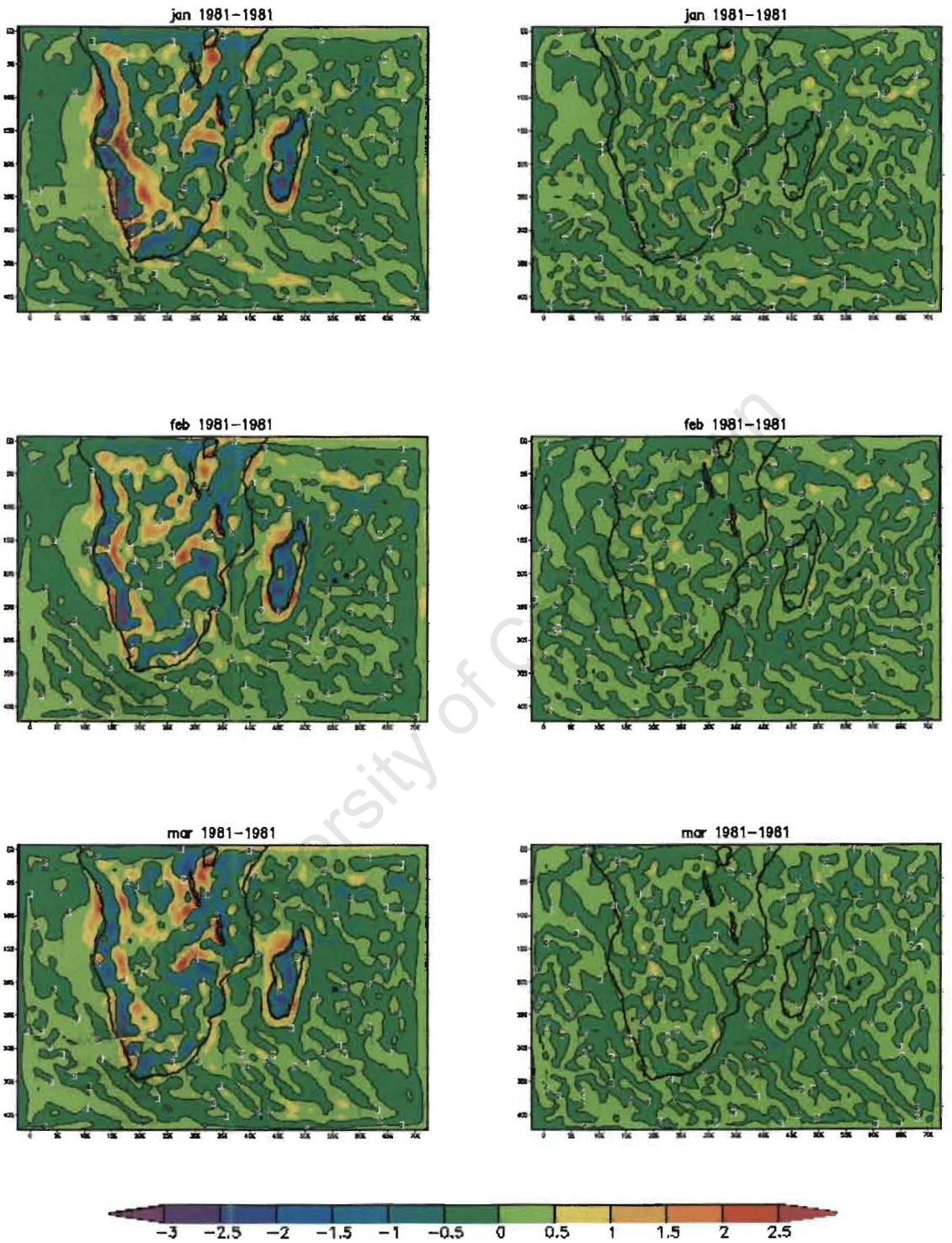

Fig 6.5 *Surface divergence anomalies for observed (Left panel) and idealised (Right panel) SST anomaly experiments. The scale is shown and contour interval is* 0.1×10^{-4}.

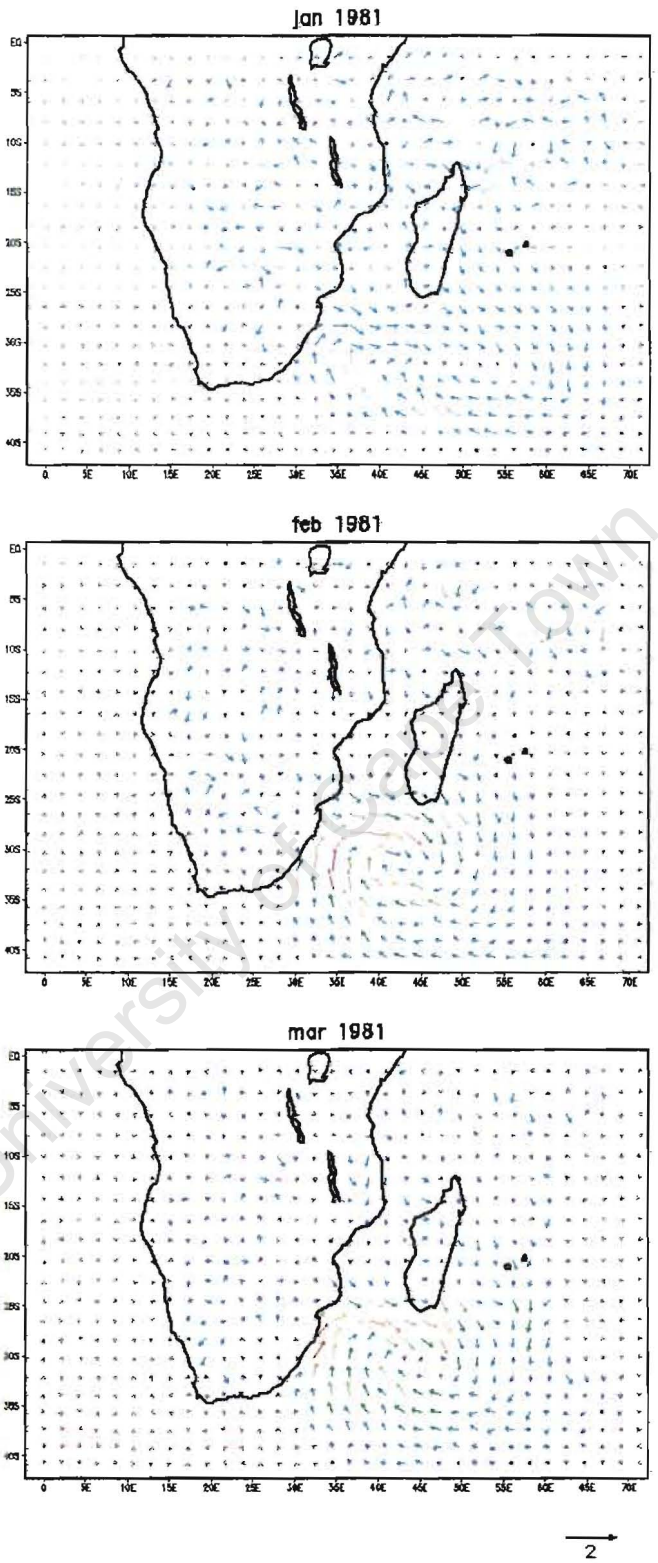

Fig 6.6 *Surface wind (0.995) anomalies for idealised SST anomaly experiment. A scale anomaly vector is shown.*

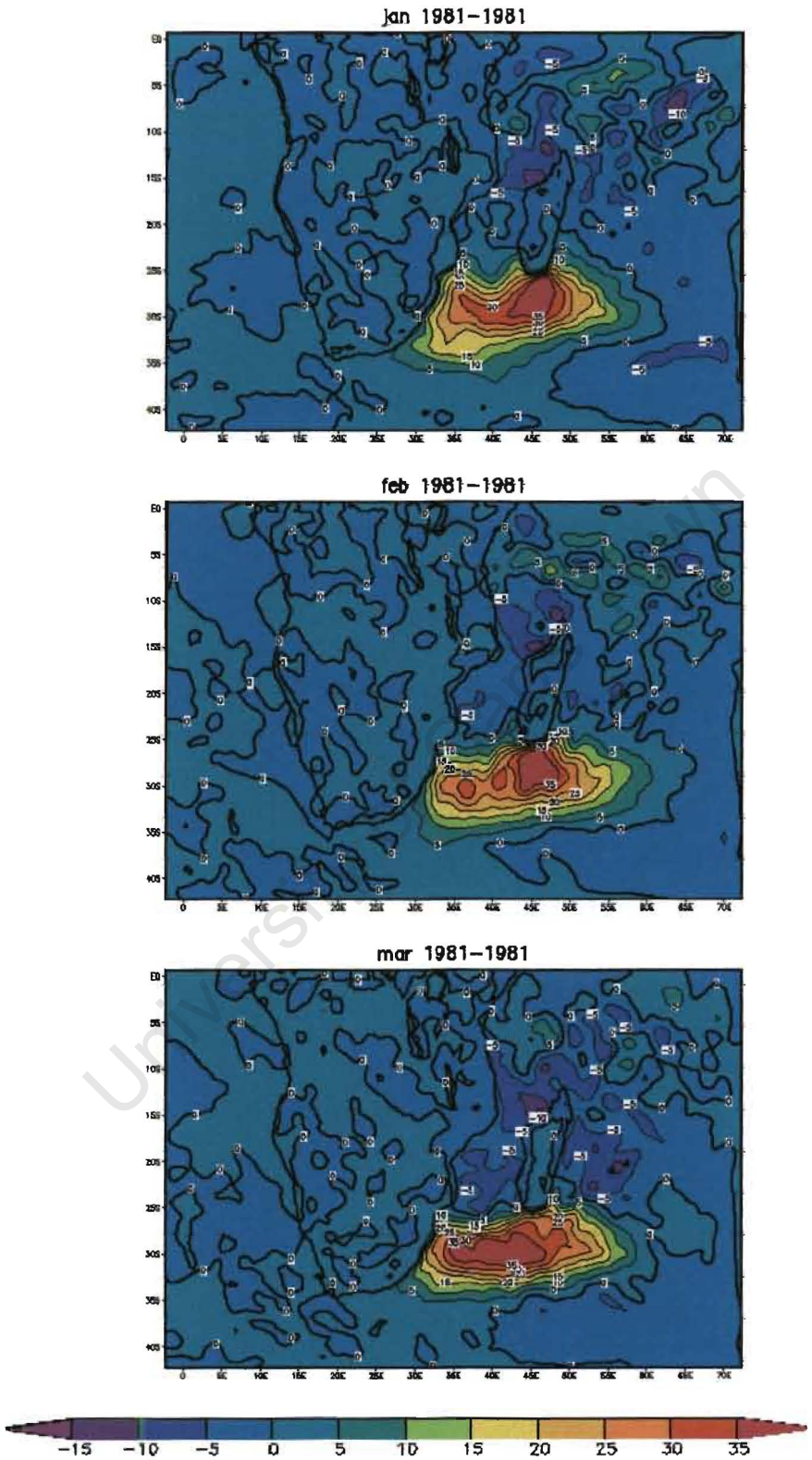

Fig 6.7 *Latent heat flux difference for the idealised SST anomaly experiment. The scale is shown and contour interval is 5.0 Wm^{-2}.*

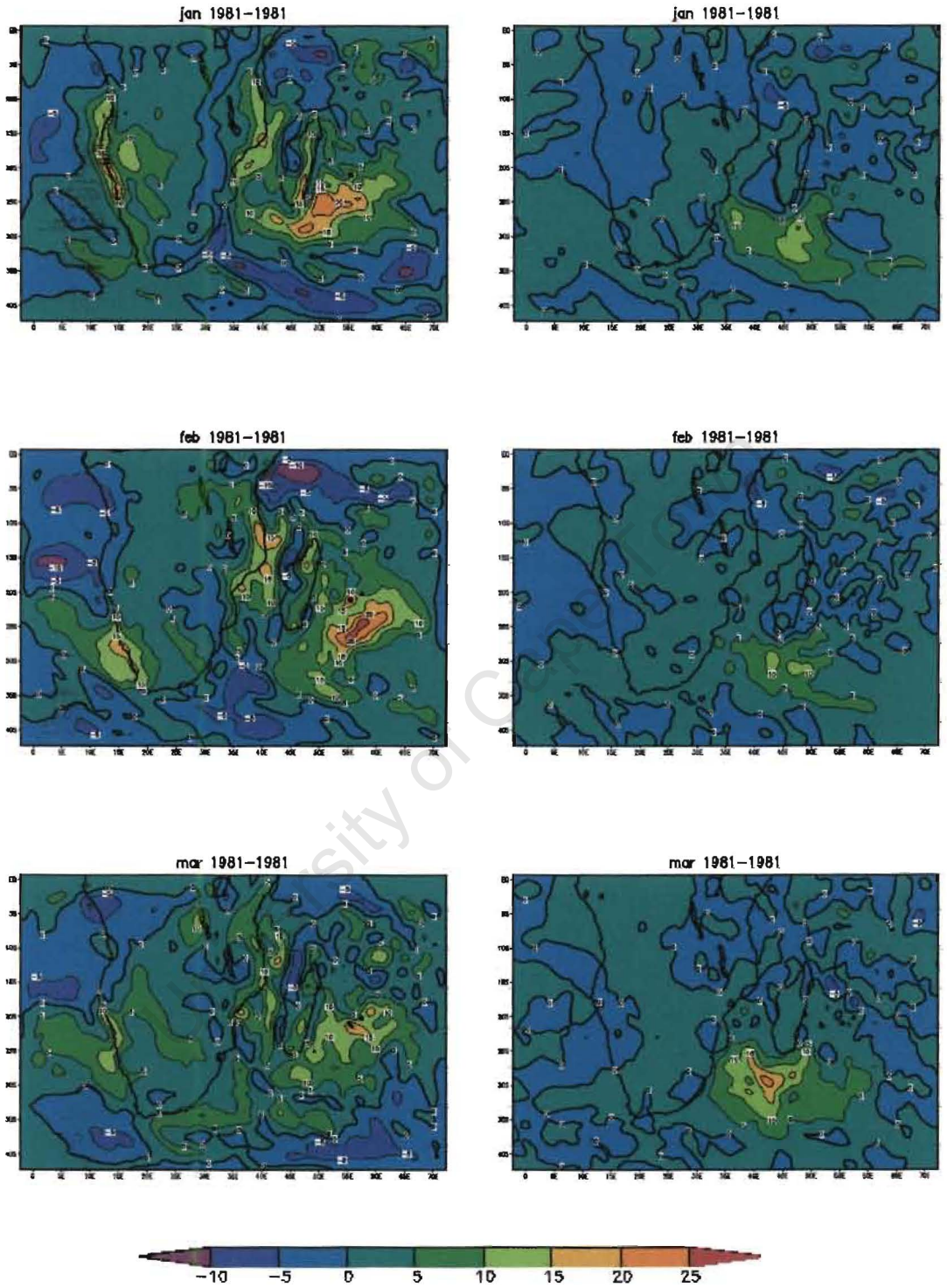

Fig 6.8 *850 hPa specific humidity anomalies for the idealised (Right panel) and observed (Left panel) SST anomaly experiments. The scale is shown and contour interval is* $5g^{-kg}$.

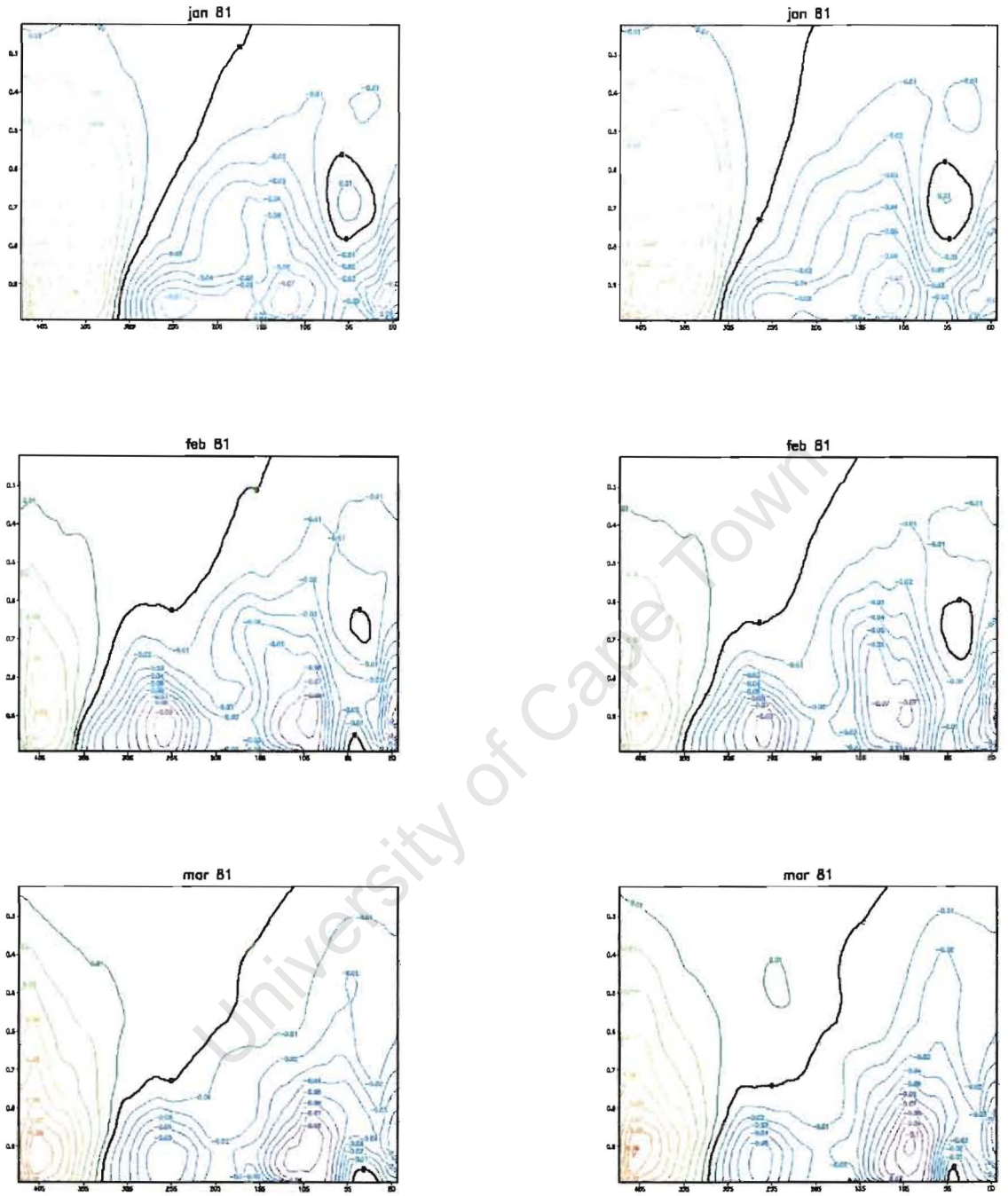

Fig 6.9 *Moisture flux transects through 40°E for idealised (Left panel) and observed (Right panel) SST anomaly experiments. Contour interval is* $0.01ms^{-1}.g^{-kg}$

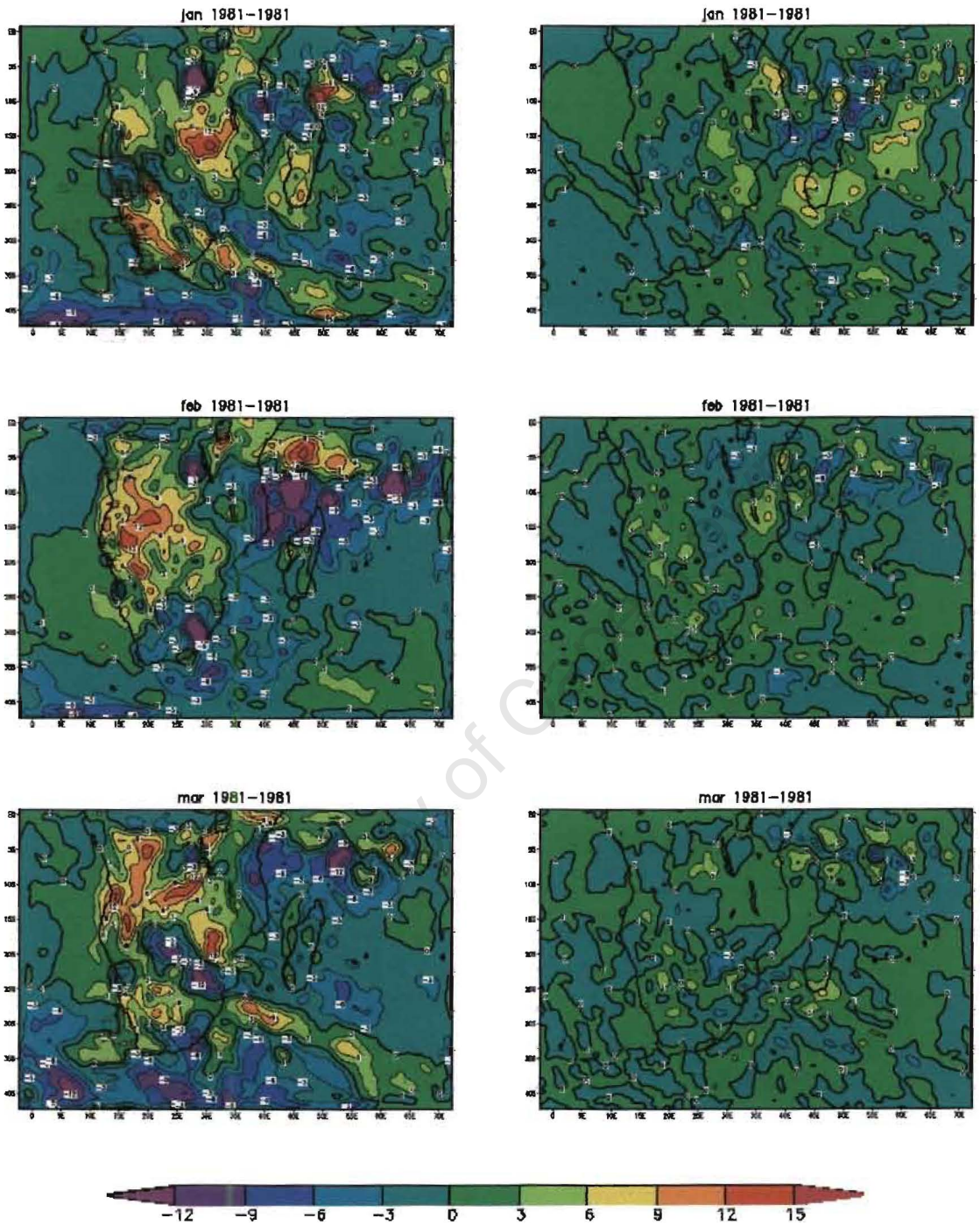

Fig 6.10 *Out-going Longwave Radiation anomalies for observed (Left panel) and idealised (Right panel) SST anomaly experiments. The scale is shown and contour interval is* $3Wm^{-2}$.

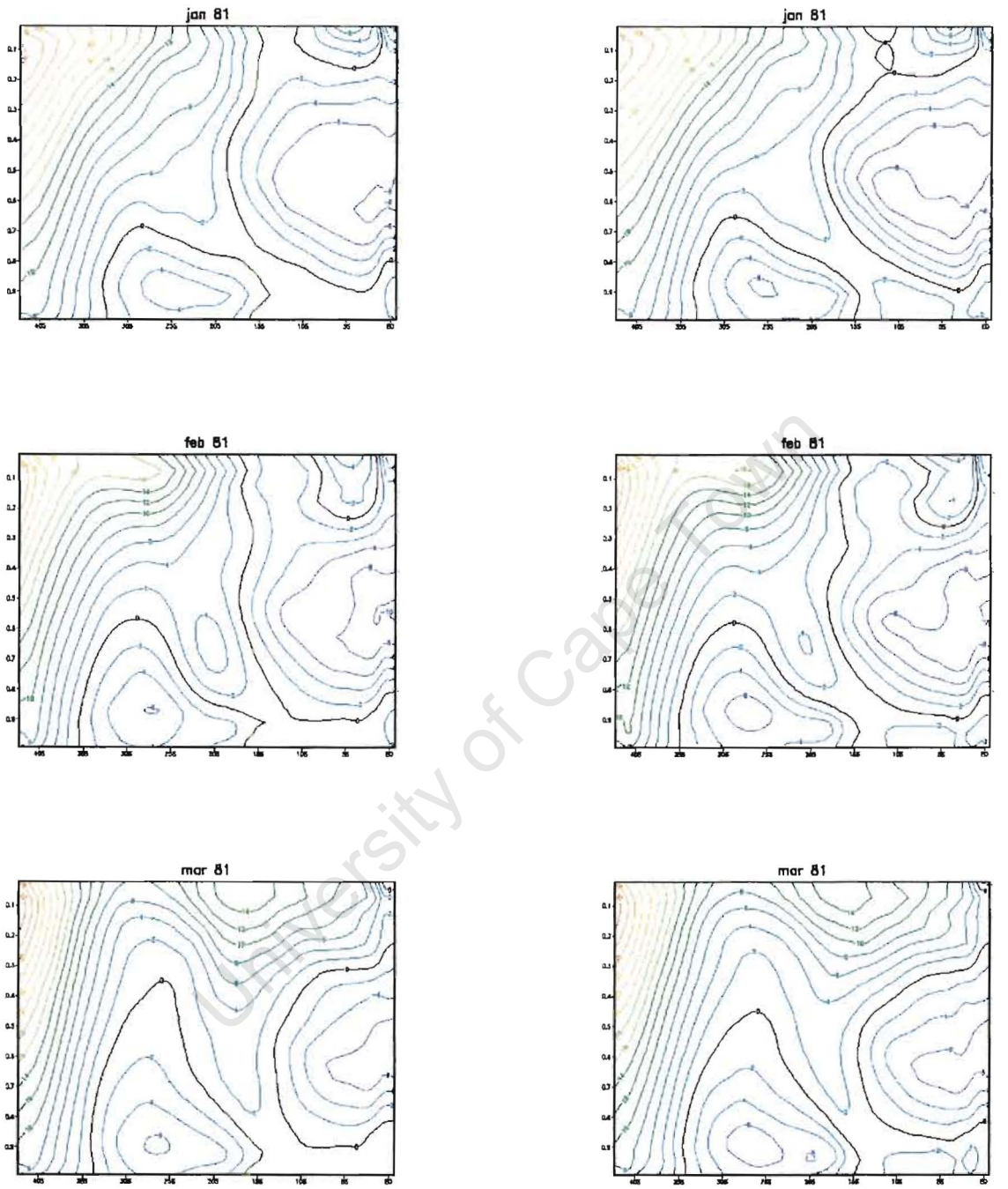

***Fig 6.11** A 10°E transect of zonal winds for observed (left panel) and idealised (right panel) SST anomaly experiment. Contour interval is 2ms^{-1}.*

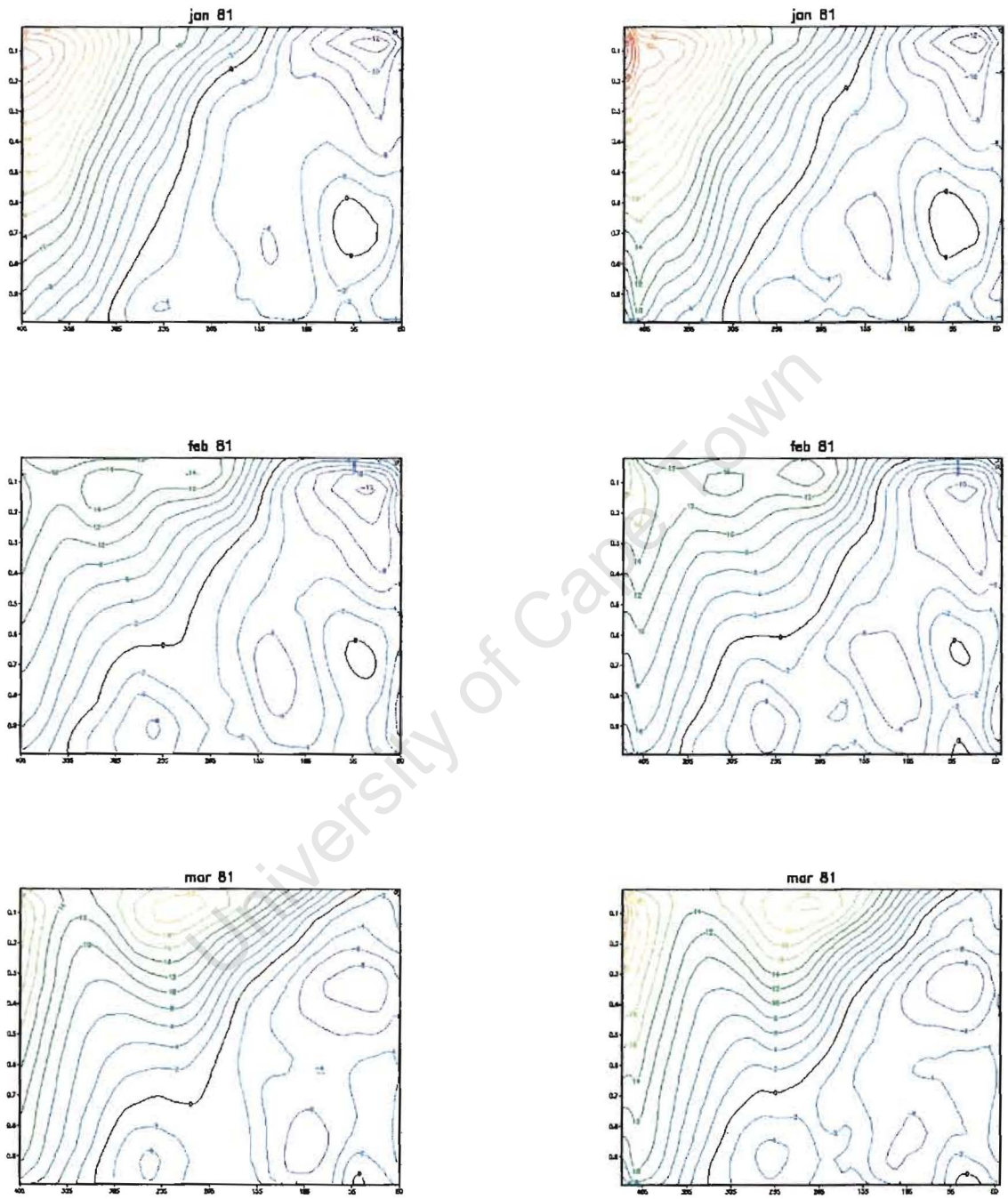

***Fig 6.12** A 40°E transect of zonal winds for observed (left panel) and idealised (right panel) SST anomaly experiments. Contour interval is 2ms^{-1}.*

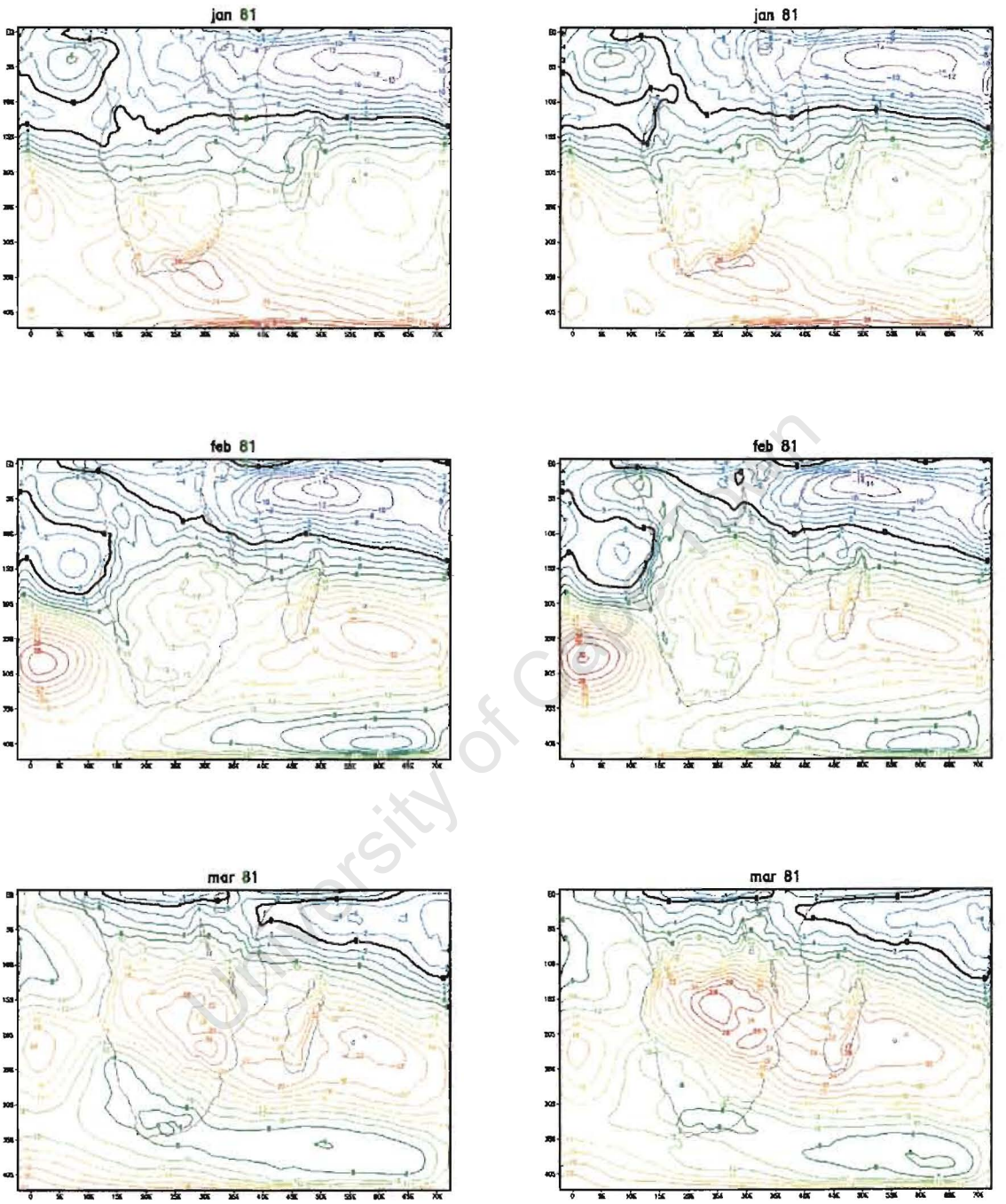

Fig 6.13 *Zonal wind shear (200-850 hPa) for observed (Left panel) and idealised (Right panel) SST anomaly experiments. Contour interval is 2ms^{-1}.*

Chapter 7

Summary and Conclusions

The aim of this thesis was to use a regional climate model, MM5, to investigate the response over Southern Africa to the subtropical South Indian Ocean SST dipole pattern. A sea surface temperature dipole pattern in the subtropical South Indian Ocean, known as the subtropical South Indian Ocean dipole, is characterised by warm (cool) SST anomalies in the southwest (southeast) Indian Ocean during the positive phase. During the negative phase, the opposite orientation of the SST anomalies is observed.

From the review of the literature in **chapter two**, it is evident that variations in SSTs in the Indian Ocean may influence austral summer rainfall over southern Africa. This may be through the influence the SSTs may have on the frequency and intensity of major rainfall-producing systems such as easterly waves and tropical temperate troughs over the region. One of several modes of SST variability in the Indian Ocean, the subtropical South Indian dipole has previously been shown to be linked with summer rainfall over Southern Africa. The positive phase of this phenomenon was found to be associated with above normal austral summer rainfall while below normal rainfall was associated with the negative phase. Though this phenomenon was observed to peak in February during austral summer, it does not occur every year and depends on the location and intensity of the South Indian Ocean anticyclone during a particular year. The mechanisms behind the evolution of the subtropical south Indian Ocean dipole are not well understood. However, this phenomenon is reported to be a manifestation the strong ocean-atmosphere coupling in the subtropics.

7.1 Findings of Study

In order to assess the strength and frequency of the event, the subtropical dipole index (SDI), was produced using GISST 2.3b dataset in **chapter four**. This index was obtained from the SST anomaly difference between the western (55-65°E, 37-27°S) and eastern (90-100°E, 28-18°S) subtropical South Indian Ocean. Strong events of both phases, with index values of about ∀1 and greater, were identified from the index. Amongst these the strongest positive (1981) and negative (1998) events were identified. These two events were then simulated with the MM5 model to investigate the atmospheric response over Southern Africa. The model domain extended from 0-45°S, -5W-70°E, covering the whole of southern Africa, Madagascar and part of the southern Indian and Atlantic Oceans. This domain did not include the eastern part of the South Indian Ocean where the other pole is located. Computational resources could not allow for a larger domain. An idealised experiment of the 1981 event, forced with warm SST anomalies of about 2.0°C to the south of Madagascar, was also carried out. The model was run over a period of five months, starting from November of the previous year to April of the following year, at resolution of 60km grid distance.

From the SDI, nine strong positive and negative events were identified. Variations among events of a particular phase were observed. The variations were mainly in the orientation, strength and pole sizes. Some events were seen to have weaker and smaller poles than others. Of the nine positive events identified, six showed the orientation of the boxes used to obtain the SDI and were used in the positive phase composite. All the nine negative events identified were used in the negative phase composite because most of the events did not show as clear an expression of the dipole as the positive events. Two strongest events, of opposite phase, were identified from among the nine positive and negative events. These two events, the 1980/1 and 1997/8 positive and negative events respectively, also happened to be the most recent strong events.

Although the positive and negative composites showed opposite dipole patterns, it was found that the processes involved during their evolution were not necessary opposite,

contrary to the suggestion of Behera and Yamagata (2001). The winds in particular, which were found to play a major role in the evolution of the dipole, may change direction. However, the opposite implied by these authors may be in the mean sea level pressure anomalies in which a cyclonic anomaly is associated with the negative phase and the anticyclonic anomaly with the positive phase of the dipole. It is not clear whether the circulation, wind direction in particular, and other features associated with the positive phase are opposite during the negative phase. Therefore, the suggestion that the opposite situation occurs during an opposite event may be misleading.

In the analysis of individual positive and negative events in this thesis, it was found that although composites may bring out certain features that are associated with a particular phenomenon, they also tend to leave out features or patterns that are not generic to the phenomenon but important to specific events. Therefore use of composites must be used with caution especially when analysing phenomena that occur on interanual, but vary on intraseasonal time scales.

It was also found that although the index indicated occurrences of strong events during some years, plots of the summer SST anomalies for particular years did not show dipole patterns at all. The season in which the dipole peaks appeared to matter. Therefore, picking out strong events from the index must be done cautiously when a particular season is of interest.

The two strongest opposite events identified from the nine positive and negative events were simulated, in **chapter five**, using NCEP data for MM5's boundary conditions. These simulations were carried out for the purpose of validating the model and to explore differences in atmospheric conditions over southern Africa during the two opposite events. In order to do this, the January, February and March sea level pressure, 850 hPa and 500 hPa geopotential differences of the two simulations (1981-1998) as well as zonal wind shear were compared with those of the NCEP model. Transects of zonal winds and moisture fluxes for the two models were also compared. Other rainfall related fields such as OLR, latent heat flux and specific humidity were also considered. Similarities were

observed between MM5 and NCEP difference plots of the variables mention above, particularly in the 500 hPa geopotential height. Examination of rainfall related variables were generally consistent with wetter conditions occurring during the 1980/1 event than in 1997/8.

Given that the atmosphere is generally more responsive to warm than cool SST anomalies and that previous experiments with general circulation models suggest that the atmospheric response over southern Africa is stronger when warm SST anomalies are close to the subcontinent, an idealised experiment for 1980/1 was done with the SST forcing south of Madagascar in **chapter six**. The model was forced with 30-year climatological surface temperatures on which a warm pole anomaly of about 2.0°C was imposed with centre at 30°S, 40°E while maintaining the 1980/1 conditions for other variables. A similar experiment, but with the model forced with climatological SST only, served as a control run. In response to this forcing, a low pressure anomaly was generated over the warm pole. This is in agreement with AGCM experiments (Reason, 2001 and 2002). An examination of the geopotential height indicated the weakening of the low pressure in the low troposphere consistent with the linear quasi-geostrophic theory. Therefore the MM5 response to the forcing is in broad agreement with both the linear quasi-geostrophic theory and AGCM experiments at least between the 1000 and 850 hPa levels.

A low level cyclonic wind anomaly, in association with the low pressure, was generated over the warm pole. This wind anomaly was observed to evaporate a lot of moisture over the warm pole as indicated by anomalous latent heat fluxes. However, there was no strong indication of moist air advected over the southeastern parts of subcontinent. The low-level cyclonic wind anomalies in the southwest South Indian Ocean tend to weaken the prevailing southeasterlies, which are observed to transport moist air to the subcontinent during austral summer. Weakened divergence, and increased OLR were observed over the subcontinent. These conditions suggest reduced rainfall over southern Africa.

7.2 Directions for future research

The subtropical South Indian Ocean dipole is a recently proposed phenomenon whose mechanisms and its effect on the southern African atmospheric circulation are not yet well understood. The results of this research appear to be in broad agreement with previous GCM experiments. As a result of the caveats encountered, there is need to further investigate the dipole's influence on southern African atmospheric circulation at higher resolution than can better represent the tight SST, topographic and vegetation gradient of the region. It would also be important to study the possible relationship of the subtropical South Indian Ocean dipole to other climatic phenomena, such as ENSO .

7.3 Conclusion

This thesis has tried to examine a phenomenon, which may be responsible for observed intra-seasonal and interannual rainfall variations that are not linked to well known phenomena like ENSO. Understanding this mode of SST variability in the subtropical south Indian Ocean may help identify local or external phenomena, which are related to rainfall variability, that may drive or may be driven by this mode of variability. Rainfall variability has a strong socio-economic impact in regions around the Indian Ocean because of the large population, this phenomenon may be used to enhance intra- to inter seasonal rainfall forecasting over Southern Africa thereby giving regional governments ample time to organise necessary resources to mitigate the effects of calamities associated with rainfall variability.

References

Allan, R. J., Lindesay, J. A. and Reason, C. J. C. 1995: Multidecadal variability in the climate system over the Indian Ocean region during the austral summer. *J. Climate*, **8**, no.7, 1853-73.

Allan, R., Chambers, D., Drosdowsky, W., Hendon, H.,. Latif, M.,N. Nicholls, I. Smith, R. Stone, and Y. Tourre, 2001: Is there an Indian Ocean dipole, and is it independent of the El Nino – Southern Oscillation? *CLIVAR Exchanges*, **6**, 3, 18-22.

Ansell, T., C. J. C. Reason, and G. Meyers, 2000: Variability in the tropical southeast Indian Ocean and links with southeast Australian winter rainfall. *Geophys. Res. Lett.*, **27**, 24, 3977-80.

Anyamba, A., C. J. Tucker, and R. J. Eastman, 2001: NDVI anomaly patterns over Africa during the 1997/98 ENSO warm event. *Int. J. Remot. Sense.*, **22**,10, 1847-59

Baquero-Bernal, A., M. Latif, and S. Legutke, 2002: On dipolelike variability of sea surface temperature in the tropical Indian Ocean. *J. Climate,* **15**, 1358-63.

Behera, S.K., and T. Yamagata, 2001: Subtropical SST dipole events in the southern Indian Ocean. *Geophys. Res. Lett.*, **28**, 327-330.

Behera, S.K., R. Krishnan, and T. Yamagata, 1999: Unusual ocean-atmosphere conditions in the tropical Indian Ocean during 1994. *Geophys. Res. Lett.*, **26**, 19, 3001-4.

Behera, S.K., P.S. Salvekar, and T. Yamagata, 2000: Simulation of interannual SST variability in the tropical Indian Ocean. *J. Climate,* **13**, 3487-99.

Black, E., J. Slingo, and K. R. Sperber, 2003: An observational study of the relationship between excessively strong short rains in coastal East Africa and Indian Ocean SSTs. *Mon. Wea. Rev.*, **131**, 71-94

Bromwich, D. H., Cassano J. J., Klein T., G. Heinemann, K. M. Hines, K. Steffen, and J. E. Box, 2001: Mesoscale Modeling of Katabatic Winds over Greenland with the Polar MM5. *Mon. Wea. Rev.*, **129**, 2290-309.

Cadet, D. L., 1985: The Southern Oscillation over the Indian Ocean. *J. Climatol.*, **2**, 189-212.

Chambers, D. P., B. D. Tapley, and R. H. Stewart, 1999: Anomalous warming in the Indian Ocean coincident with El Nino. *J. Geophys. Res.*,**104** (C2), 3035-47.

Clark, C. O., J. E. Cole, and P. J. Webster, 2000: Indian Ocean SST and Indian summer rainfall: Predictive relationships and their decadal variability. *J. Climate,* **13**, 2503-19.

Colle, B. A. and C. F. Mass, 2000; The 5-9 February 1996 flooding event over the Pacific Northwest: Sensitivity studies and evaluation of the MM5 precipitation forecasts. *Mon. Wea. Rev.*,**128**, 593-617.

Cook, K. H., 2001: A Southern hemisphere wave response to ENSO with implications for Southern Africa precipitation. J. Atmos. Sci., **58**, 15, 2146-62.

Cook, K.H., 2000: The South Indian Convergence Zone and Interannual Rainfall Variability over Southern Africa. *J. Climate*, **13**, 3789-3804.

D'Abreton, P. C. and P. D. Tyson, 1995: Divergent and non-divergent water vapour transport over southern Africa during wet and dry conditions. *Meteor. Atmos. Phys.*, **55**, 47-59.

Dabberdt, W. F., and T. W. Schlatter, 1996: Research opportunities from emerging atmospheric observing and modeling capabilities. *Bull. Amer. Meteor. Soc.*, **77**, 305-323.

Drosdowsky, W., 1993: Potential predictability of winter rainfall over southern and eastern Australia using Indian Ocean sea surface temperature anomalies. *Australian Meteor. Mag.*, **42**, 1-6.

Fandry, C. B. and L. M. Leslie, 1984: A two-layer quasi-geostrophic model of summer trough formation in the Australian subtropical easterlies. *J. Atmos. Sci.*, **14**, 807-18.

Gill, A. E., 1980: Some simple solutions for heat-induced tropical circulations. *Quart. J. Roy. Meteor. Soc.*, **106**, 447-462.

Goddard, L. and N. E. Graham, 1999: Importance of the Indian Ocean for simulating rainfall anomalies over eastern and southern Africa. *J. Geophys. Res.*, **104** (D16), 19099-116.

Grotzner, A., M. Latif, and D. Dommenget, 2000: Atmospheric response to sea surface temperature anomalies during El Nino 1997/98 as simulated by ECHAM4. *Quart. J. Roy. Meteor. Soc.*, **126**, 2175-98.

Hasternrath, S., A. Nicklis and L. Greishar, 1993: Atmospheric-Hydrospheric mechanisms of climate anomalies in the western equatorial Indian Ocean. *J. Geophys. Res.*, **98** (C11), 20219-35.

Hasternrath, S., 2002: Dipoles, Temperature Gradients, and Tropical Climate Anomalies. *Bull. Amer. Meteor. Soc.*, **83**, 735-738.

Hirst, A. C. and J. S. Godfrey, 1993: The role of Indonesian throughflow in a global ocean GCM. *J. Phys. Oceano.*, **23**, 6, 1057-86.

Hoerling, M. P., M. L. Blackmon, and M. Ting, 1992: Simulating the atmospheric response to the 1985-87 El Nino cycle. *J. Climate,* **5**, 669-82.

Hurrell, W. J., Van Loon H. and Shea D. J., 1998, 'The Mean State of the Troposphere' in *Meteorology of the Southern Hemisphere* eds Karoly, D. J. and Vincent, D. G., American Meteorological Society.

Lindesay, J.A., 1988: South African rainfall, the Southern Oscillation and Southern Hemisphere semi-annual cycle. *Int. J. Climatology*, **8**, 17-30.

Iizuka, S., T. Matsuura, and T. Yamagata, 2000: The Indian Ocean SST dipole simulated in a coupled general circulation model. *Geophys. Res. Lett.*, **27**, 20, 3369-72.

Jury, M. R., B. Pathack, and B. Parker, 1999: Climatic determinants and statistical prediction of tropical cyclone days in the southwest Indian Ocean. *J. Climate,* **12**, 6, 1738-46

Jury, M. R., H. M. Mulenga, and S. J. Mason, 1999: Exploratory long-range models to estimate summer climate variability over Southern Africa. *J. Climate,* **12**, 1892-99

Jury, M. R., 1996: Regional teleconnection patterns associated with summer rainfall over South Africa, Namibia and Zimbabwe. *Int. J. Climatol.*, **16**, 135-53.

Jury, M. R. and B. Pathack, 1991: A study of climate and weather variability over the tropical southwest Indian Ocean. *Meteor. Atmos. Phys.*, **47**, 1, 37-48.

Kalnay, E., M. Kanamitsu, R. Kistler, W. Collins, D. Deaven, L. Gandin, M. Iredell, S. Saha, G. White, J. Woollen, Y. Zhu, M. Chelliah, W. Ebisuzaki, W. Higgins, J. Janowiak, K. C. Mo, C. Ropelewski, J. Wang, A. Leetmaa, R. Reynolds, R. Jenne, and D. Joseph, 1996: The NCEP/NCAR 40-Year Reanalysis Project. *Bull. Amer. Meteor. Soc.*, **77**, 437-71.

Klopper, E., W. A. Landhan, and J. Van Heerden, 1998: The predictability of seasonal maximum temperature in South Africa. *Int. J. Climatol.*, **18**, 741-58.

Koracin, D. and C. E. Dorman, 2001: Marine Atmospheric Boundary Layer Divergence and Clouds along California in June 1996. *Mon. Wea. Rev.*, **129**, 2040-56.

Landman, W. A. and S. J. Mason, 1999: Change in the association between Indian Ocean sea-surface temperature and summer rainfall over South Africa and Namibia. *Int. J. Climatol.*, **19**, 1477-92.

Latif, M., D. Dommenget, M. Dima, and A. Grotzner, 1999: The role of Indian Ocean sea surface temperature in forcing East African rainfall anomalies during December-January 1997/98. *J. Climate*, **12**, 12, 3497-504.

Latif, M., D. Dommenget, and M. Dima, 1998: Role of Indian Ocean sea surface temperature in forcing East African climate anomalies. *Max-Planck-Inst. Meteorol.* **16** pp...

Lau, N. C. and M. J. Nath, 1990: A General circulation model study of the atmospheric response to extratropical SST anomalies observed in 1950-79. *J. Climate*, **3**, 965-89.

Li, T., Z. Yongsheng, C. P. Chang, and W. Bin, 2001: On the relationship between Indian Ocean sea surface temperature and Asian summer monsoon. *Geophys. Res. Lett.*, **28**, 14, 2843-6.

Logan, J. A., Jones, D. B. A., Megretskaia, I. A., Oltmans, S. J., Johnson, B. J., Vömel, H., Randel, W. J., Kimani, W. and Schmidlin, F. J., 2002: Quasibiennial oscillation in tropical ozone as revealed by ozonesonde and satellite data. J. Geophy. Res., 108, D8, 4244-

Mason, S. J. and M. R. Jury, 1997: Climate variability and change over southern Africa: a reflection on underlying processes. *Prog. Phys. Geo.*, **21**, 1, 23-50.

Mason, S. J., 1995: Sea-Surface temperature – South African rainfall associations, 1910 –

1989. *Int. J. Climatol.*,**15**, 119-35.

Nicholls, N., 1989: Sea surface temperatures and Australian winter rainfall. *J. Climate*, **2**, 965-73

Nicholls, N. and W. Drosdowsky, 2001: Is there an equatorial Indian Ocean SST dipole, independent of the El Niño Southern Oscillation? 81st American Meteorological Society Annual Meeting Albuquerque, New Mexico, USA, 14-19 January 2001

Nicholson, S., 2003: Comment on "The South Indian convergence zone and interannual rainfall variability over Southern Africa" and the question of ENSO's influence on Southern Africa. *J. Climate*, **16**, 555-62.

Palmer, T. N. and D. A. Mansfield, 1986: A study of wintertime circulation anomalies during past El Nino events using a high resolution general circulation model. I: Influence of model climatology. *Quart J. Roy. Meteor. Soc.*, **112**, 613-38.

Peng, S., W. A. Robinson, and M. P. Hoerling, 1997: The modeled atmospheric response to midlatitude SST anomalies and its dependence on background circulation states. *J. Climate*, **10**, 971-87.

Peng, S. and J. S. Whitaker, 1998: Mechanisms determining the atmospheric response to midlatitude SST anomalies. *J. Climate*, **12**, 1393-408

Peng, S and R. Walter, 2001: Relationships between atmospheric internal variability and the responses to an Extratropical anomaly. *J. Climate*, **14**, 2743-59

Preston-Whyte, R. A. and Tyson, P.D. 1988, The Atmosphere and Weather of Southern Africa, Oxford University Press, Cape Town.

Rao, S. A., S. K. Behera, Y. Masumoto, and T. Yamagata, 2002: Interannual subsurface

variability in the tropical Indian Ocean with a special emphasis on the Indian Ocean dipole. *Deep-Sea Res. Part II*, **49**, 1549-72.

Reason, C. J. C., R. J. Allan, and J. A. Lindesay, 1996: Evidence of the influence remote forcing on interdecadal variability in the southern Indian Ocean. *J. Geophys. Res.*, **101** (C5), 11867-82.

Reason, C. J. C., 1998: Warm and cool events in the southeast Atlantic/southwest Indian Ocean region and potential impacts on circulation and rainfall over southern Africa. *Met. Atmos. Phys*, **69**, 49-65.

Reason, C. J. C., C. R. Godfred-Spenning, R. J. Allan, and J. A. Lindesay, 1998: Air-Sea interaction mechanisms and low-frequency climate variability in the south Indian Ocean region. *Int. J. Climatol.*, **18**, 391-405.

Reason, C. J. C., 1999: Interannual warm and cool events in the subtropical/mid-latitude South Indian Ocean region. *Geophys. Res. Lett.*, **26**, 2, 215-18.

Reason, C. J. C. and H. Mulenga, 1999: Relationships between South African rainfall and SST anomalies in the south west Indian Ocean. *Int. J. Climatol.*, **19**, 1651-1673.

Reason, C. J. C., R. J. Allan, J. A. Lindesay, and T. J. Ansell, 2000: ENSO and climatic signals across the Indian Ocean basin in the global context: Part I, interannual composite patterns. *Int. J. Climatol.*, **20**, 1285-327.

Reason, C. J. C., 2001: Subtropical Indian Ocean SST dipole events and southern African rainfall. *Geophys. Res. Lett.*, **28**, 11, 2225-7.

Reason, C. J. C., 2001b: Evidence for the influence of the Agulhas current on regional atmospheric patterns. *J. Climate*, **14**, 2769-78.

Reason, C. J. C. and R. J. Murray, 2001: Modelling low frequency variability in southern

hemisphere extra-tropical cyclone characteristics and sensitivity to sea-surface temperature. *Int. J. Climatol.*, **21**, 249-267.

Reason, C. J. C., 2002: Sensitivity of the southern African circulation to dipole sea-surface temperature patterns in the south Indian Ocean. *Int. J. Climatol.*, **22**, 377-393.

Reason, C. J. C. and M. Rouault, 2002: ENSO-like decadal variability and South African rainfall. *Geophy. Res. Lett.*, **29**, no.13, 16-1-4

Rocha, A. and I. H. Simmonds, 1997: Interannual variability of southern African summer rainfall. Part I: Relationships with air-sea interactions processes. *Int. J. Climatol.*, **17**, 235-65.

Rocha, A. and I. H. Simmonds, 1997: Interannual variability of southern African summer rainfall. Part II: modeling the impact of sea surface temperatures on rainfall and circulation. *Int. J. Climatol.*, **17**, 267-90.

Roebber, P. J. and G. W. Reuter, 2002: The Sensitivity of Precipitation to Circulation Details. Part II: Mesoscale Modeling. *Mon. Wea. Rev.*, **130**, 3-23.

Ropelewski, C. F. and M. S. Halpert, 1987: Global and regional scale precipitation patterns associated with the El Nino/Southern Oscillation. *Mon. Wea. Rev.*, **115**, 1606-26.

Rouault, M., White, S. A., Reason, C. J. C., Lutjeharms, J. R. E., and Jobard, I., 2002: Ocean-Atmosphere Interaction in the Agulhas Current Region and a South African Extreme Weather Event. *Weather and Forecasting*, **17**, 655-669.

Rouault, M., P. Florenchie, N. Fauchereau, and C. J. C. Reason, 2003: South East Tropical Atlantic Warm Events and Southern African Rainfall. *Geophys. Res. Lett.*, **30** (5),10.1029/2002/GL014840.

Saji, N. H., B. N. Goswami, P. N. Vinayachandran, and T. Yamagata, 1999: A dipole

mode in the tropical Indian Ocean. *Nat.*, **401**, 360-63.

Smith, I, 1994: Indian Ocean sea-surface temperature patterns and Australian winter rainfall. *Int. J. Climatol.*, **14**, 287-305.

Smith, I. N., P. Mcintosh, T. J. Ansell, C. J. C. Reason, and K. Mcinnes, 2000: Southwest Western Australia winter rainfall and its association with Indian Ocean climate variability. *Int. J. Climatol.*, **20**, 1913-30.

Streten, N. A., 1981: Southern hemisphere sea surface temperature variability and apparent associations with Australian rainfall. *J. Geophys. Res.*, **86**, 485-97.

Trenberth, E. K. (ed.) 1992: Climate system modeling, Cambridge University Press.

Van Heerden, J. and Taljaard, J. J., 1998, 'Africa and Surrounding Waters' in *Meteorology of the Southern Hemisphere* eds Karoly, D. J. and Vincent, D. G., American Meteorological Society.

Venzke, S., M. Latif, and A. Villwock, 2000: The coupled GCM ECHO-2. Part II: Indian Ocean response to ENSO. *J. Climate*, **13**, 8, 1371-83.

Vinayachandran, P. N., N. H. Saji, and T. Yamagata, 1999: Response of the Equatorial Indian Ocean to an unusual wind event during 1994. *Geophys. Res. Lett.*, **26**, 11, 1613-16.

Vinayachandran, P. N., S. Lizuka and T. Yamagata, 2002: Indian Ocean dipole mode events in an ocean general circulation model. *Deep-Sea Res. II*, **49**, 1573-96.

Walker, N. D., 1990: Links between South African summer rainfall and temperature variability of the Agulhas and Benguela Current systems. *J. Geophys. Res.*, **95**, 3297-319.
Washington, R. and Todd, M., 1999: Tropical-Temperate links in Southern African and

southwest Indian Ocean Satellite-Derived daily rainfall. *Int. J. Climatol.* **19**, 1601-16.

Wang, R., 2001: Prediction of seasonal climate in a low-dimension phase space derived from the observed SST forcing. *J. Climate*, **14**, 77-97.

Webster, P. J., A. M. Moore, and J. P. Loschnigg, 1999: Coupled ocean – atmosphere dynamics in the Indian Ocean during 1997-98. *Nat.*, **401**, 6751, 356-60.

Yamagata, T., S. K. Behera, S. A. Rao, Z. Guan, K. Ashok, and H. N. Saji, 2002: The Indian Ocean Dipole: a Physical Entity. *CLIVAR Exchanges*, **7**, 2, 15-18

Yu, L. and M. M. Rienecker, 1999: Mechanisms for the Indian Ocean warming during the 1997-98 El Nino. *Geophys. Res. Lett.*, **26**, 6, 735-8.

Zou, X., Y. H. Kuo, and S. Low-Nam, 1998: Medium-Range prediction of an extratropical oceanic cyclone: Impact of initial state. *Mon. Wea. Rev.*, **126**, 2737-63.

http://www.mmm.ucar.edu/mm5/mm5v3/tutorial/regrid/sst_note.html, 20/06/02: A note about sea-surface temperatures and skin temperatures.

Appendix

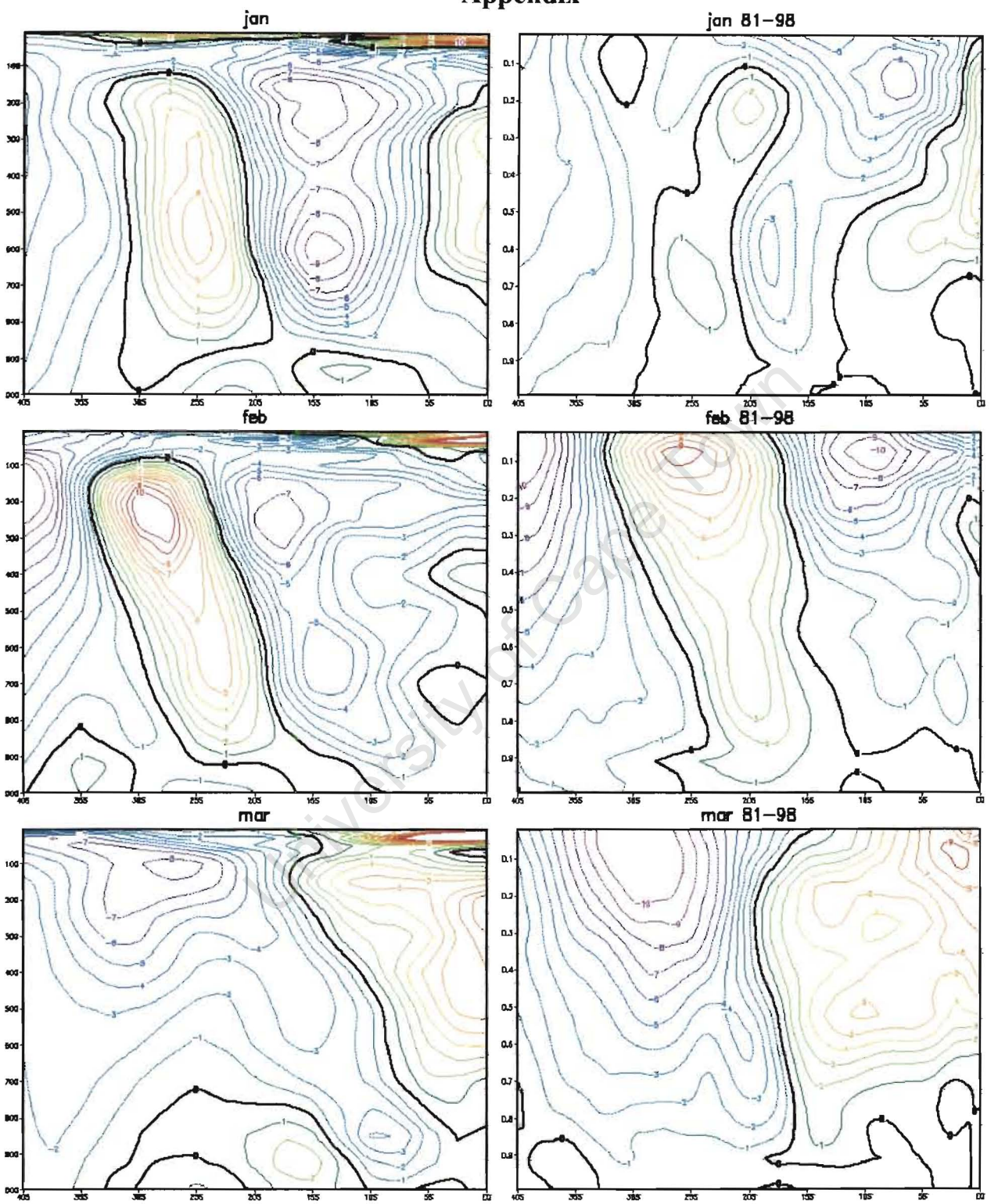

Fig A.1 *A transect of zonal wind difference for 1981 and 1998; taken along* ***10°E****. MM5: Right panel and NCEP: Left panel. Contour interval is* $2ms^{-1}$.

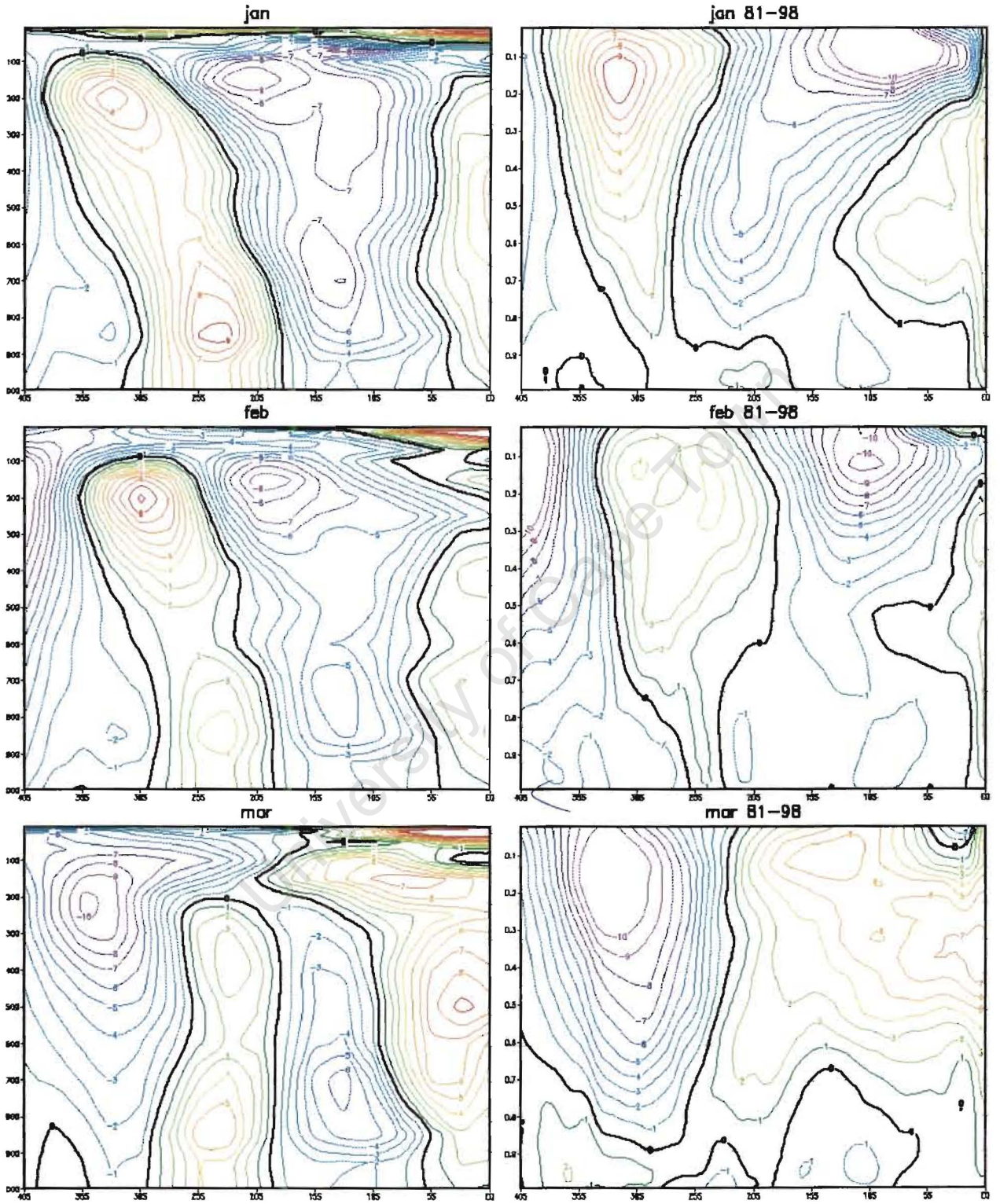

Fig A.2 *A transect of zonal wind difference for 1981 and 1998; taken along* ***20°E****. MM5: Right panel and NCEP: Left panel. Contour interval is* $2ms^{-1}$.

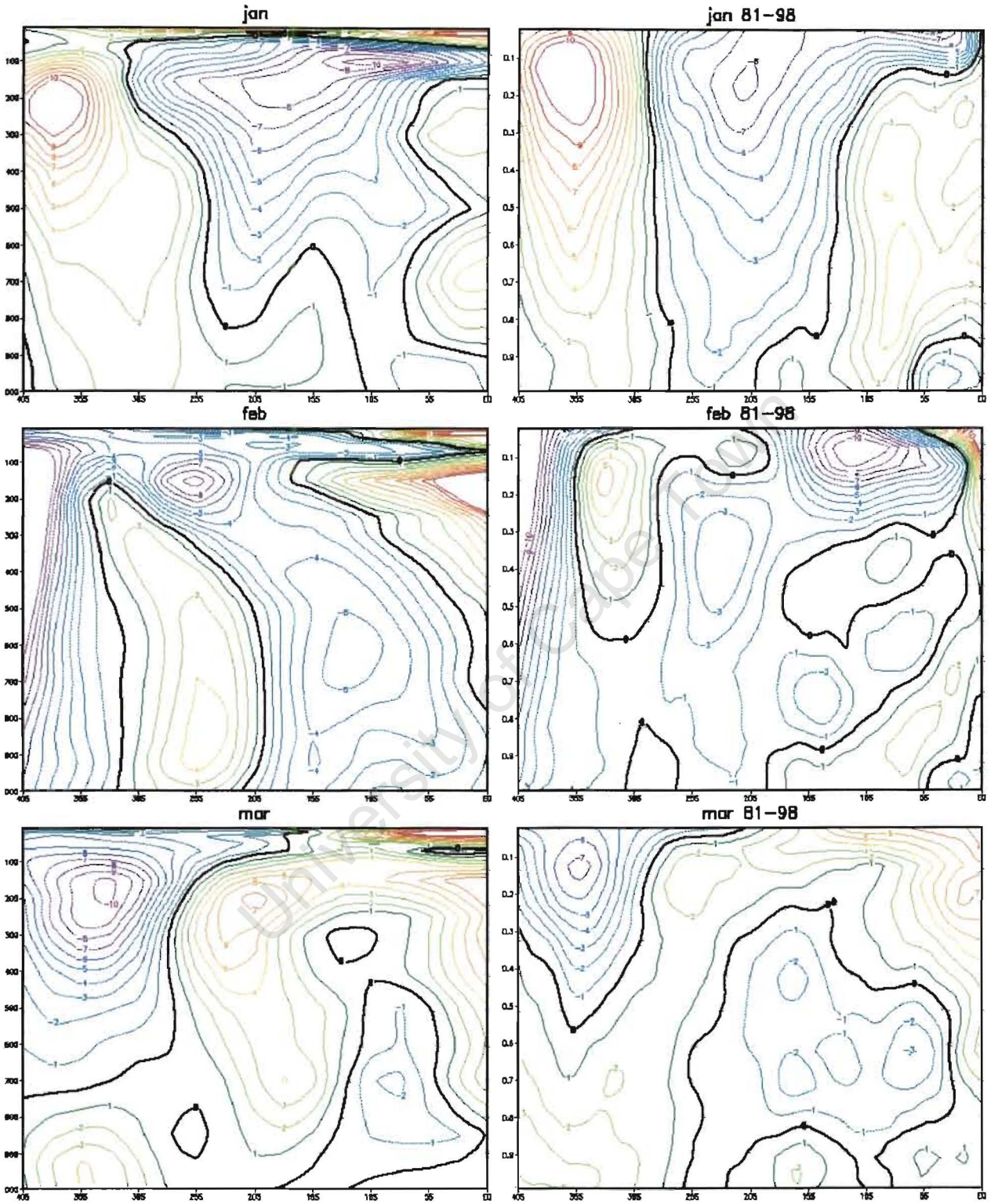

Fig A.3 *A transect of zonal wind difference for 1981 and 1998; taken along* ***40°E****. MM5: Right panel and NCEP: Left panel. Contour interval is* $2ms^{-1}$.